Measuring the Muon Anomalous Magnetic Moment to High Precision

David Flay

Electromagnetic Interactions with Nucleons and Nuclei, Paphos, Cyprus

31 October 2019

Outline

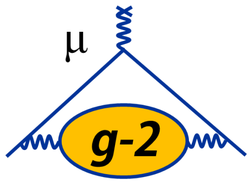

Introduction

- The Magnetic Moment and the Anomaly
- Recent Theoretical Efforts

The Muon g-2 Experiment at Fermilab

- Experimental Technique
- Overview of Operations to Date
- Analysis Status

Summary

The Magnetic Moment and the Anomaly

The Magnetic Moment

$$\vec{\mu} = g\frac{q}{2m}\vec{s}$$

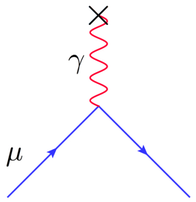

- Magnetic moment connected to spin via dimensionless g-factor
- Dirac: g = 2 for s = 1/2 particles (1928)
- Hyperfine structure experiments on hydrogen: g ≠ 2 (Nafe, Nelson, Rabi 1947)
  - Anomalous contribution $a \equiv (g-2)/2 = \alpha/2\pi$ (Schwinger, QED, 1948)
  - Radiative corrections from virtual particles in loops

The Magnetic Moment and the Anomaly

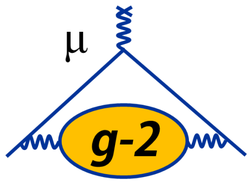

The Magnetic Moment

$$\vec{\mu} = g\frac{q}{2m}\vec{s}$$

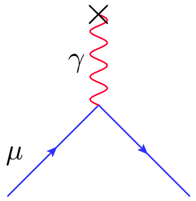

- Magnetic moment connected to spin via dimensionless g-factor
- Dirac: g = 2 for s = 1/2 particles (1928)
- Hyperfine structure experiments on hydrogen: g ≠ 2 (Nafe, Nelson, Rabi 1947)
  - Anomalous contribution a ≡ (g-2)/2 = α/2π (Schwinger, QED, 1948)
  - Radiative corrections from virtual particles in loops

The Muon Anomaly a_μ

Schwinger O(α) Vacuum polarization O(α^2)

$a_\mu =$

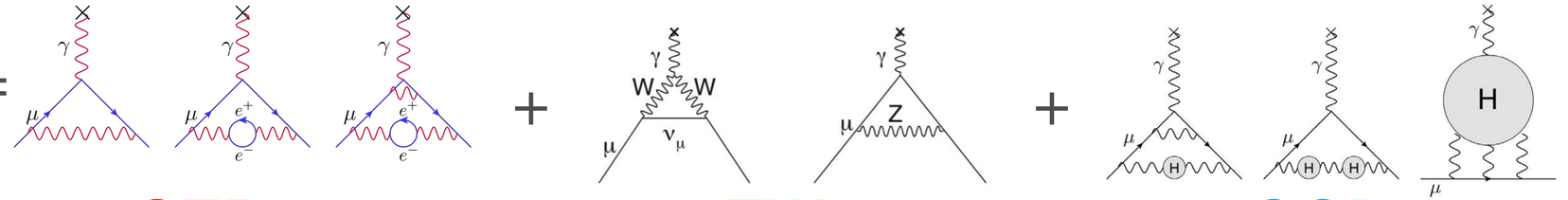

QED **EW** **QCD**

The Magnetic Moment and the Anomaly

The Magnetic Moment

$$\vec{\mu} = g\frac{q}{2m}\vec{s}$$

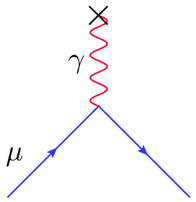

- Magnetic moment connected to spin via dimensionless g-factor
- Dirac: g = 2 for s = 1/2 particles (1928)
- Hyperfine structure experiments on hydrogen: g ≠ 2 (Nafe, Nelson, Rabi 1947)
  - Anomalous contribution a ≡ (g-2)/2 = α/2π (Schwinger, QED, 1948)
  - Radiative corrections from virtual particles in loops

The Muon Anomaly a_μ

Schwinger O(α) Vacuum polarization O(α²)

$a_\mu =$

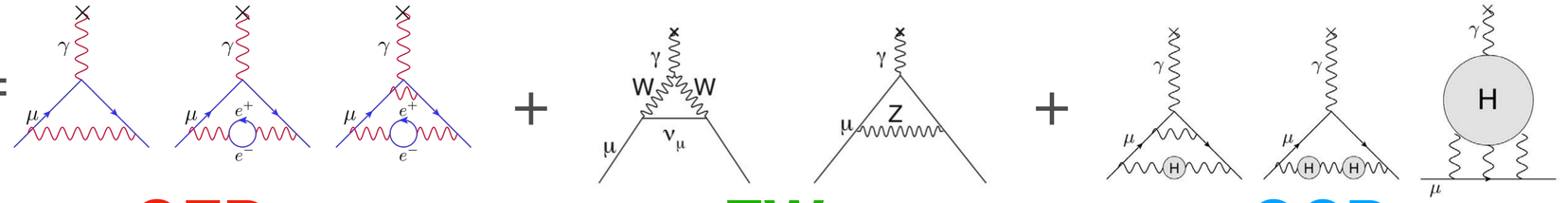

QED EW QCD

Current Status

- **Disagreement** between experiment and theory at > 3σ
- **Improvements**
  - **Experiment**: more statistics, reduced systematics
  - **Theory**: focus on QCD uncertainties

S. Corrodi

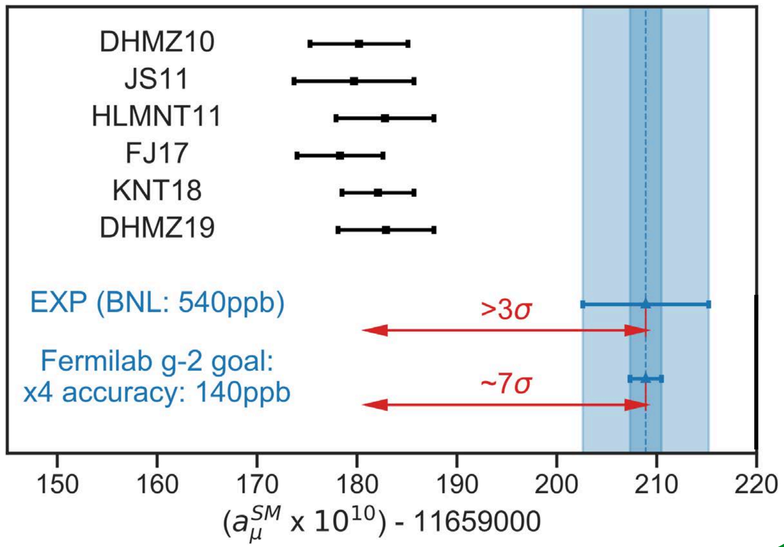

The Magnetic Moment and the Anomaly

Lattice groups making excellent progress (HVP LO, NLO, HLbL)

Calculation of the hadronic vacuum polarization contribution to the muon anomalous magnetic moment

T. Blum, P.A. Boyle, V. Gülpers, T. Izubuchi, L. Jin, C. Jung, A. Jüttner, C. Lehner, A. Portelli, J.T. Tsang

(Submitted on 22 Jan 2018)

We present a first-principles lattice QCD+QED calculation at physical pion mass of the leading-order hadronic vacuum polarization contribution to the muon anomalous magnetic moment. The total contribution of up, down, strange, and charm quarks including QED and strong isospin breaking effects is found to be $a_\mu^{\mathrm{HVP\,LO}} = 715.4(16.3)(9.2) \times 10^{-10}$, where the first error is statistical and the second is systematic. By supplementing lattice data for very s
we significantly improve the precision of our calcul
systematic, R-ratio statistical, and R-ratio systemat
leading-order hadronic vacuum polarization contril
calculation of the light-quark QED correction at ph

Comments: 12 pages, 11 figures
Subjects: **High Energy Physics - Lattice (hep-lat)**; Hi
Cite as: **arXiv:1801.07224 [hep-lat]**
(or **arXiv:1801.07224v1 [hep-lat]** for this ve

Higher-order hadronic-vacuum-polarization contribution to the muon $g-2$ from lattice QCD

B. Chakraborty, C. T. H. Davies, J. Koponen, G. P. Lepage, and R. S. Van de Water (Fermilab Lattice, HPQCD, and MILC Collaborations)
Phys. Rev. D **98**, 094503 – Published 9 November 2018

Article | References | Citing Articles (1) | PDF | HTML | Export Citation

ABSTRACT

We introduce a new method for calculating the $\mathrm{O}(\alpha^3)$ hadronic-vacuum-polarization contribution to the muon anomalous magnetic moment from *ab initio* lattice QCD. We first derive expressions suitable for computing the higher-order contributions either from the renormalized vacuum polarization function $\hat{\Pi}(q^2)$ or directly from the lattice vector-current correlator in Euclidean space. We then demonstrate the approach using previously published results for the Taylor coefficients of $\hat{\Pi}(q^2)$ that were obtained on four-flavor QCD gauge-field configurations with physical light-quark masses. We

virtual particles in loops

a_μ

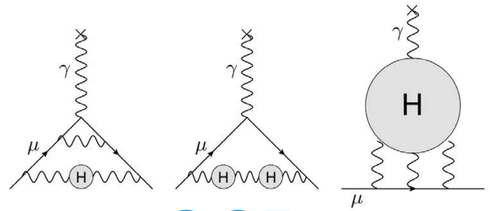

S. Corrodi

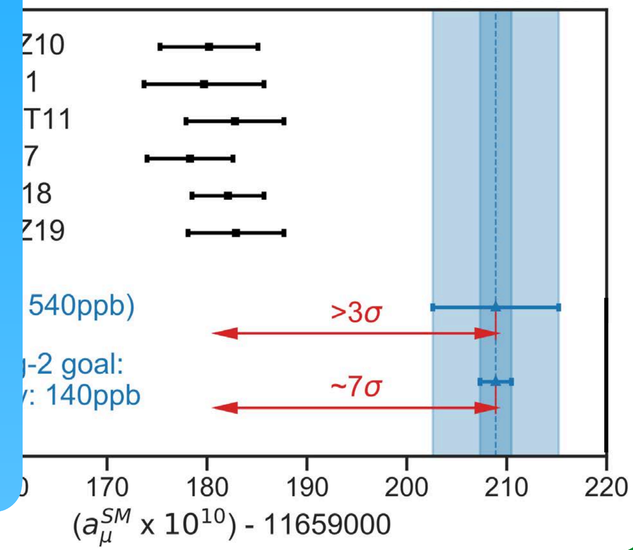

UMassAmherst

The Magnetic Moment and the Anomaly

Lattice groups making excellent progress (HVP LO, NLO, HLbL)

Calculation of the hadronic vacuum polarizat
anomalous magnetic moment

T. Blum, P.A. Boyle, V. Gülpers, T. Izubuchi, L. Jin, C. Jung, A. Jüttner, C

(Submitted on 22 Jan 2018)

We present a first-principles lattice QCD+QED calculation at physical pion mas
contribution to the muon anomalous magnetic moment. The total contributior
strong isospin breaking effects is found to be $a_\mu^{\mathrm{HVP\,LO}} = 715.4(16.3)(9.2) \times 10$
systematic. By supplementing lattice data for very s
we significantly improve the precision of our calcul
systematic, R-ratio statistical, and R-ratio systemat
leading-order hadronic vacuum polarization contril
calculation of the light-quark QED correction at ph

Comments: 12 pages, 11 figures
Subjects: **High Energy Physics - Lattice (hep-lat)**; Hi
Cite as: **arXiv:1801.07224 [hep-lat]**
(or **arXiv:1801.07224v1 [hep-lat]** for this ve

Higher-order
muon $g-2$ fr

B. Chakraborty, C. T. H
MILC Collaborations)
Phys. Rev. D **98**, 0945

Article | References

ABS

We int
the mu
for cor
function $\hat{\Pi}(q^2)$ or directly from the lattice vector-current correlator in Euclidean space. We then demonstrate the approach using previously published results for the Taylor coefficients of $\hat{\Pi}(q^2)$ that
were obtained on four-flavor QCD gauge-field configurations with physical light-quark masses. We

virtual particles in loops

2nd g-2 Theory Initiative Meeting in June 2018

JOHANNES GUTENBERG UNIVERSITÄT MAINZ

Theory Group
Institute for Nuclear Physics

HOME | SEARCH | SITEMAP | CONTACT

HOME RESEARCH PEOPLE PUBLICATIONS TEACHING EVENTS PRESS AND MEDIA SERVICES CONTACT

- Home
- Research
- People
- Publications
- Teaching
- Events
  - Talks and Guest Speakers
  - Previous Events
  - g-2 Workshop
- Press and Media
- Services
- Contact

Second Plenary Workshop of the Muon g-2 Theory Initiative

18 June 2018 - 22 June 2018

In the coming years, experiments at Fermilab and at J-PARC plan to reduce the uncertainties on the already very precisely measured anomalous magnetic moment of the muon by a factor of four. The goal is to resolve the current tantalizing tension between theory and experiment of three to four standard deviations. On the theory side the hadronic corrections to the anomalous magnetic moment are the dominant sources of uncertainty. They must be determined with better precision in order to unambiguously discover whether or not new physics effects contribute to this quantity.

There are a number of complementary theoretical efforts underway to better understand and quantify the hadronic corrections, including dispersive methods, lattice QCD, effective field theories, and QCD models. The Muon (g-2) Theory Initiative was formed in order to facilitate interactions between the different groups through organizing a series of workshops. The goal of this workshop is to bring together theorists from the different communities to discuss, assess, and compare the status of the various efforts, and to map out strategies for obtaining the best theoretical predictions for these hadronic corrections in advance of the experimental results.

First Circular

Second Circular

Indico website

Dates	June 18, 2018 - June 22, 2018
Timezone	GMT+2
Location	**Helmholtz-Institut Mainz** Staudinger Weg 18, 55128 Mainz, Ground Floor

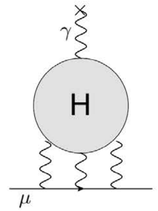

Corrodi

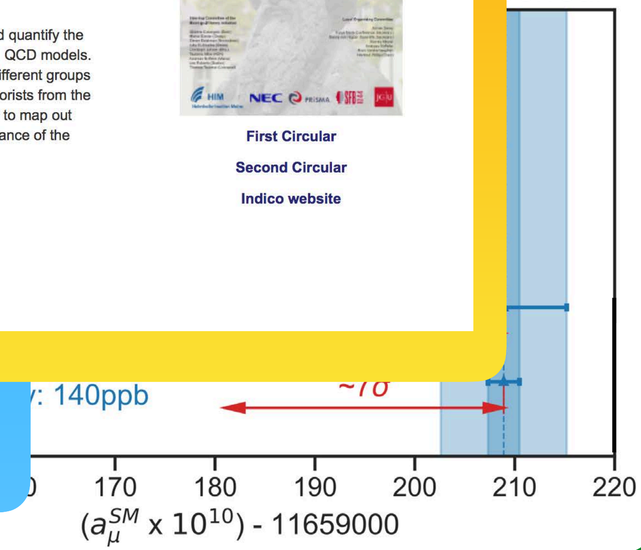

The Magnetic Moment and the Anomaly

Lattice groups making excellent progress (HVP LO, NLO, HLbL)

Calculation of the hadronic vacuum polarizat
anomalous magnetic moment

T. Blum, P.A. Boyle, V. Gülpers, T. Izubuchi, L. Jin, C. Jung, A. Jüttner, C

(Submitted on 22 Jan 2018)

We present a first-principles lattice QCD+QED calculation at physical pion mas
contribution to the muon anomalous magnetic moment. The total contributior
strong isospin breaking effects is found to be $a_\mu^{\mathrm{HVP\,LO}} = 715.4(16.3)(9.2) \times 10$
systematic. By supplementing lattice data for very s
we significantly improve the precision of our calcul
systematic, R-ratio statistical, and R-ratio systemat
leading-order hadronic vacuum polarization contril
calculation of the light-quark QED correction at ph

Comments: 12 pages, 11 figures
Subjects: **High Energy Physics - Lattice (hep-lat)**; Hi
Cite as: **arXiv:1801.07224 [hep-lat]**
(or **arXiv:1801.07224v1 [hep-lat]** for this ve

Higher-order
muon $g-2$ fr

B. Chakraborty, C. T. H
MILC Collaborations)
Phys. Rev. D **98**, 0945

Article | References

ABS

We int
the mu
for cor
function $\hat{\Pi}(q^2)$ or directly from the lattic
demonstrate the approach using previo
were obtained on four-flavor QCD gaug

virtual particles in loops

2nd g-2 Theory Initiative Meeting in June 2018

JOHANNES GUTENBERG UNIVERSITÄT MAINZ

- Home
- Research
- People
- Publications
- Teaching
- **Events**
  - Talks and Guest Speakers
  - Previous Events
  - **g-2 Workshop**
- Press and Media
- Services
- Contact

3rd g-2 Theory Initiative Meeting in Sept 2019

INT Workshop INT-19-74W

Hadronic contributions to $(g-2)_\mu$

September 9 - 13, 2019

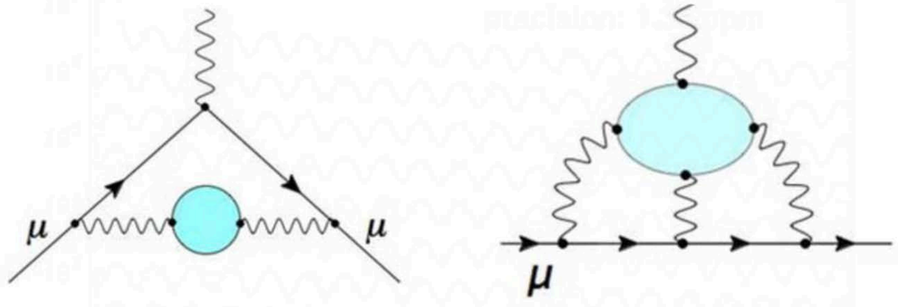

a_μ Theoretical Status

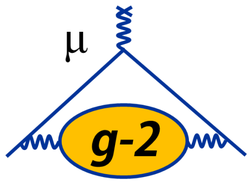

Contribution	Value (x 10^{-11})	Reference
QED	116 584 718.95 ± 0.08	PRL **109** 111808 (2012)
EW	153.6 ± 1.0	PRD **88** 053005 (2013)

a_μ Theoretical Status

Contribution	Value (x 10^{-11})	Reference
QED	116 584 718.95 ± 0.08	PRL **109** 111808 (2012)
EW	153.6 ± 1.0	PRD **88** 053005 (2013)
HVP (LO)	**6931 ± 34**	EPJ C **77** 827 (2017)
HVP (LO)	**6933 ± 25**	PRD **97** 114025 (2018)

HVP (LO): Lowest-Order Hadronic Vacuum Polarization

- **Critical input** from e^+e^- colliders (data from SND, CMD3, BaBar, KLOE, Belle, BESIII), extensive physics program running to reduce δa_μ^{HVP} to ~ 0.3% in coming years
- **Progress on the lattice**: Calculations at physical π mass; approaching goal of δa_μ^{HVP} ~ 1% (cross-check with e^+e^- data)

$$a_\mu^{\mathrm{had;LO}} = \left(\frac{\alpha m_\mu}{3\pi}\right)^2 \int_{m_\pi^2}^{\infty} \frac{ds}{s^2} K(s) R(s)$$

$$R \equiv \frac{\sigma_{\mathrm{tot}}(e^+e^- \to \mathrm{hadrons})}{\sigma(e^+e^- \to \mu^+\mu^-)}$$

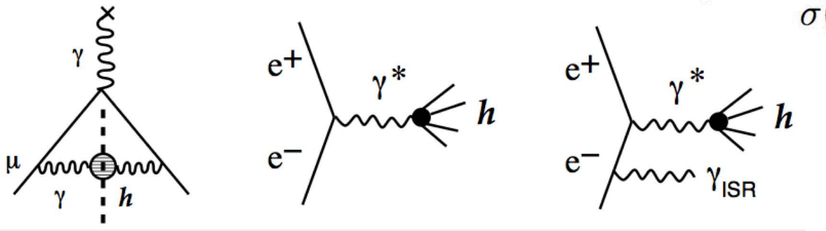

a_μ Theoretical Status

Contribution	Value (x 10^{-11})	Reference
QED	116 584 718.95 ± 0.08	PRL **109** 111808 (2012)
EW	153.6 ± 1.0	PRD **88** 053005 (2013)
HVP (LO)	**6931 ± 34**	EPJ C **77** 827 (2017)
HVP (LO)	**6933 ± 25**	PRD **97** 114025 (2018)

[prepared by K. Miura for WP]

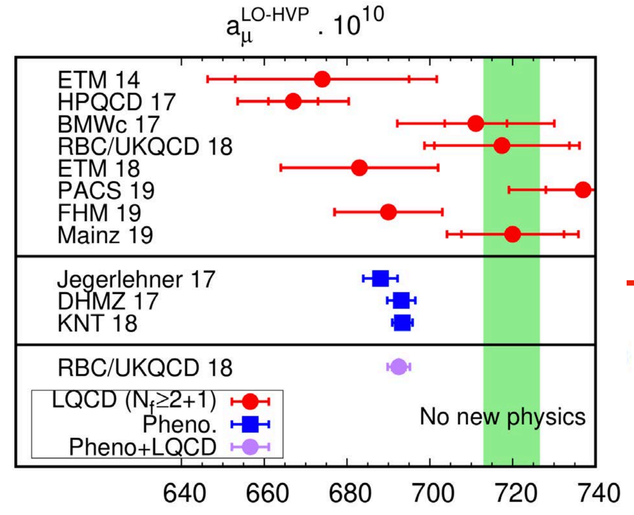

HVP (LO): Lowest-Order Hadronic Va

- **Critical input** from e^+e^- colliders (data from S
  BaBar, KLOE, Belle, BESIII), extensive physic
  running to reduce δa_μ^{HVP} to ~ 0.3% in coming
- **Progress on the lattice**: Calculations at physical π mass;
  approaching goal of δa_μ^{HVP} ~ 1% (cross-check with e^+e^- data)

$$= \left(\frac{\alpha m_\mu}{3\pi}\right)^2 \int_{m_\pi^2}^{\infty} \frac{ds}{s^2} K(s) R(s)$$

$$R \equiv \frac{\sigma_{\text{tot}}(e^+e^- \to \text{hadrons})}{\sigma(e^+e^- \to \mu^+\mu^-)}$$

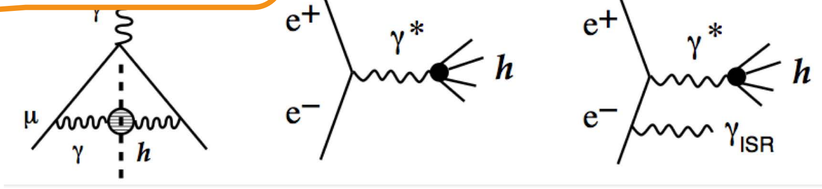

a_μ Theoretical Status

Contribution	Value (x 10^{-11})	Reference
QED	116 584 718.95 ± 0.08	PRL **109** 111808 (2012)
EW	153.6 ± 1.0	PRD **88** 053005 (2013)
HVP (LO)	**6931 ± 34**	EPJ C **77** 827 (2017)
HVP (LO)	**6933 ± 25**	PRD **97** 114025 (2018)
HVP (NLO)	**-98.7 ± 0.7**	EPJ C **77** 827 (2017)
HVP (NLO)	**-98.2 ± 0.4**	PRD **97** 114025 (2018)
HVP (NNLO)	12.4 ± 0.1	PLB 734 144 (2014)

HVP (LO): Lowest-Order Hadronic Vacuum Polarization

- **Critical input** from e^+e^- colliders (data from SND, CMD3, BaBar, KLOE, Belle, BESIII), extensive physics program running to reduce δa_μ^{HVP} to ~ 0.3% in coming years
- **Progress on the lattice**: Calculations at physical π mass; approaching goal of δa_μ^{HVP} ~ 1% (cross-check with e^+e^- data)

$$a_\mu^{\mathrm{had;LO}} = \left(\frac{\alpha m_\mu}{3\pi}\right)^2 \int_{m_\pi^2}^{\infty} \frac{ds}{s^2} K(s) R(s)$$

$$R \equiv \frac{\sigma_{\mathrm{tot}}(e^+e^- \to \mathrm{hadrons})}{\sigma(e^+e^- \to \mu^+\mu^-)}$$

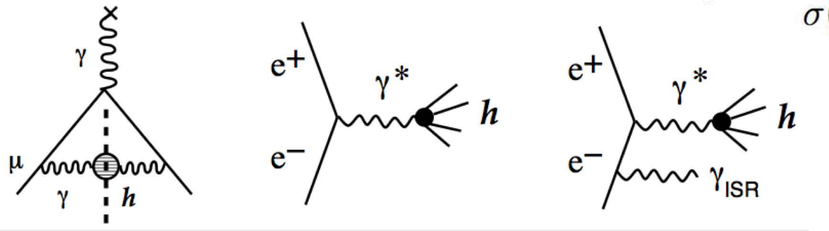

UMassAmherst

a_μ Theoretical Status

New *ab initio* approaches [PRD **98** 094503 (2018)] finding consistent result of (-93 ± 13) x 10^{-11} — **lattice making big strides**

		012)
		013)
		7)
		018)
HV (NLO)	**-98.7 ± 0.7**	EPJ C **77** 827 (2017)
HVP (NLO)	**-98.2 ± 0.4**	PRD **97** 114025 (2018)
HVP (NNLO)	12.4 ± 0.1	PLB 734 144 (2014)

HVP (LO): Lowest-Order Hadronic Vacuum Polarization

- **Critical input** from e^+e^- colliders (data from SND, CMD3, BaBar, KLOE, Belle, BESIII), extensive physics program running to reduce δa_μ^{HVP} to ~ 0.3% in coming years
- **Progress on the lattice**: Calculations at physical π mass; approaching goal of δa_μ^{HVP} ~ 1% (cross-check with e^+e^- data)

$$a_\mu^{\mathrm{had;LO}} = \left(\frac{\alpha m_\mu}{3\pi}\right)^2 \int_{m_\pi^2}^{\infty} \frac{ds}{s^2} K(s) R(s)$$

$$R \equiv \frac{\sigma_{\mathrm{tot}}(e^+e^- \to \mathrm{hadrons})}{\sigma(e^+e^- \to \mu^+\mu^-)}$$

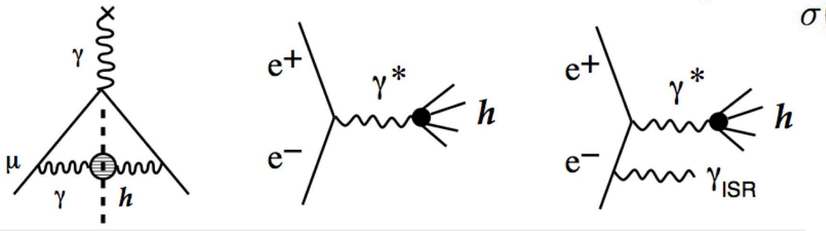

UMassAmherst

a_μ Theoretical Status

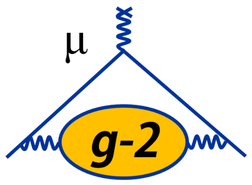

New *ab initio* approaches [PRD **98** 094503 (2018)] finding consistent result of (-93 ± 13) x 10^{-11} — **lattice making big strides**

		012)
		013)
		7)
		018)
HV (NLO)	**-98.7 ± 0.7**	EPJ C **77** 827 (2017)
HVP (NLO)	**-98.2 ± 0.4**	PRD **97** 114025 (2018)
HVP (NNLO)	12.4 ± 0.1	PLB 734 144 (2014)
HLbL (LO + NLO)	101 ± 26	PLB 735 90 (2014), EPJ Web Conf 118 01016 (2016)
Total SM	**116 591 818 ± 43 (368 ppb)** **116 591 821 ± 36 (309 ppb)**	

HLbL: Hadronic Light-by-Light

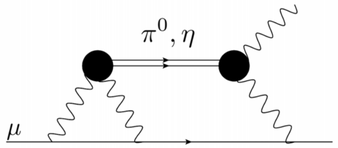

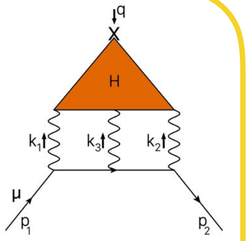

- Model dependent: based on χPT + short-distance constraints (operator product expansion)
- Difficult to relate to data like HVP (LO); γ* physics, π^0 data (BESIII, KLOE) important for constraining models
- **Theory Progress**: New dispersive calculation approach; extend the lattice (finite volume, disconnected diagrams); Blum et al. making excellent progress

HVP (LO): Lowest-Order Hadronic Vacuum Polarization

- **Critical input** from e^+e^- colliders (data from SND, CMD3, BaBar, KLOE, Belle, BESIII), extensive physics program running to reduce δa_μ^{HVP} to ~ 0.3% in coming years
- **Progress on the lattice**: Calculations at physical π mass; approaching goal of δa_μ^{HVP} ~ 1% (cross-check with e^+e^- data)

$$a_\mu^{\mathrm{had;LO}} = \left(\frac{\alpha m_\mu}{3\pi}\right)^2 \int_{m_\pi^2}^{\infty} \frac{ds}{s^2} K(s) R(s)$$

$$R \equiv \frac{\sigma_{\mathrm{tot}}(e^+e^- \to \mathrm{hadrons})}{\sigma(e^+e^- \to \mu^+\mu^-)}$$

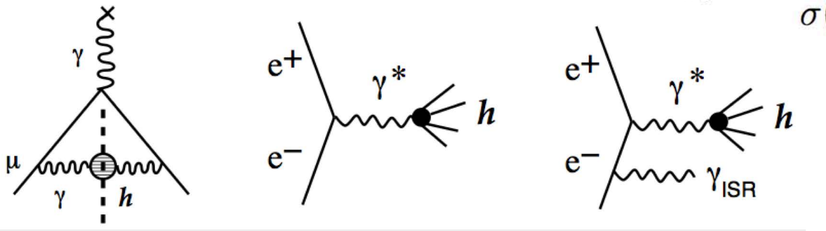

a_μ Theoretical Status

New *ab initio* approaches [PRD **98** 094503 (2018)] finding consistent result of (-93 ± 13) x 10^{-11} — **lattice making big strides**

		012)
		013)
		7)
		018)
HV (NLO)	**-98.7 ± 0.7**	EPJ C **77** 827 (2017)
HVP (NLO)	**-98.2 ± 0.4**	PRD **97** 114025 (2018)
HVP (NNLO)	12.4 ± 0.1	PLB 734 144 (2014)
HLbL (LO + NLO)	101 ± 26	PLB 735 90 (2014), EPJ Web Conf 118 01016 (2016)
Total SM	**116 591 818 ± 43 (368 ppb)** **116 591 821 ± 36 (309 ppb)**	

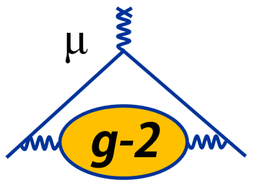

HLbL: Hadronic Light-by-Light

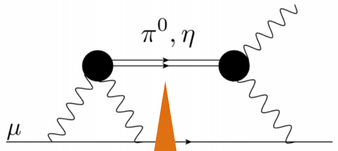

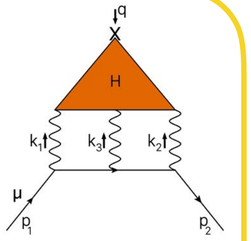

- Model depende : based on χPT + short-distance constraints (op tor product expansion)
- Difficult to rela data like HVP (LO); γ* physics, π^0 data (BESIII, KLOE portant for constraining models
- **Theory Prog** lew dispersive calculation approach; extend the la ite volume, disconnected diagrams); Blum et al. r xcellent progress

HVP (LO): Lowest-Orde

- **Critical input** from e^+e^- colli BaBar, KLOE, Belle, BESIII), running to reduce δa_μ^{HVP} to
- **Progress on the lattice**: Ca approaching goal of δa_μ^{HVP}

$$\left.\sigma(e^+e^- \to \text{hadrons})\right)_{\text{bt}}$$
$$\sigma(e^+e^- \to \mu^+\mu^-)$$

Recent lattice & data-driven estimate [PRD **100** 034520 (2019)] for $a_\mu^{\pi^0-\text{pole}}$ is consistent with lowest-meson dominance, + vector phenomenological models [PRD **51** 4939 (2005), PRL **83** 5230 (1999), EJC **21** 659 (2001), PRD **65** 073034 (2002), PRD **94** 053006 (2016), EJC **75** 586 (2015)]

a_μ Theoretical Status

New *ab initio* approaches [PRD **98** 094503 (2018)] finding consistent result of (-93 ± 13) x 10^{-11} — **lattice making big strides**

HV[illegible](NLO)	-98.7 ± 0.7	EPJ C **77** 827 (2017)
HVP (NLO)	-98.2 ± 0.4	PRD **97** 114025 (2018)
HVP (NNLO)	12.4 ± 0.1	
HLbL (LO + NLO)	101 ± 26	
	91 818 ± 43 (368	
	91 821 ± 36 (309	

Builds confidence in HLbL term

See **T. Blum**'s talk for updates on the lattice

HLbL: Hadronic Light-by-Light

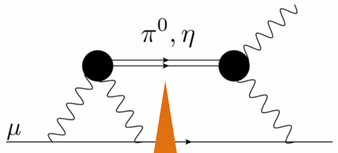

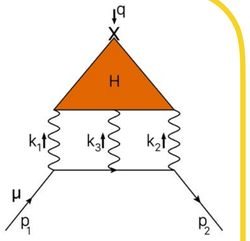

- Model dependent: based on χPT + short-distance constraints (operator product expansion)
- Difficult to relate to data like HVP (LO); γ* physics, π^0 data (BESIII, KLOE important for constraining models
- **Theory Prog** lew dispersive calculation approach; extend the la ite volume, disconnected diagrams); Blum et al. r xcellent progress

HVP (LO): Lowest-Order Hadronic Vacuum Polarization

- **Critical input** from e^+e^- colli BaBar, KLOE, Belle, BESIII), running to reduce δa_μ^{HVP} to
- **Progress on the lattice**: Ca approaching goal of δa_μ^{HVP}

$$\left.\sigma(e^+e^- \to \text{hadrons})\right)$$
$$\sigma(e^+e^- \to \mu^+\mu^-)$$

Recent lattice & data-driven estimate [PRD **100** 034520 (2019)] for $a_\mu^{\pi^0-\text{pole}}$ is consistent with lowest-meson dominance, + vector phenomenological models [PRD **51** 4939 (2005), PRL **83** 5230 (1999), EJC **21** 659 (2001), PRD **65** 073034 (2002), PRD **94** 053006 (2016), EJC **75** 586 (2015)]

a_μ Theoretical Status

New *ab initio* approaches [PRD **98** 094503 (2018)] finding consistent result of $(-93 \pm 13) \times 10^{-11}$ —

- **Theory groups are making steady progress** to achieve competitive uncertainties on the same time scale as the FNAL experiment result
- **White paper** discussing all terms forthcoming

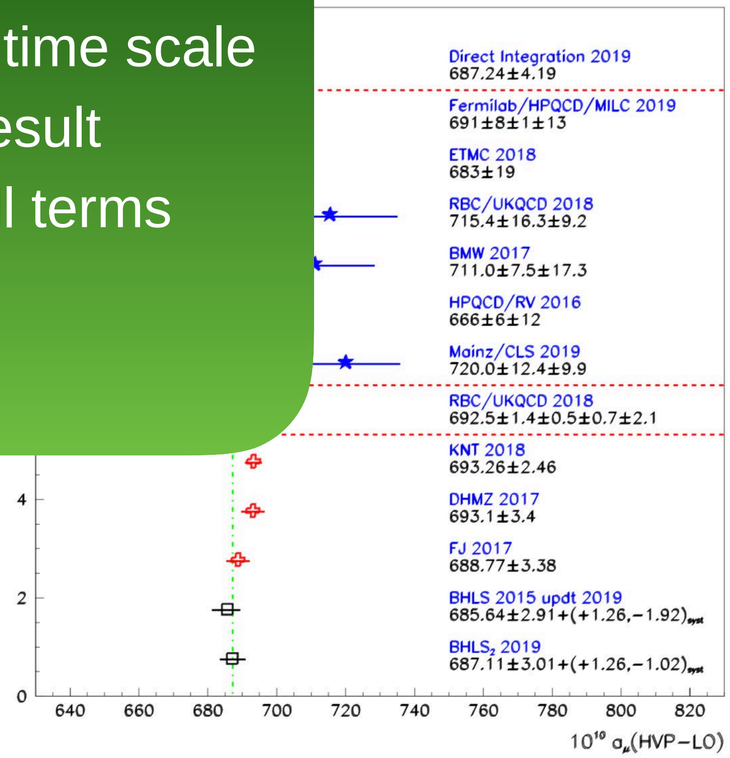

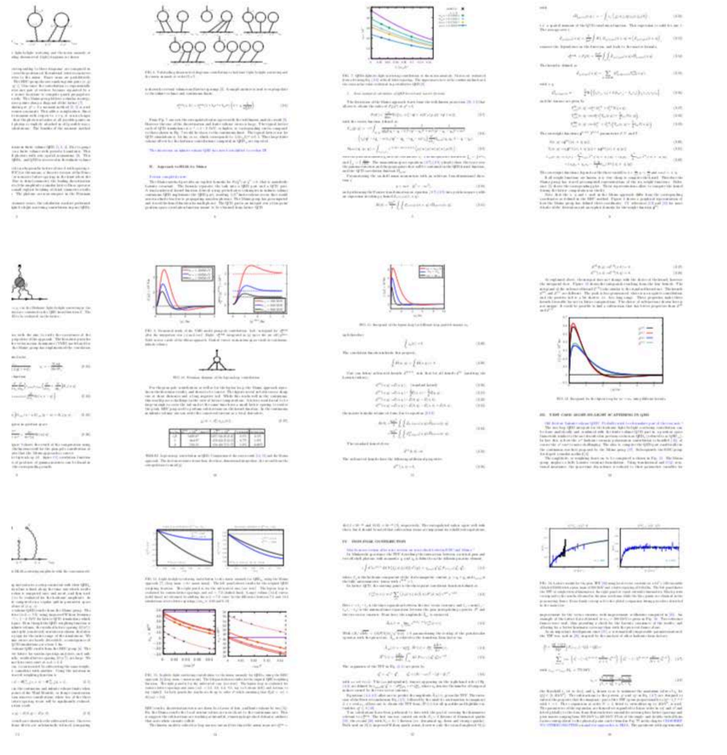

The Muon g-2 Experiment at Fermilab

Muon g-2: 33 Institutions, 7 countries, 203 Members

Why Fermilab?

- BNL limited by statistics
  (540 ppb on 9 x 10^9 detected e^+)
- E989 goal: Factor of 21 more statistics
  (2 x 10^{11} detected e^+)

Fermilab advantages

- ✓ Long beam line to collect $\pi^+ \rightarrow \mu^+$
- ✓ Much reduced amount of p, π in ring
- ✓ 4x higher fill frequency than BNL

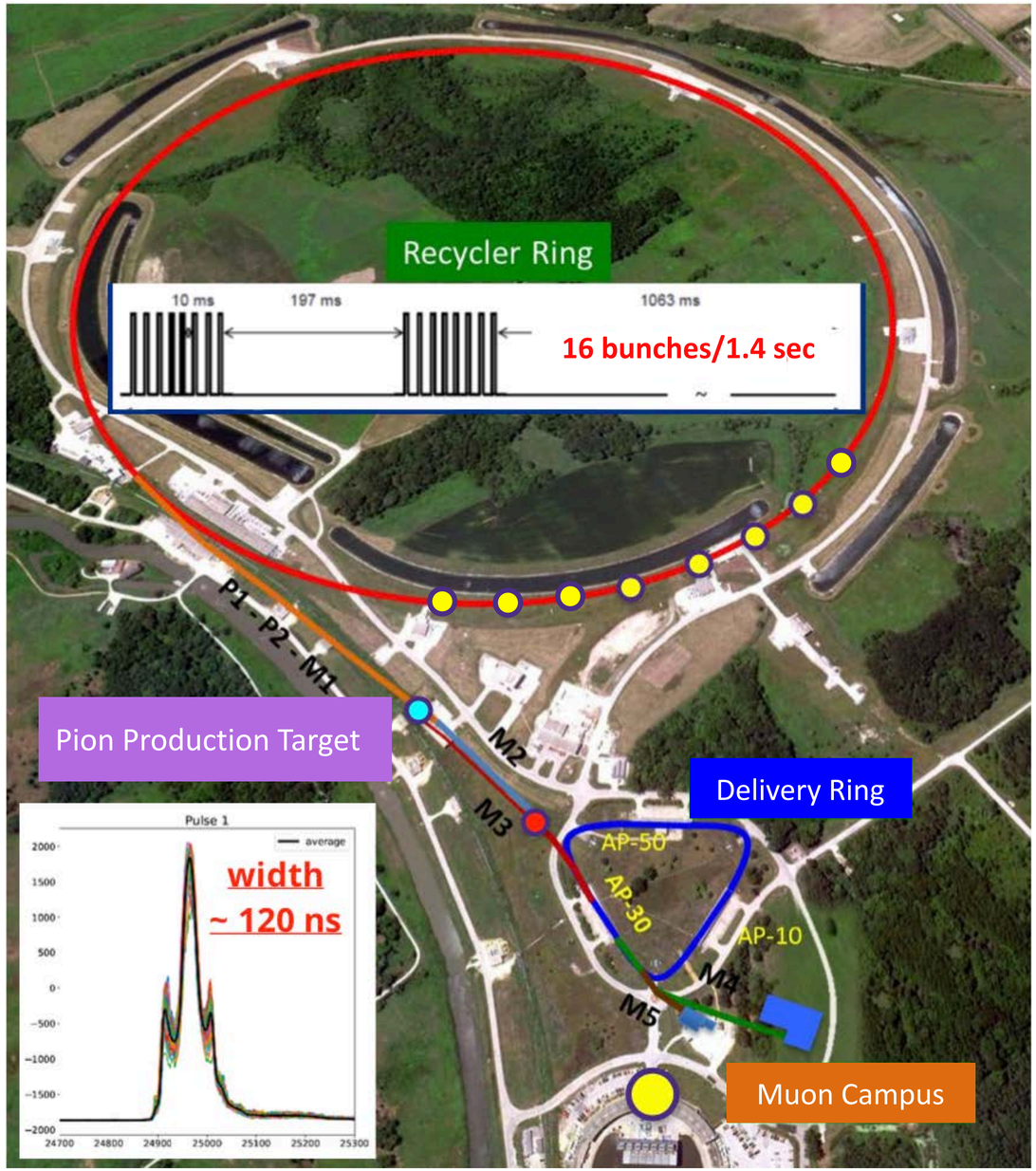

UMassAmherst

Measuring the Muon Anomaly

- Inject polarized muon beam into magnetic storage ring
- Measure **difference** between spin precession and cyclotron frequencies
- If g = 2, $\omega_a = 0$
- $g \neq 2$, $\omega_a \cong (e/m_\mu)a_\mu B$

$$\vec{\omega}_C = -\frac{e}{\gamma m}\vec{B}$$ cyclotron frequency

$$\vec{\omega}_S = -\frac{e}{\gamma m}\vec{B}\left(1 + \gamma a_\mu\right)$$ spin precession frequency (Larmor, Thomas precession)

$$\vec{\omega}_a \equiv \vec{\omega}_S - \vec{\omega}_C$$

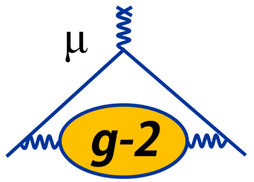

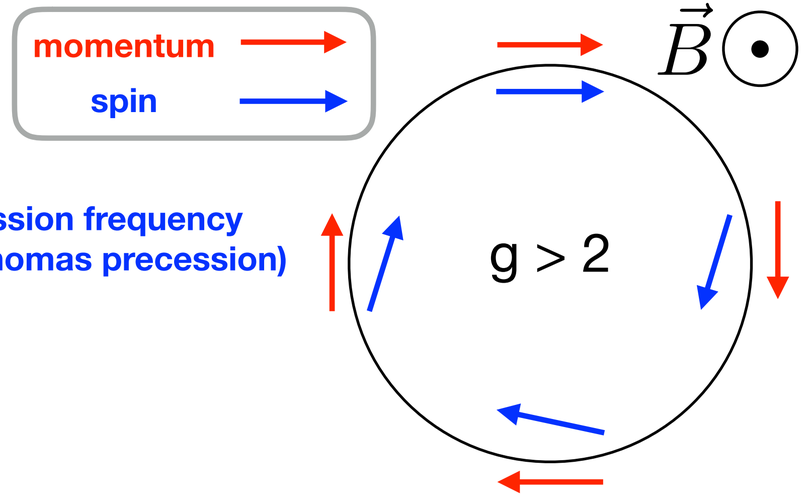

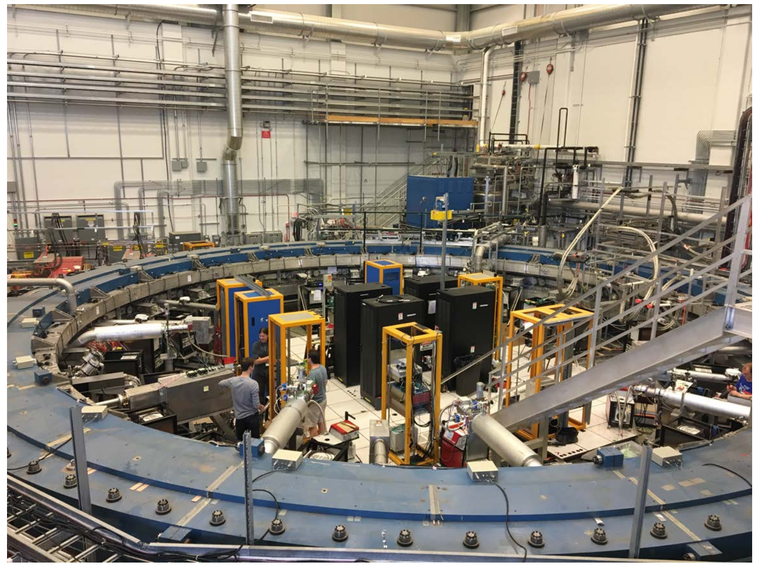

Measuring the Muon Anomaly

- Inject polarized muon beam into magnetic storage ring
- Measure **difference** between spin precession and cyclotron frequencies
- If g = 2, $\omega_a = 0$
- g ≠ 2, $\omega_a \cong (e/m_\mu)a_\mu B$
- Using $\hbar\omega_p = 2\mu_p|\vec{B}|$:

$$\vec{\omega}_C = -\frac{e}{\gamma m}\vec{B}$$ cyclotron frequency

$$\vec{\omega}_S = -\frac{e}{\gamma m}\vec{B}\left(1 + \gamma a_\mu\right)$$ spin precession frequency (Larmor, Thomas precession)

$$\vec{\omega}_a \equiv \vec{\omega}_S - \vec{\omega}_C$$

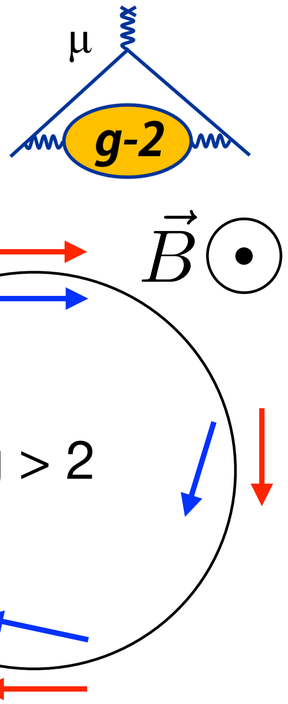

$$a_\mu = \frac{\omega_a}{\tilde{\omega}_p}\frac{\mu_p}{\mu_e}\frac{m_\mu}{m_e}\frac{g_e}{2}$$

3 ppb 22 ppb 0.3 ppt

Rev. Mod. Phys. **88**, 035009 (2016)

- We measure ω_a and ω_p separately
- Aiming for 70 ppb precision on each (systematic)
- **Target: δa_μ = 140 ppb; factor of 4 improvement over BNL**

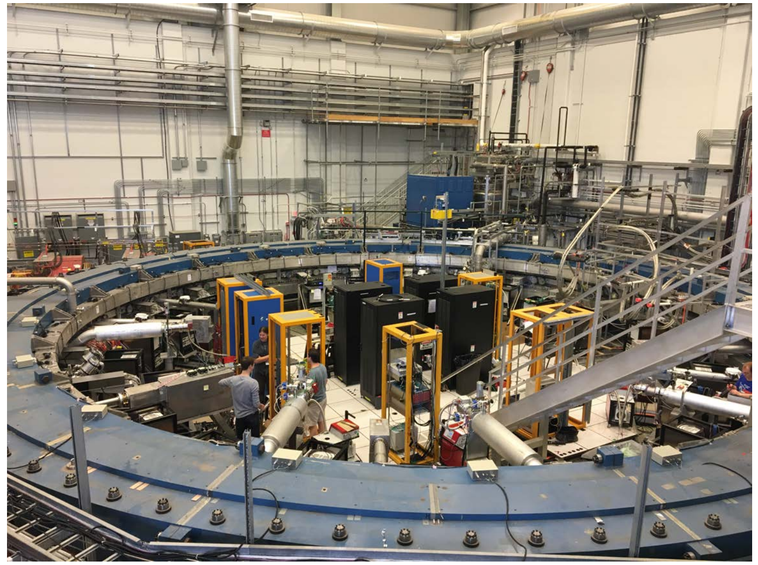

Muon Beam Injection

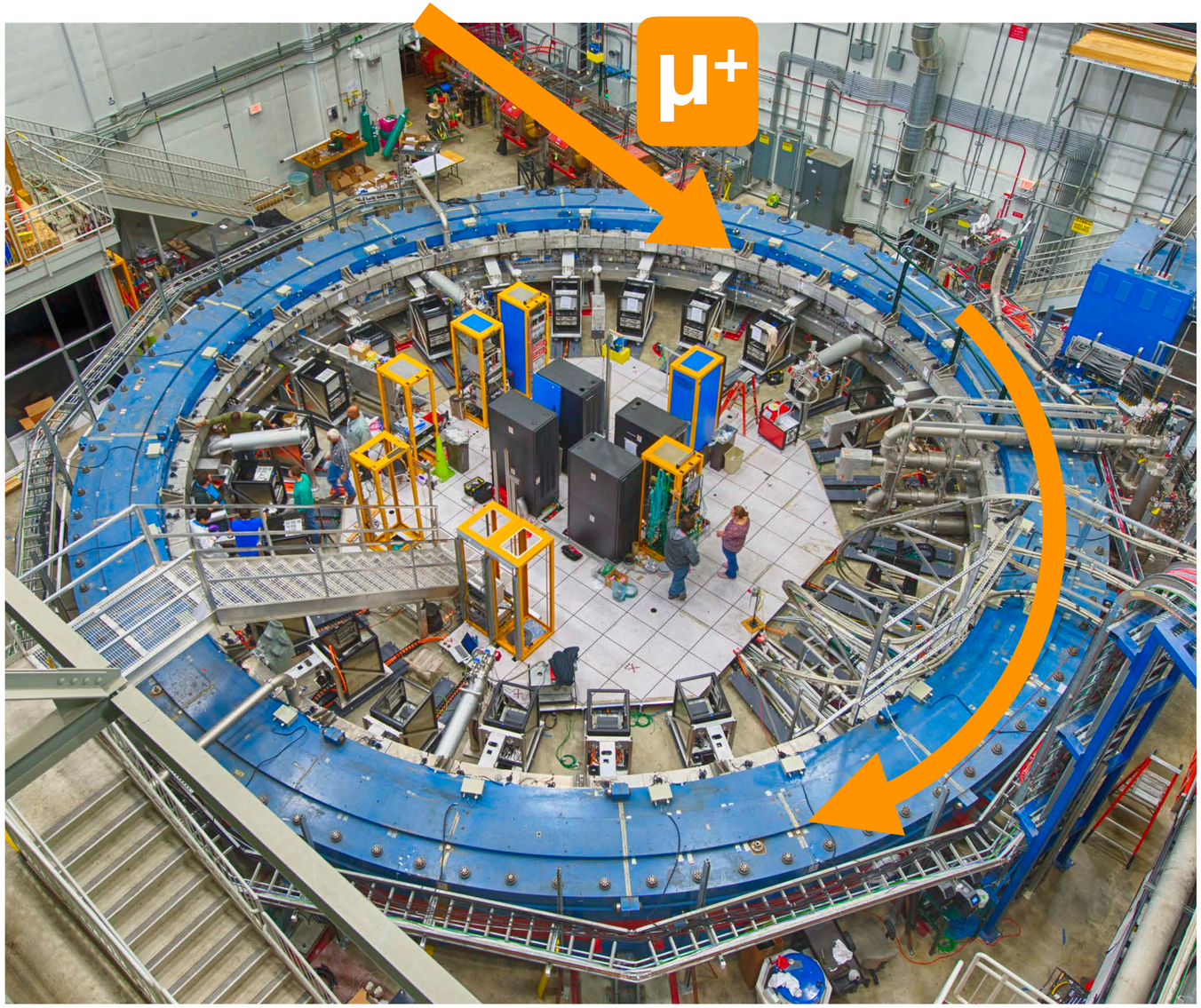

Muon Beam Injection

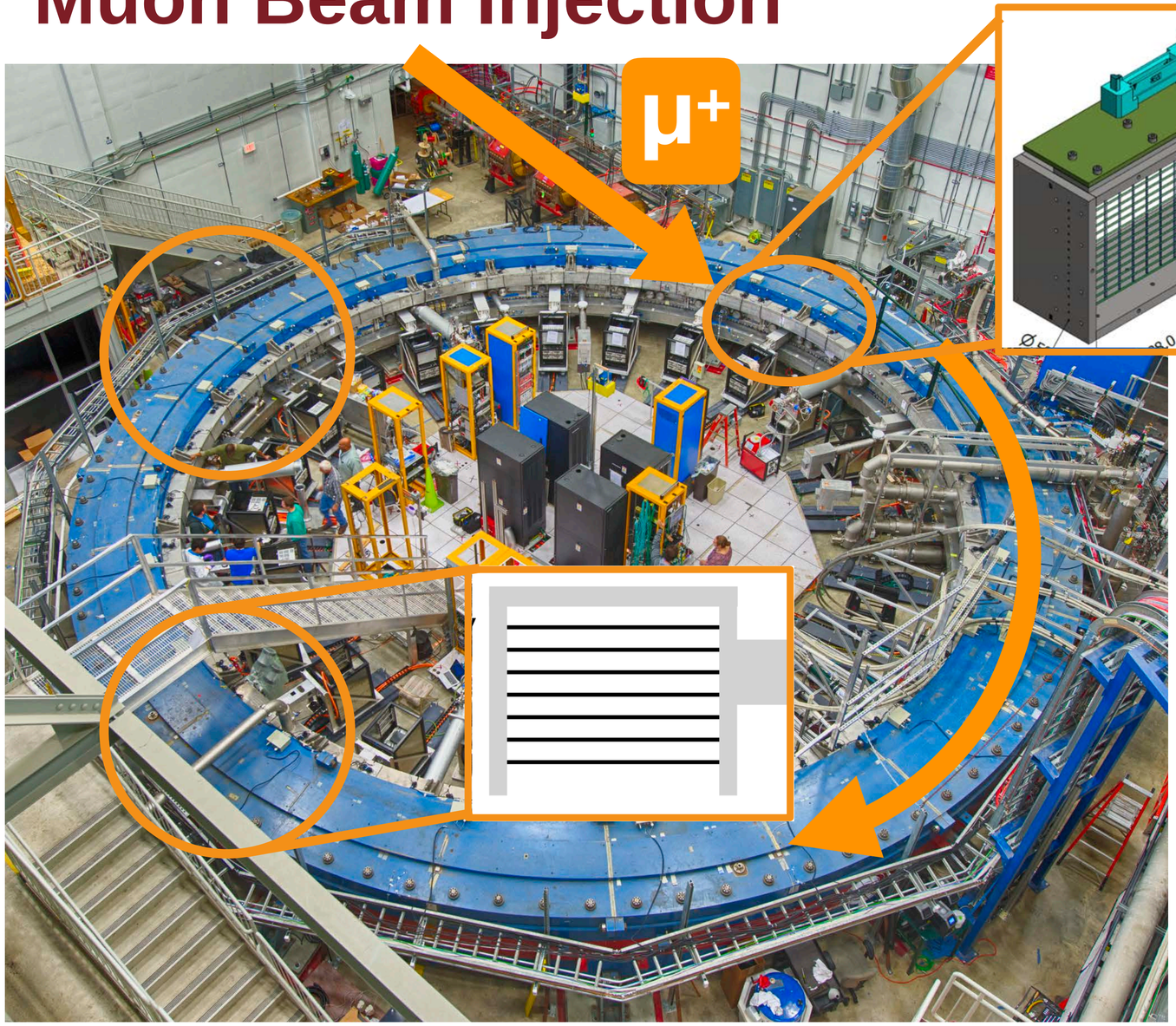

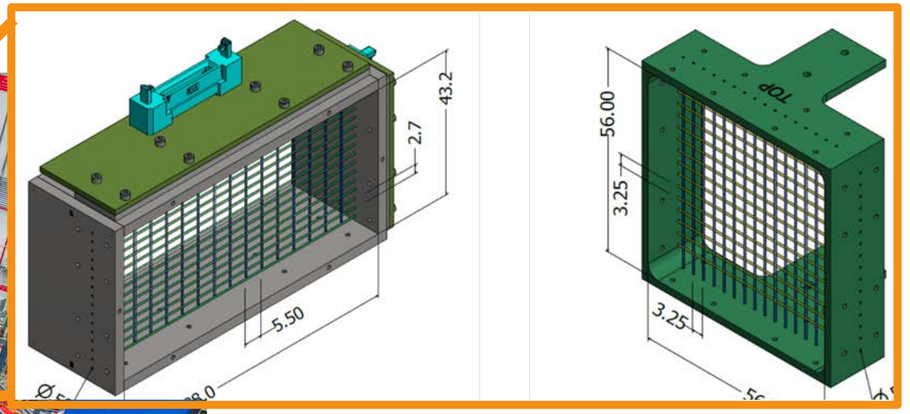

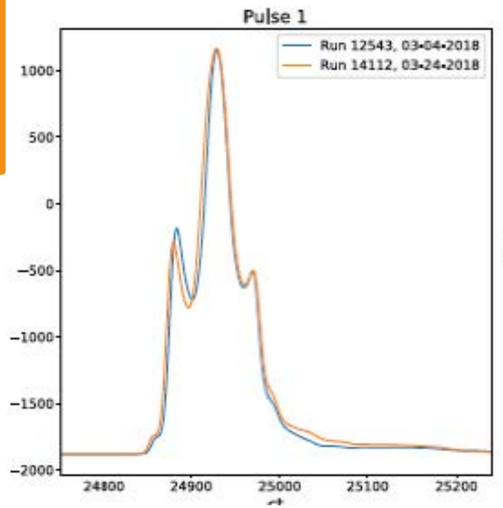

Monitoring the Incoming Muon Beam

- **Scintillating Paddles**: Monitoring temporal distribution
- **Scintillating Fibers**: Map of transverse profile, guides μ tuning into the ring

Muon Beam Injection

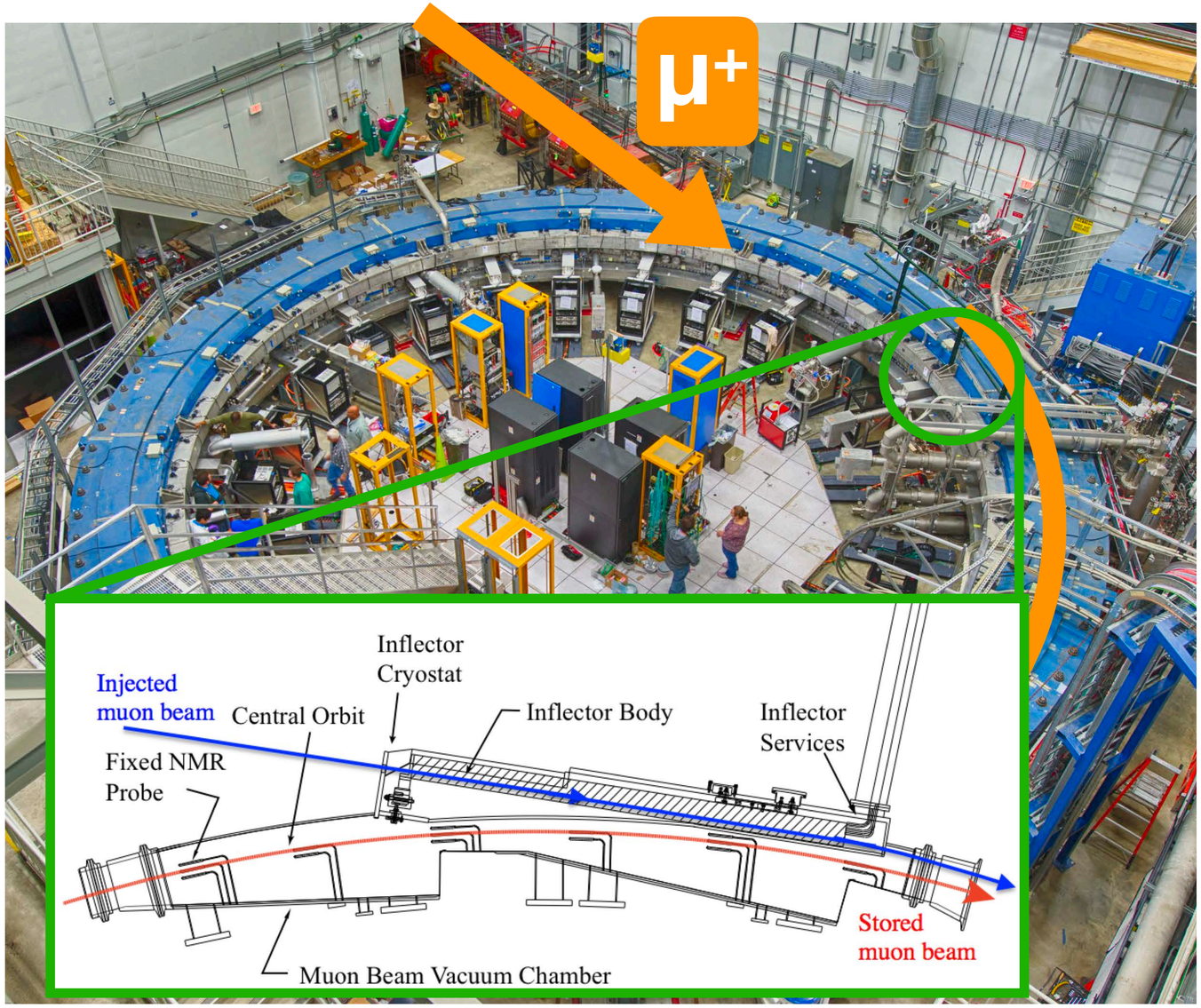

Inflector Magnet

- Need to cancel field in beam channel
- Prevents strong deflection of the beam
- Minimal perturbation to storage magnetic field

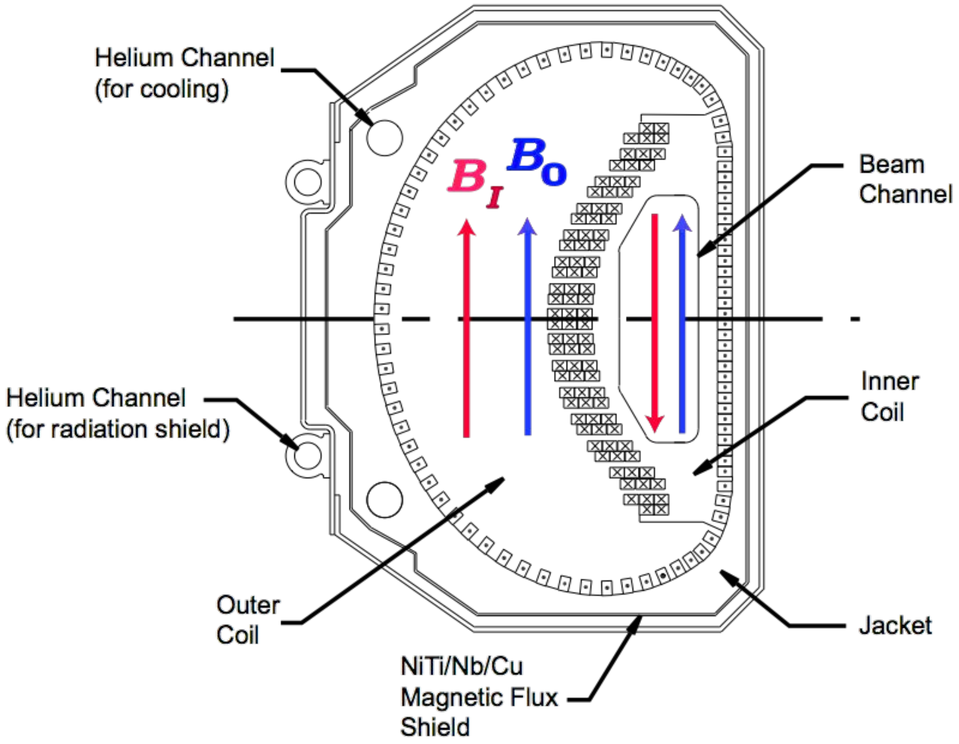

UMassAmherst

Muon Beam Storage and Focusing

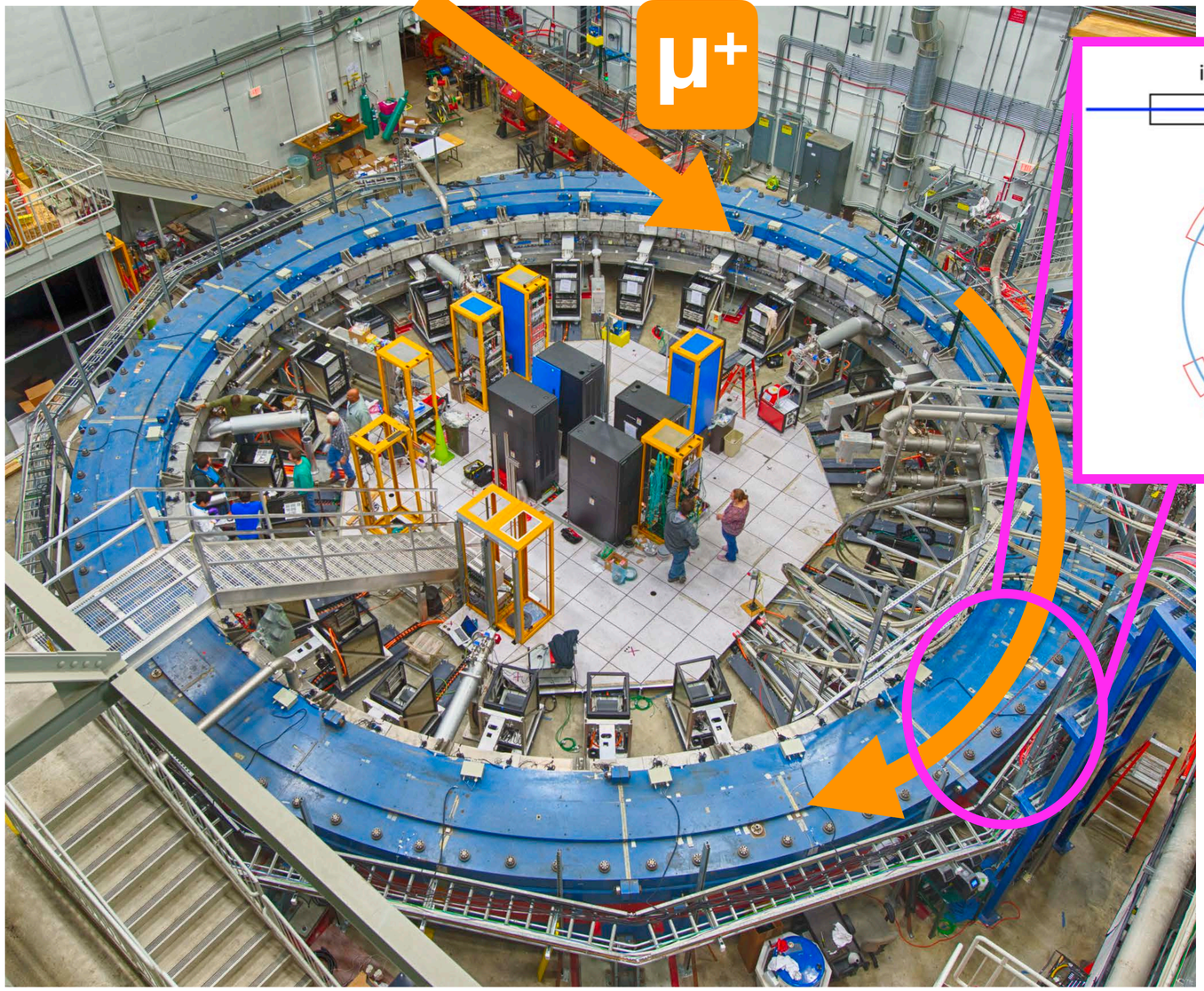

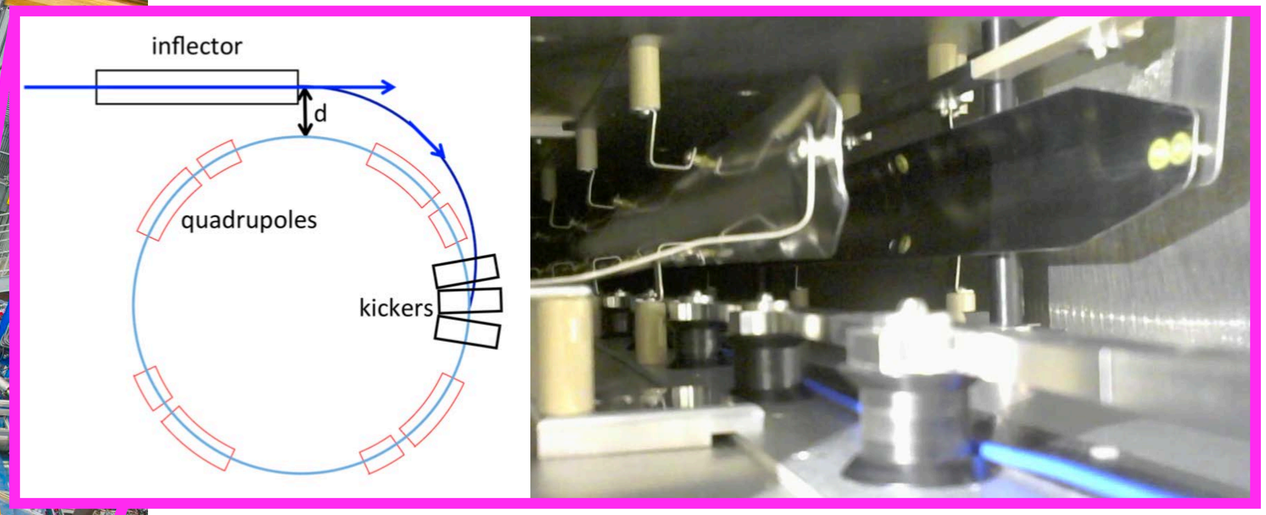

3 Kicker Magnets

- After inflector, muons enter storage region at r = 77 mm outside central closed orbit
- Deliver pulse in < 149 ns to muon beam
- Steer muons onto stored orbit

Muon Beam Storage and Focusing

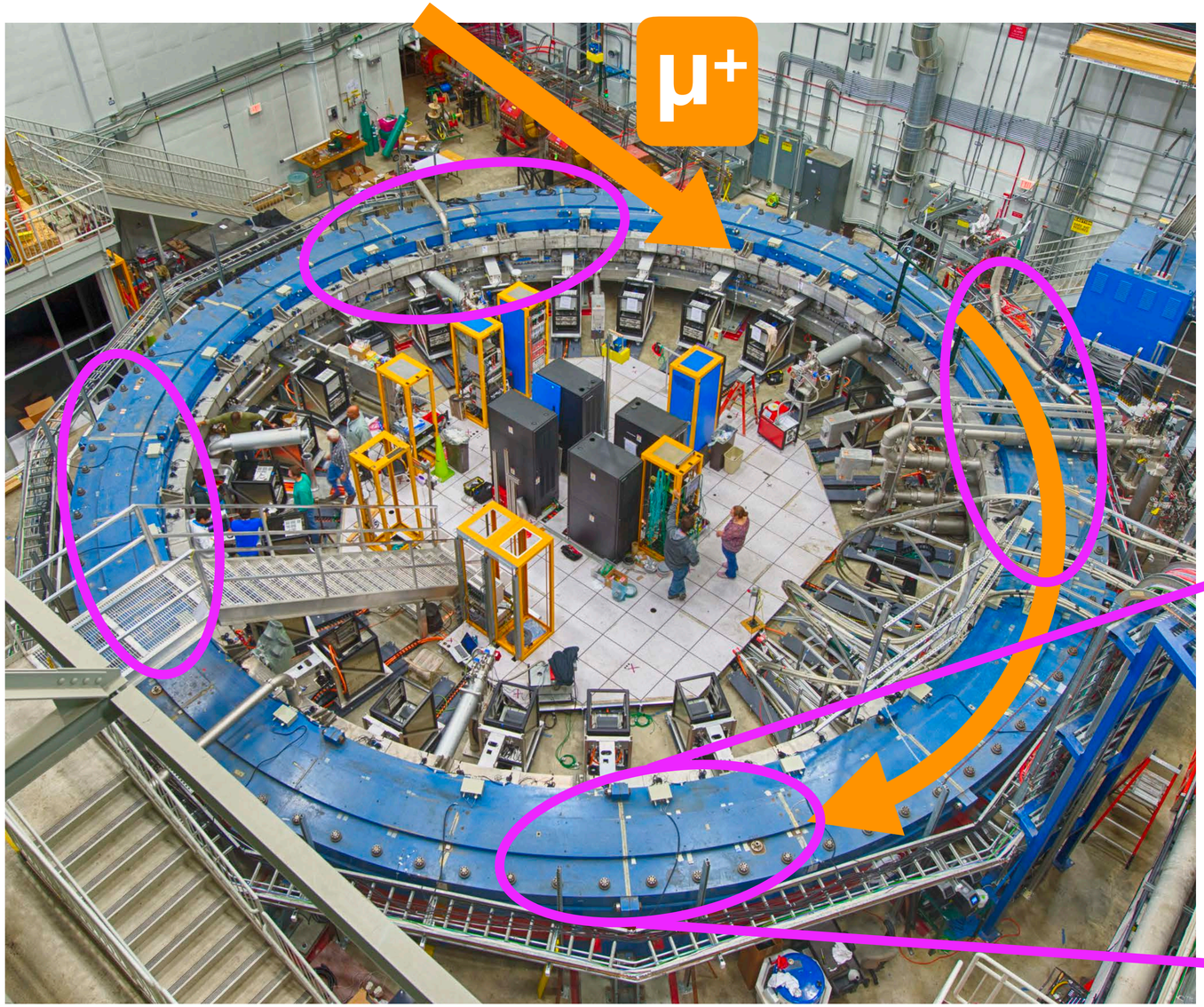

Electrostatic Quadrupoles

- Drives the muons towards the central part of storage region vertically
- Aluminum electrodes cover ~43% of total circumference

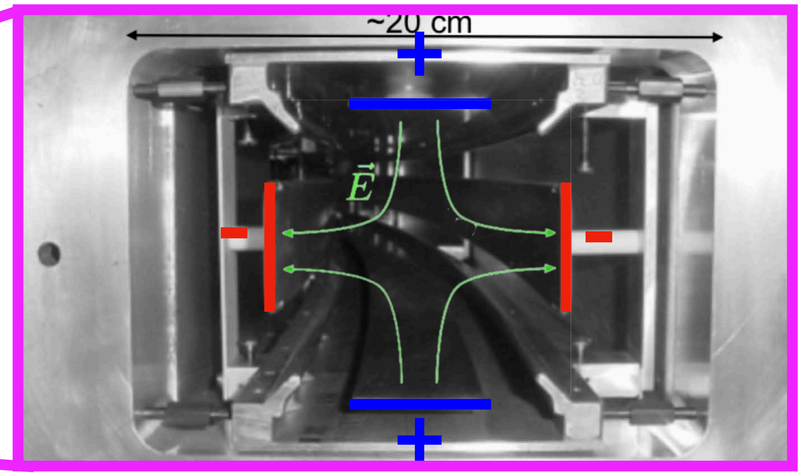

Measuring Muon Spin Precession (ω_a)

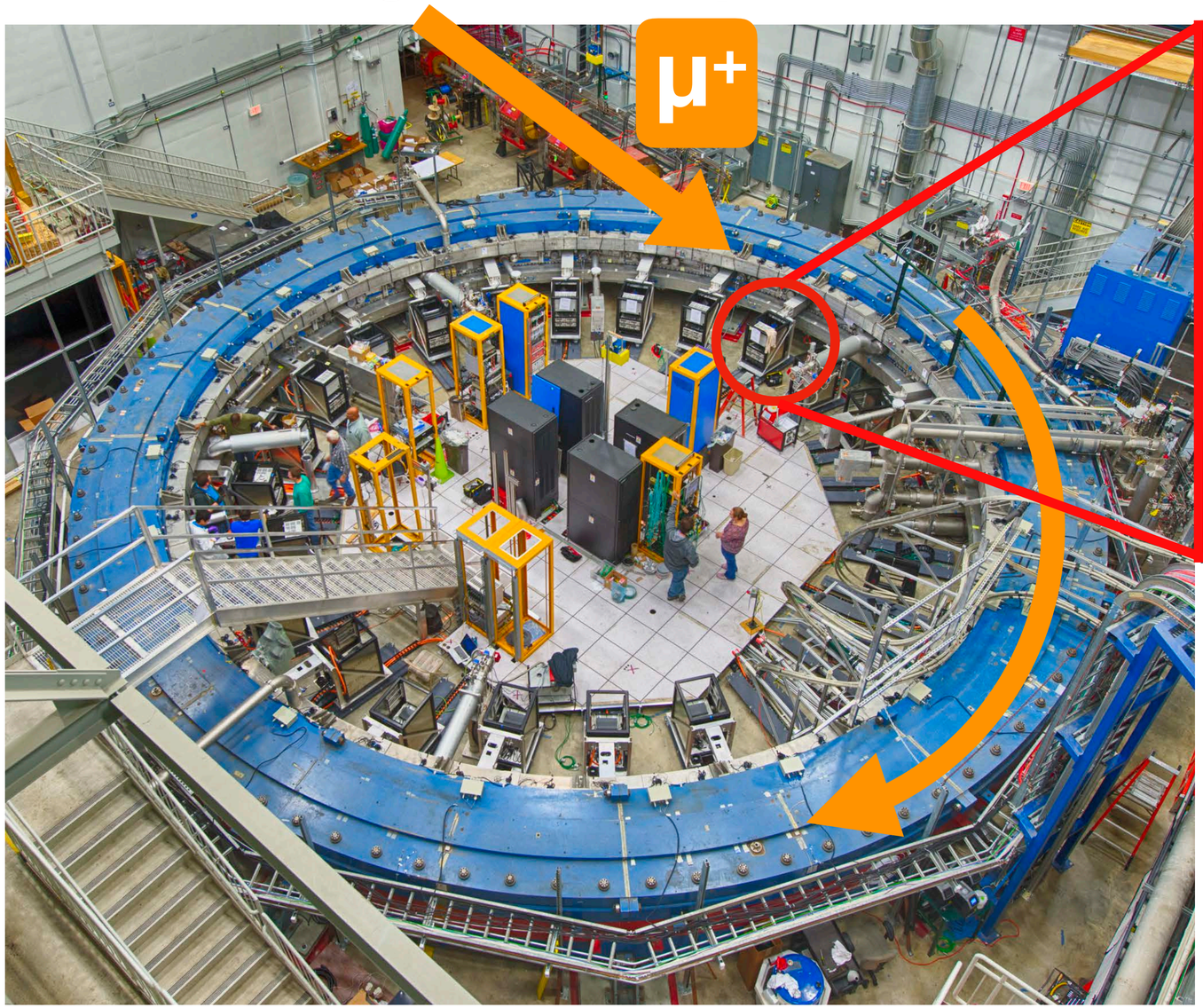

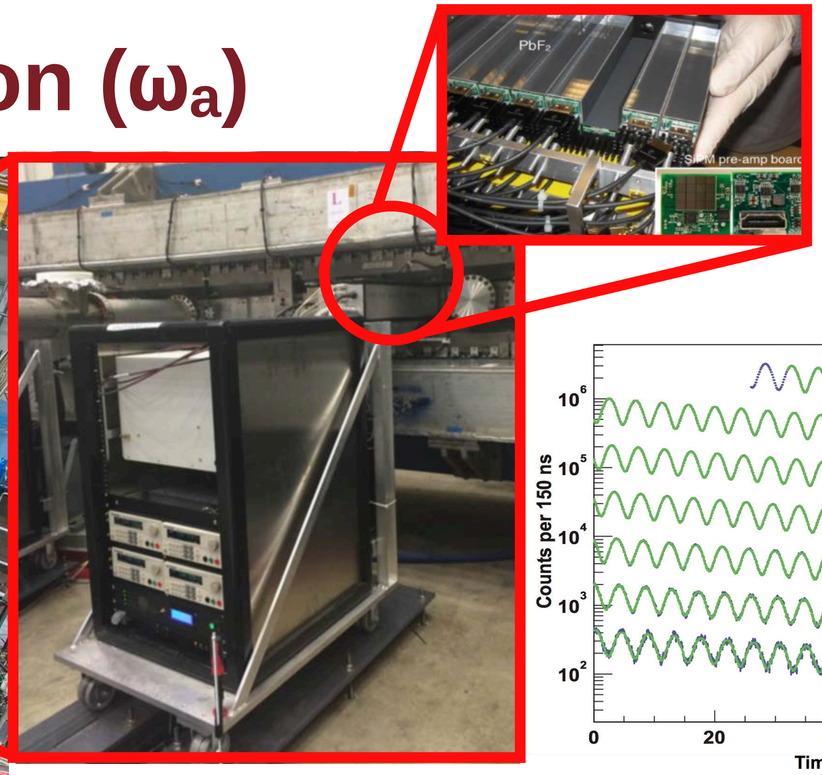

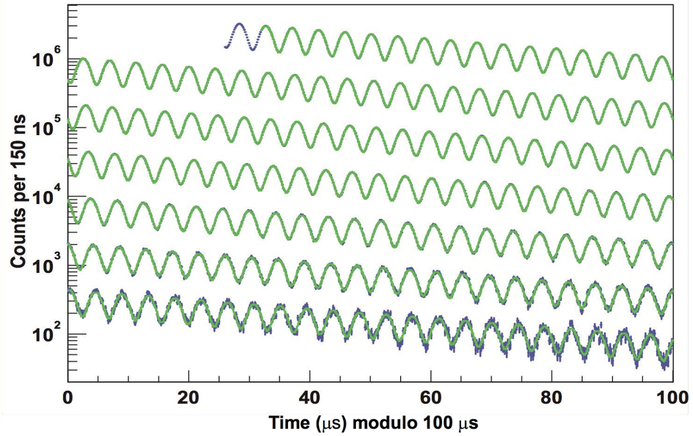

24 finely-segmented PbF_2 crystal calorimeters

- Self-analyzing decay: $\mu^+ \rightarrow e^+ \bar{\nu}_\mu \nu_e$
- Highest-energy e^+ emitted preferentially along muon spin
- Results in sinusoidally-oscillating arrival time of these e^+ in calorimeters

Measuring Muon Spin Precession (ω_a)

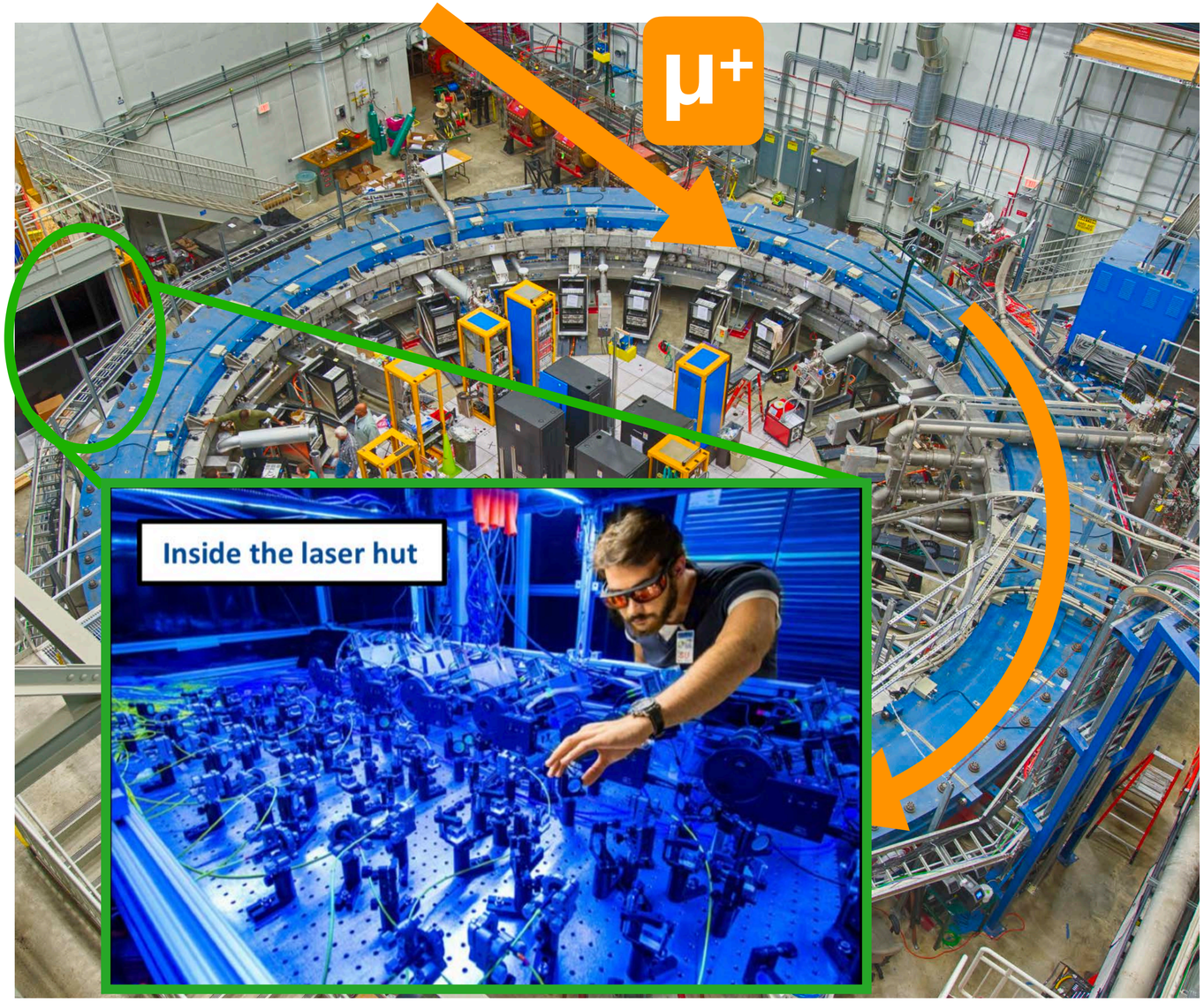

Laser System

- Calibrate calorimeter gain response throughout data taking
- Demonstrated stability to 10^{-4}/hr

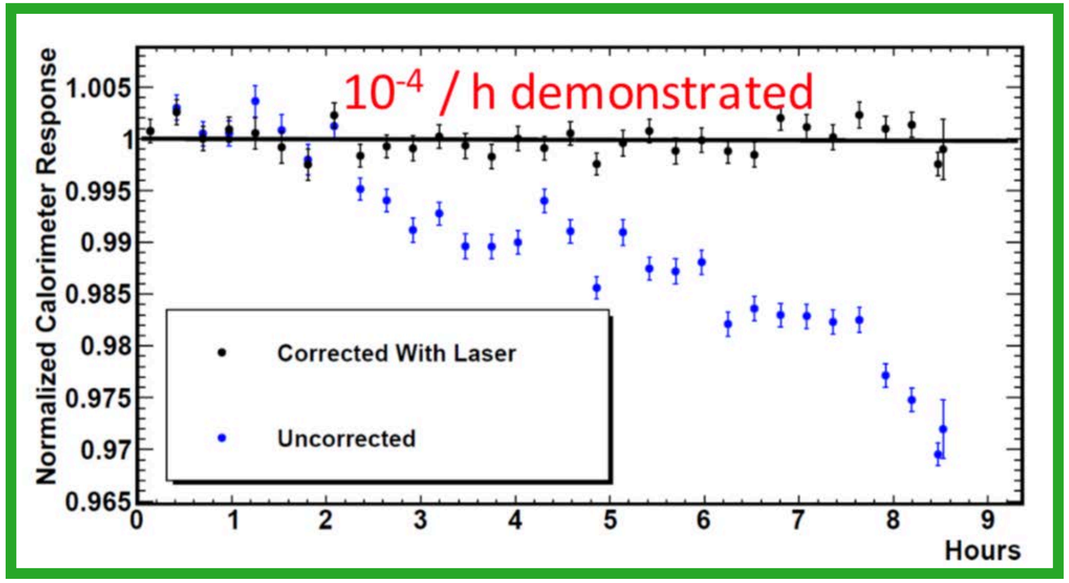

Measuring Muon Spin Precession (ω_a)

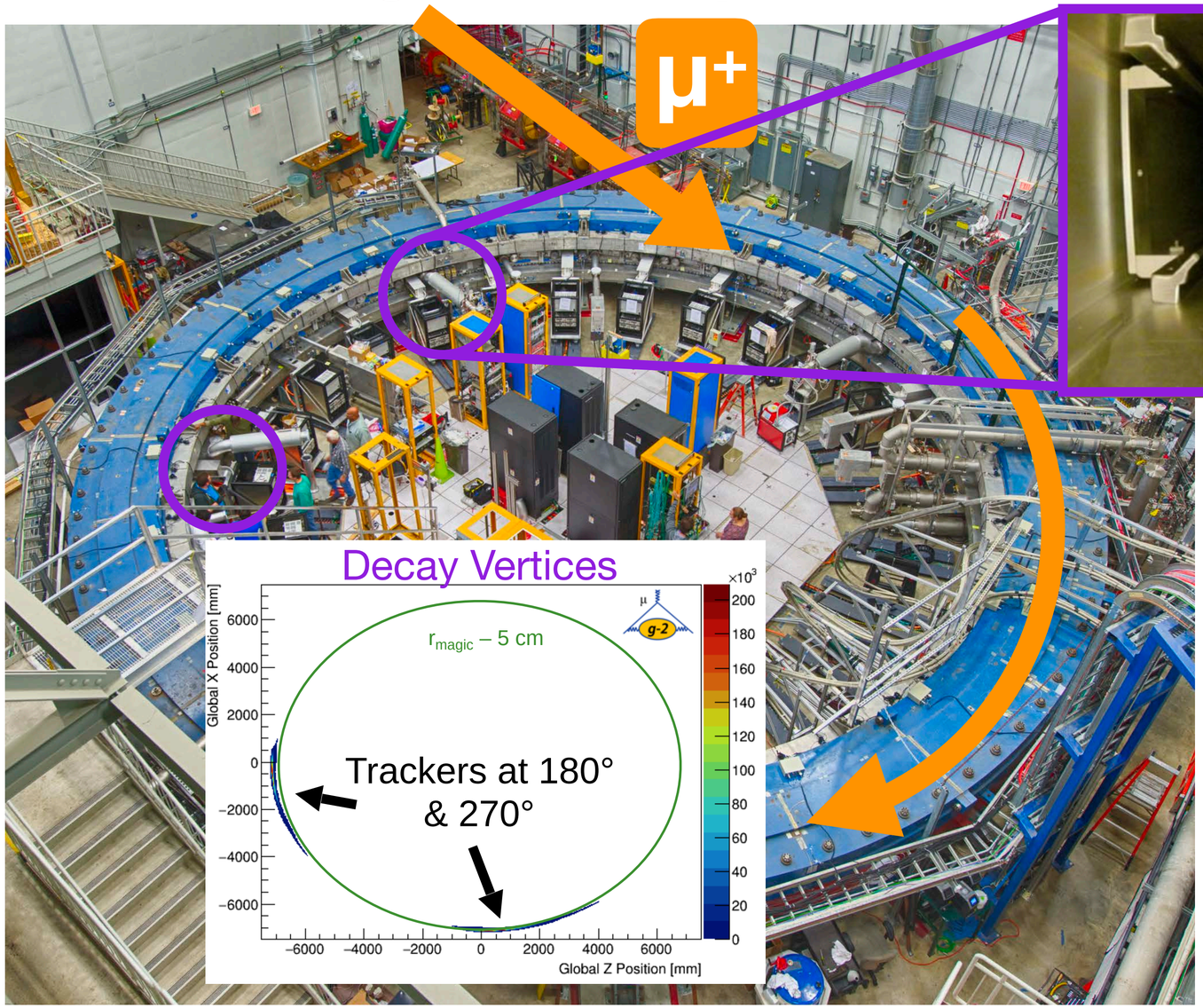

Muon's view of the storage region

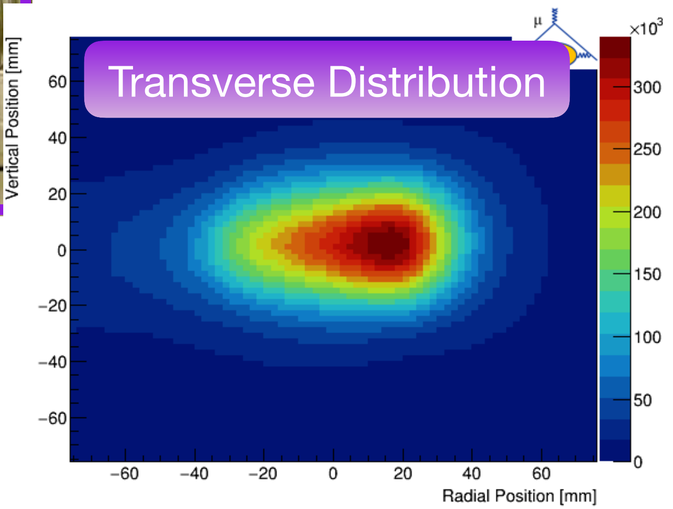

Two straw-tracker stations

- Reconstruct the muon beam distribution from e^+ hits
- Tracker module: 128 straws/module
- 8 modules per station

Magnet Anatomy

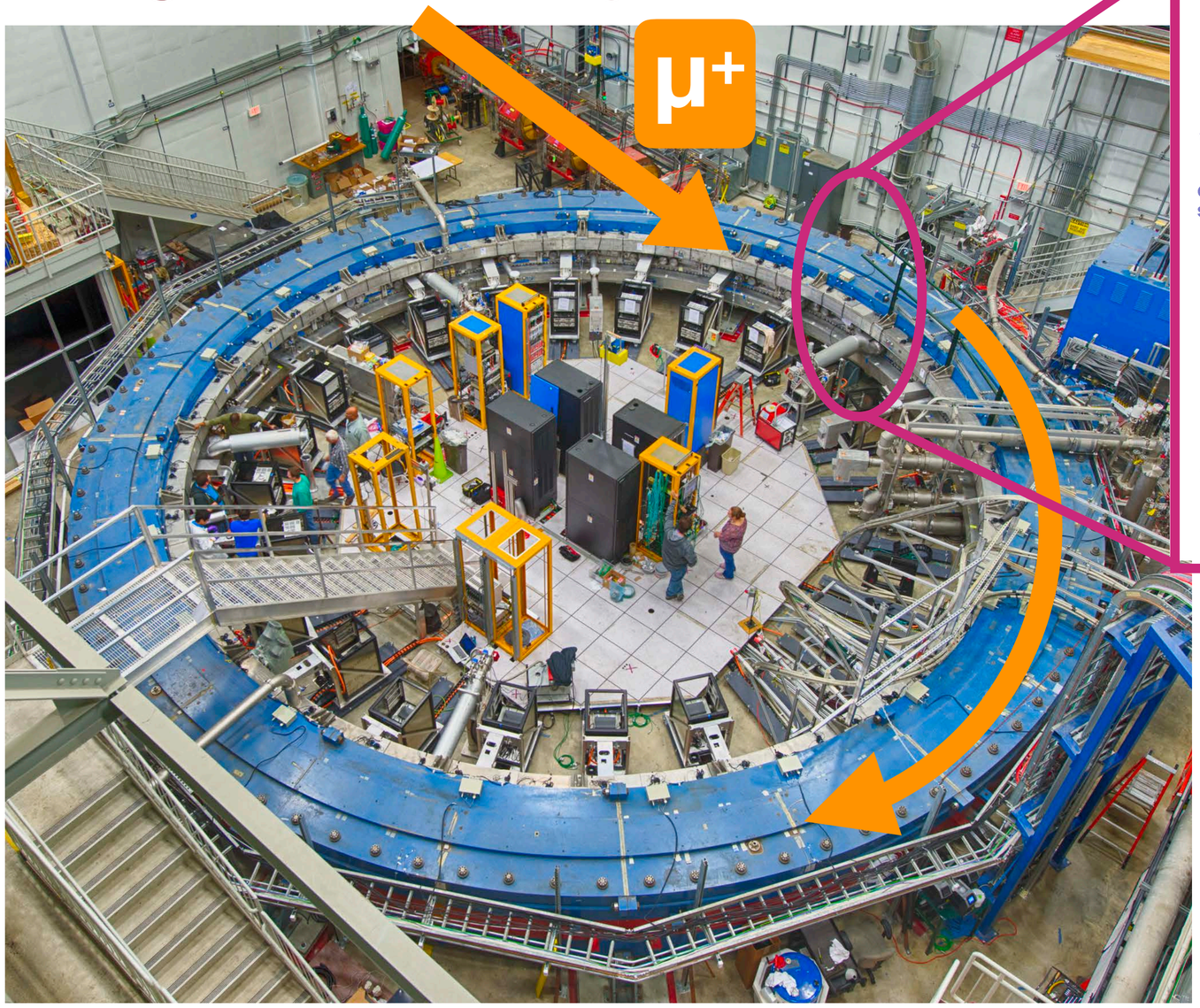

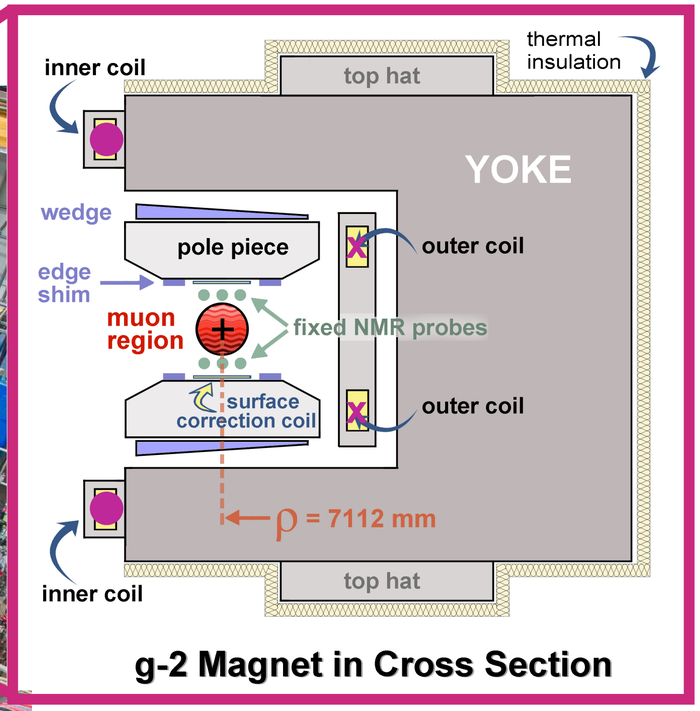

g-2 Magnet in Cross Section

Current direction indicated by ● and x

B = 1.45 T (~5200 A)

- Power supply with feedback to fine-tune field in real time

12 C-shaped yokes

- 3 upper and 3 lower poles per yoke
- 72 total poles

Field Shape

- Determined by positioning of pole pieces, wedge-shaped pieces of steel, programmable surface coils

UMassAmherst

Monitoring and Mapping the Magnetic Field

Pulsed NMR

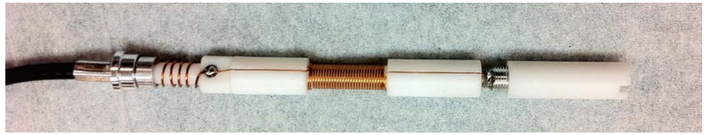

- Deliver π/2 pulse to probe, induce & record the free-induction decay (FID)
- Extracted frequency precision: 10 ppb/FID

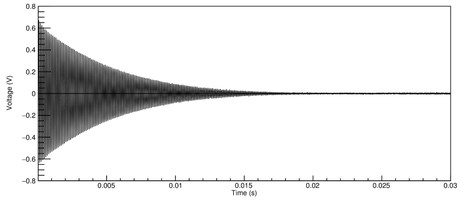

UMassAmherst

Monitoring and Mapping the Magnetic Field

Pulsed NMR

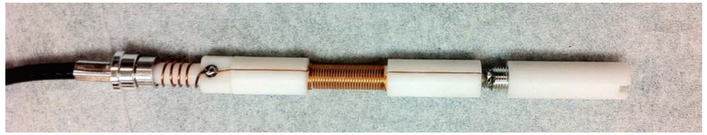

- Deliver π/2 pulse to probe, induce & record the free-induction decay (FID)
- Extracted frequency precision: 10 ppb/FID

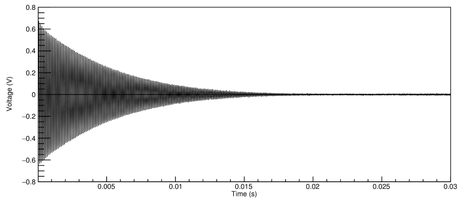

Fixed probes on vacuum chambers

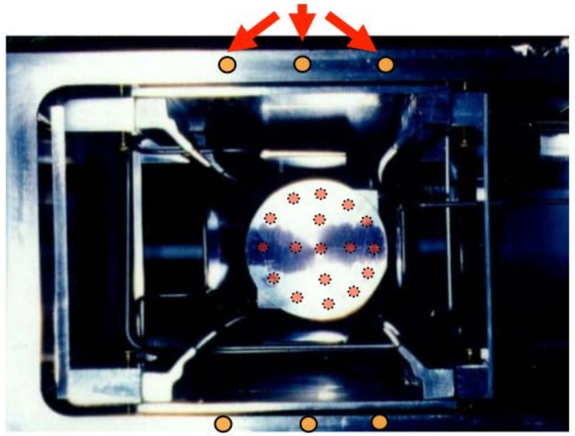

- Measure field while muons are in ring – 378 probes **outside** storage region

Trolley matrix of 17 NMR probes

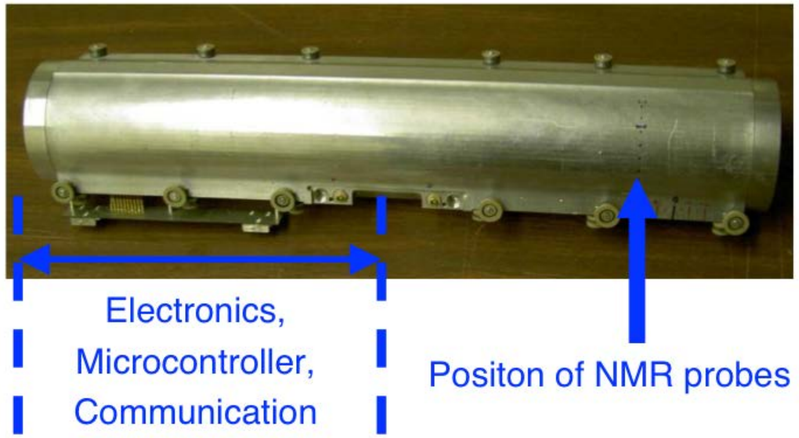

- Measure field in storage region during **specialized runs** when **muons are not being stored**

Monitoring and Mapping the Magnetic Field

Pulsed NMR

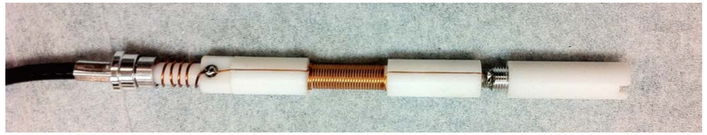

- Deliver π/2 pulse to probe, induce & record the free-induction decay (FID)
- Extracted frequency precision: 10 ppb/FID

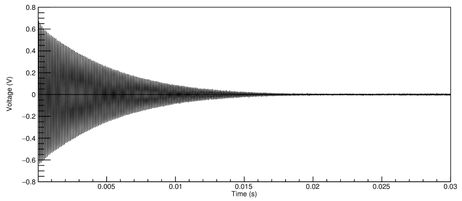

Fixed probes on vacuum chambers

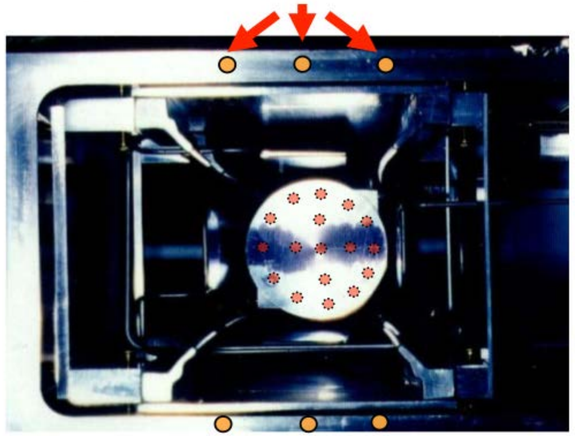

- Measure field while muons are in ring – 378 probes **outside** storage region

Trolley matrix of 17 NMR probes

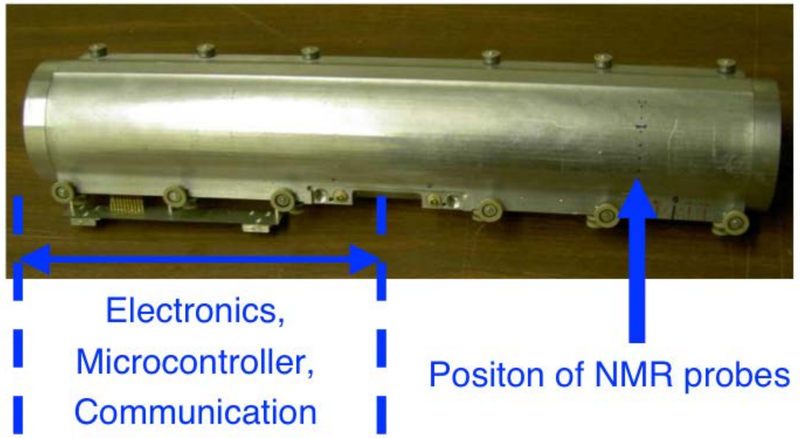

- Measure field in storage region during **specialized runs** when **muons are not being stored**

- **Trolley** probes **calibrated to free-proton Larmor frequency**
  - Calibrate trolley probes using a special probe that uses a water sample
  - Measurements in specially-shimmed region of ring

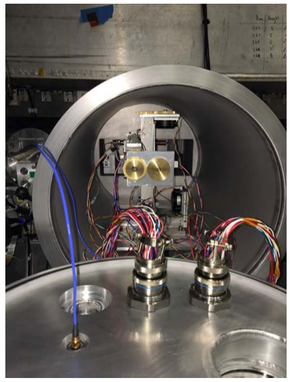

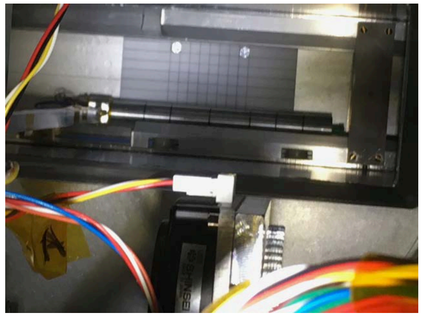

Plunging Probe

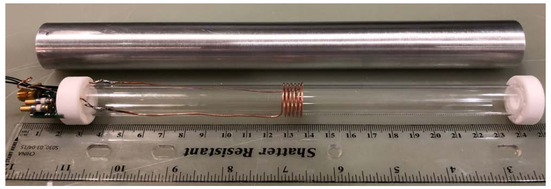

Systematic Uncertainty Comparison: E821 and E989

$$a_\mu = \frac{\omega_a}{\tilde{\omega}_p} \frac{\mu_p}{\mu_e} \frac{m_\mu}{m_e} \frac{g_e}{2}$$

- New hardware (calorimeters, trackers, NMR)
- Improved analysis techniques
- Reduce uncertainties by at least a factor of 2.5

ω_a Goal: Factor of 3 Improvement		
Category	**E821 (ppb)**	**E989 Goal (ppb)**
Gain Changes	120	20
Lost Muons	90	20
Pileup	80	40
Horizontal CBO	70	< 30
E-field/pitch	110	30
Quadrature Sum	**214**	**70**

ω_p Goal: Factor of 2.5 Improvement		
Category	**E821 (ppb)**	**E989 Goal (ppb)**
Field Calibration	50	35
Trolley Measurements	50	30
Fixed Probe Interpolation	70	30
Muon Convolution	30	10
Time-Dependent Fields	–	5
Others	100	50
Quadrature Sum	**170**	**70**

Run 1 Overview

- Data taking period: April—July 2018
- A number of changing conditions as we optimized hardware
- Accumulated ~ 1.1 x BNL statistics (after data quality cuts) — **$\delta\omega_a$(stat) ~ 410 ppb**
- Field uniformity ~ 2x better than BNL

Accumulated statistics

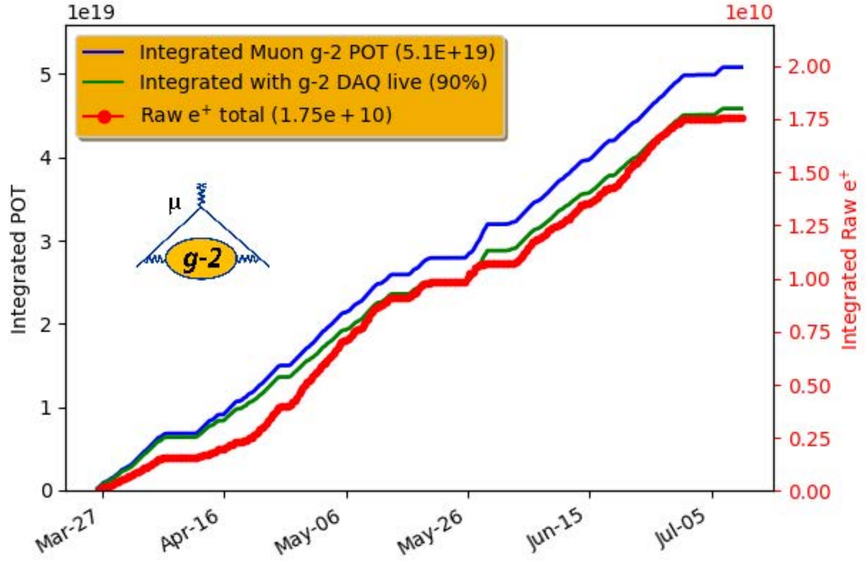

Typical Field Map

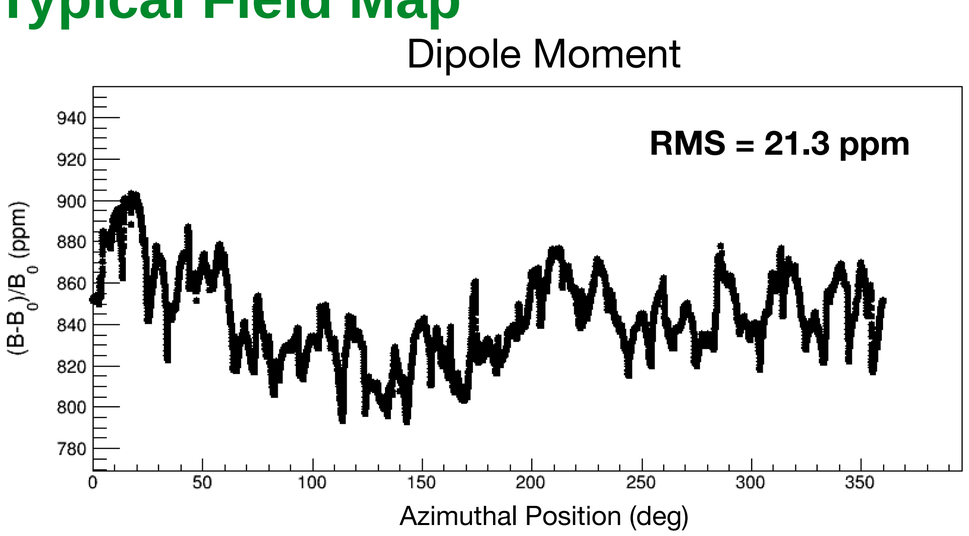

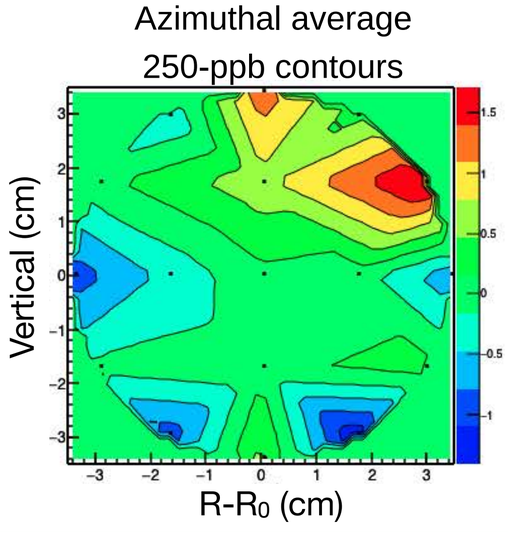

UMassAmherst

Run 2 Overview

- Data taking period: March—July 2019
- Contiguous data set
- Accumulated ~ 1.9 x BNL statistics (before data quality cuts)
- Field uniformity in very good condition

Accumulated statistics

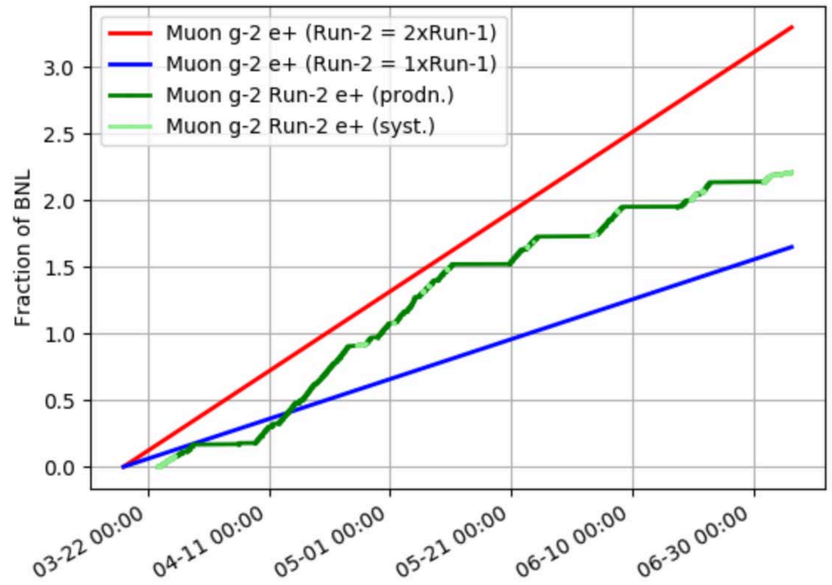

Typical Field Map

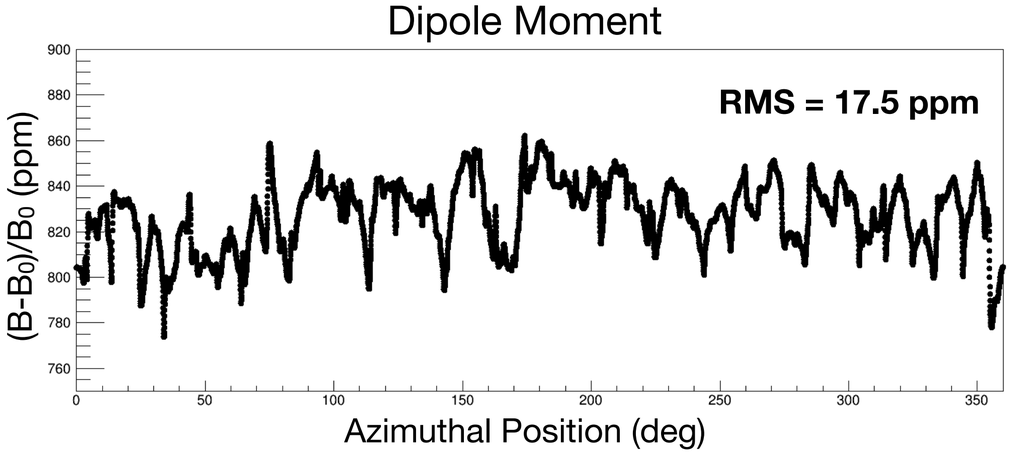

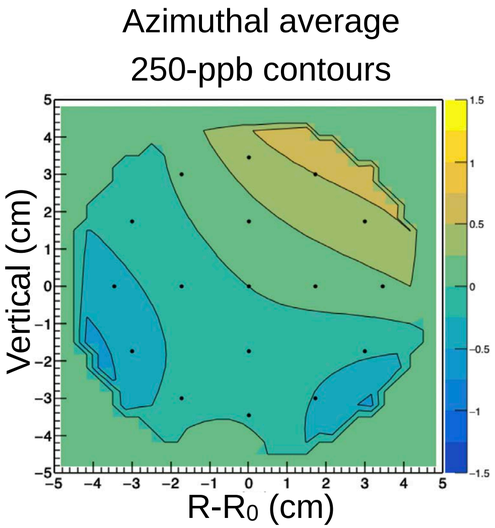

Run 3

- To start in mid-November
- Aim to **triple** statistics accumulated to date
- Direct continuation of Run 2

Run 1 Analysis Status — ω_a

$$a_\mu = \frac{\omega_a}{\tilde{\omega}_p} \frac{\mu_p}{\mu_e} \frac{m_\mu}{m_e} \frac{g_e}{2}$$

Run 1 Analysis Status: ω_a

- Account for a number of effects that can affect the extraction of ω_a

$$N(t) = N_0 e^{-t/\tau} \left[1 - A\cos\left(\omega_a t + \phi\right)\right]$$

Run 1 Analysis Status: ω_a

- Account for a number of effects that can affect the extraction of ω_a

$$N(t) = N_0 e^{-t/\tau} \left[1 - A \cos\left(\omega_a t + \phi\right)\right]$$

Detector effects

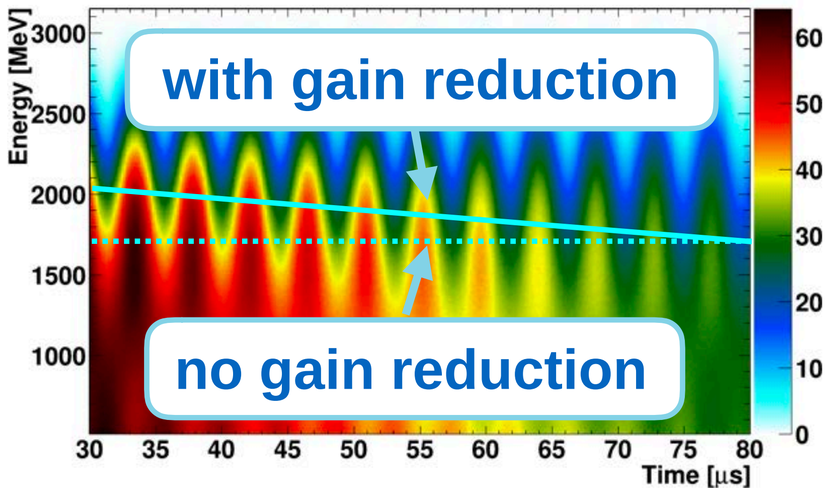

- Gain changes over time in calorimeters affects phase of signal: N → N(t), A → A(t), ϕ → ϕ(t)
- Laser system provides corrections

Run 1 Analysis Status: ω_a

- Account for a number of effects that can affect the extraction of ω_a

$$N(t) = N_0 e^{-t/\tau} \left[1 - A\cos\left(\omega_a t + \phi\right)\right]$$

Detector effects

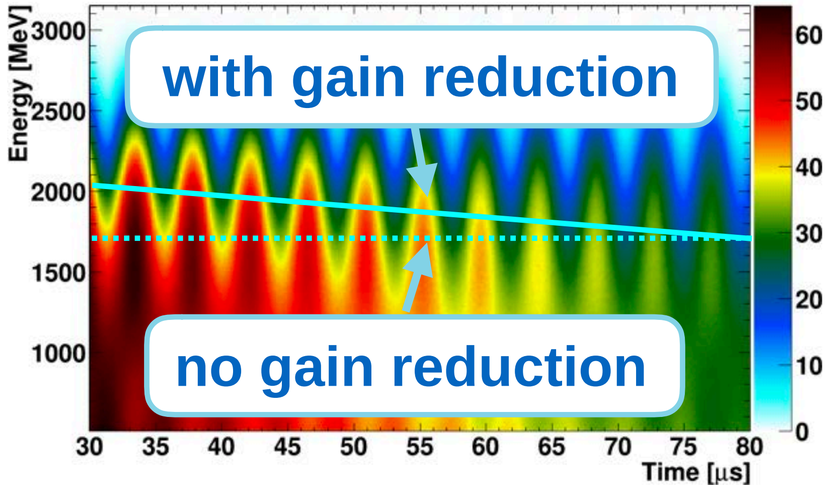

- Gain changes over time in calorimeters affects phase of signal: N → N(t), A → A(t), ϕ → ϕ(t)
- Laser system provides corrections

Event pileup

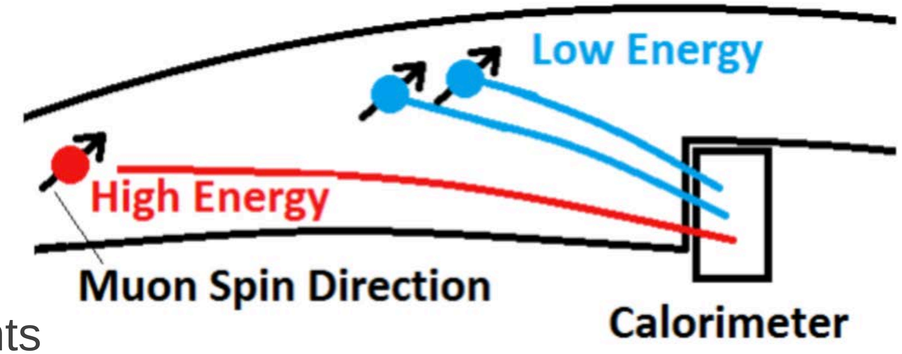

- Low-energy events can mimic high-energy events in calorimeter
- Spin precession phase varies with energy — apparent high-energy decay carries phase of low-energy decays

Run 1 Analysis Status: ω_a

- Account for a number of effects that can affect the extraction of ω_a

$$N(t) = N_0 e^{-t/\tau} \left[1 - A\cos\left(\omega_a t + \phi\right)\right]$$

Beam dynamics

Muon losses

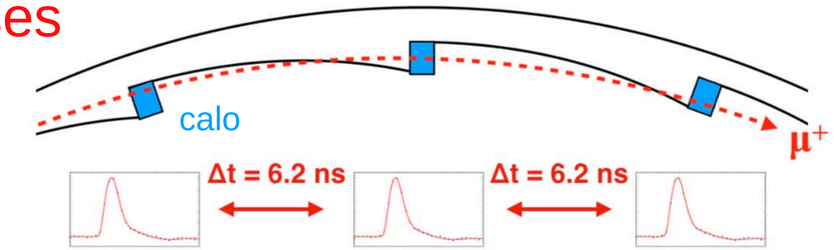

- Muons can leave storage ring by decaying or escaping
- Exhibit specific signature in multiple calorimeters
- Amplitude N_0 scaled by:

$$\Lambda(t) = 1 - K_{\text{loss}} \int_0^t e^{t'/\tau} L(t') dt'$$

Run 1 Analysis Status: ω_a

- Account for a number of effects that can affect the extraction of ω_a

$$N(t) = N_0 e^{-t/\tau} \left[1 - A\cos\left(\omega_a t + \phi\right)\right]$$

Beam dynamics

Muon losses

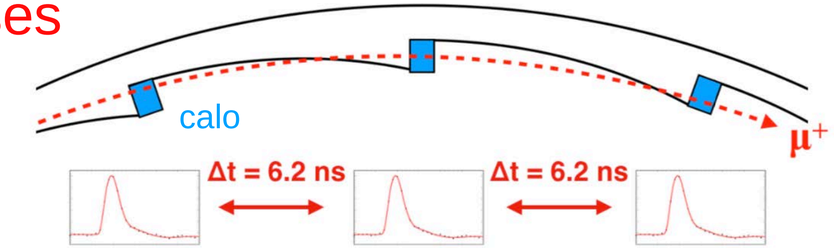

- Muons can leave storage ring by decaying or escaping
- Exhibit specific signature in multiple calorimeters
- Amplitude N_0 scaled by:

$$\Lambda(t) = 1 - K_{\text{loss}} \int_0^t e^{t'/\tau} L(t') dt'$$

Coherent betatron oscillations (CBO)

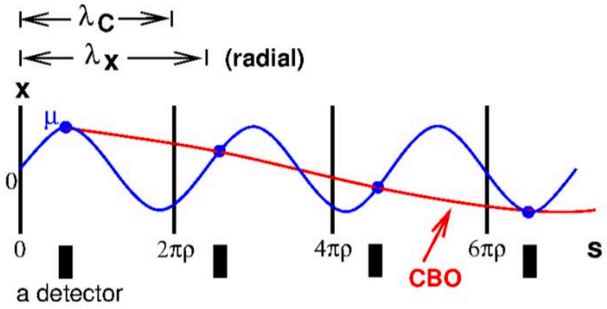

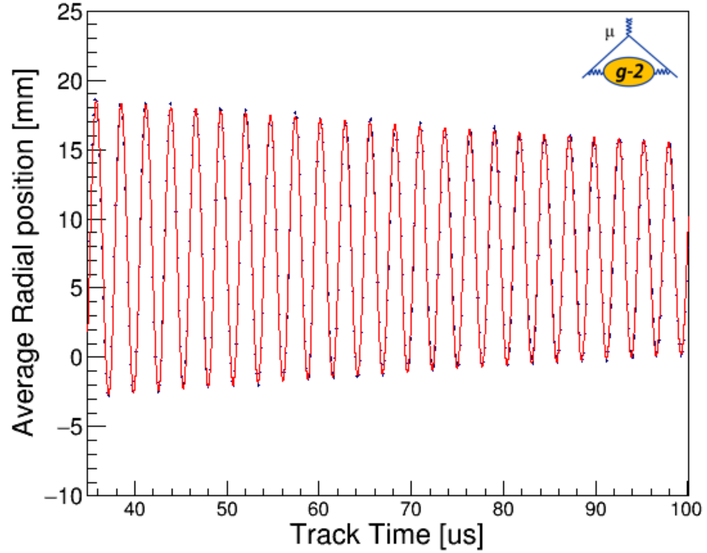

- Acceptance of calorimeters affected by coherent radial beam motion
- Amplitude N_0 scaled by:

$$C(t) = 1 - e^{-t/\tau_{\text{CBO}}} A_1 \cos\left(\omega_{\text{CBO}} t + \phi_1\right)$$

Run 1 Analysis Status: ω_a

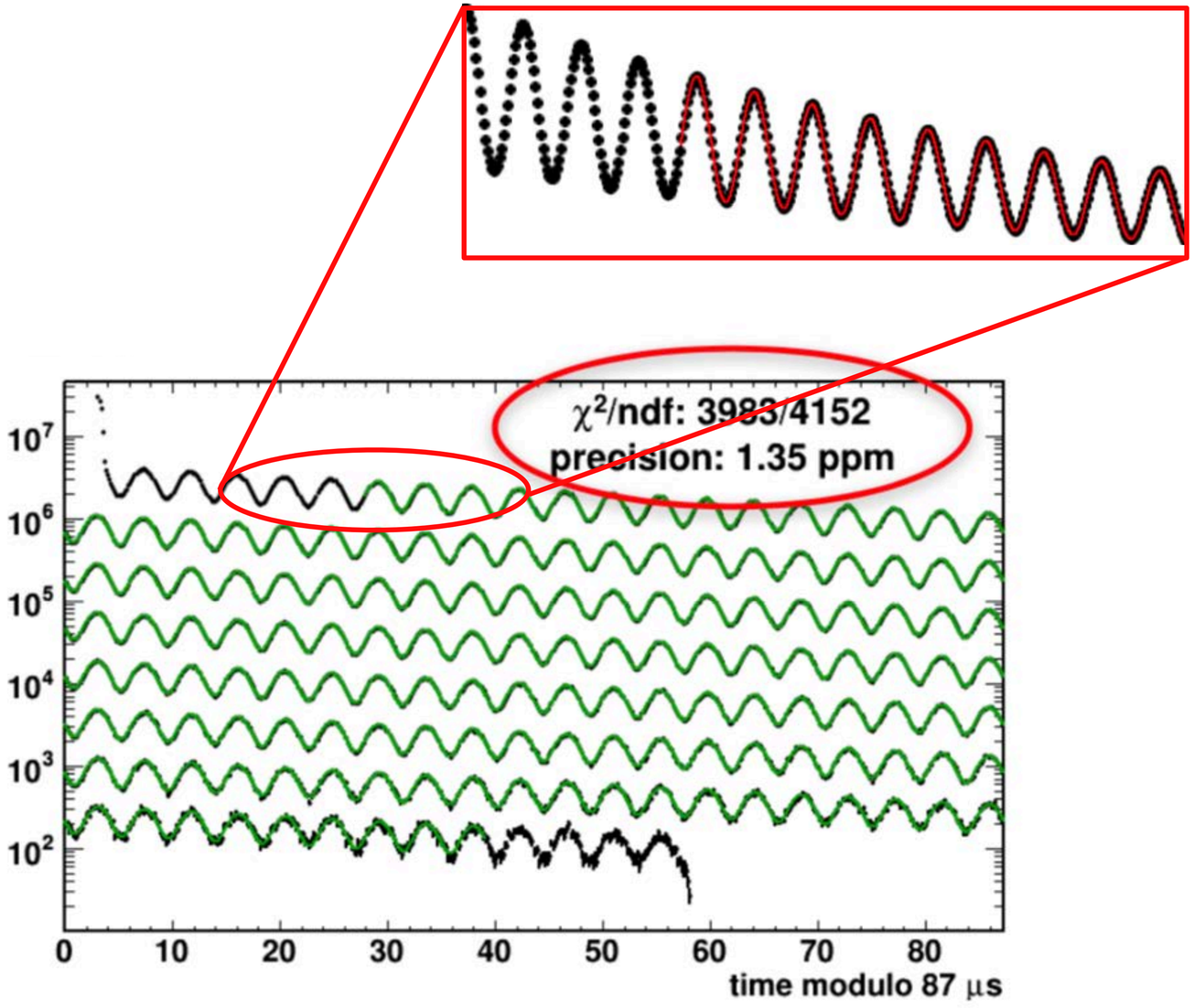

Simple five-parameter fit

FFT of fit residuals

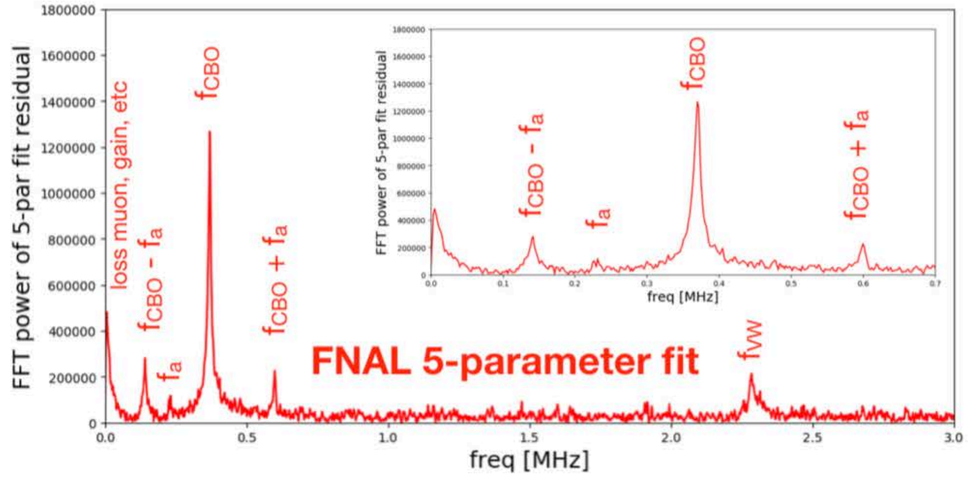

Run 1 Analysis Status: ω_a

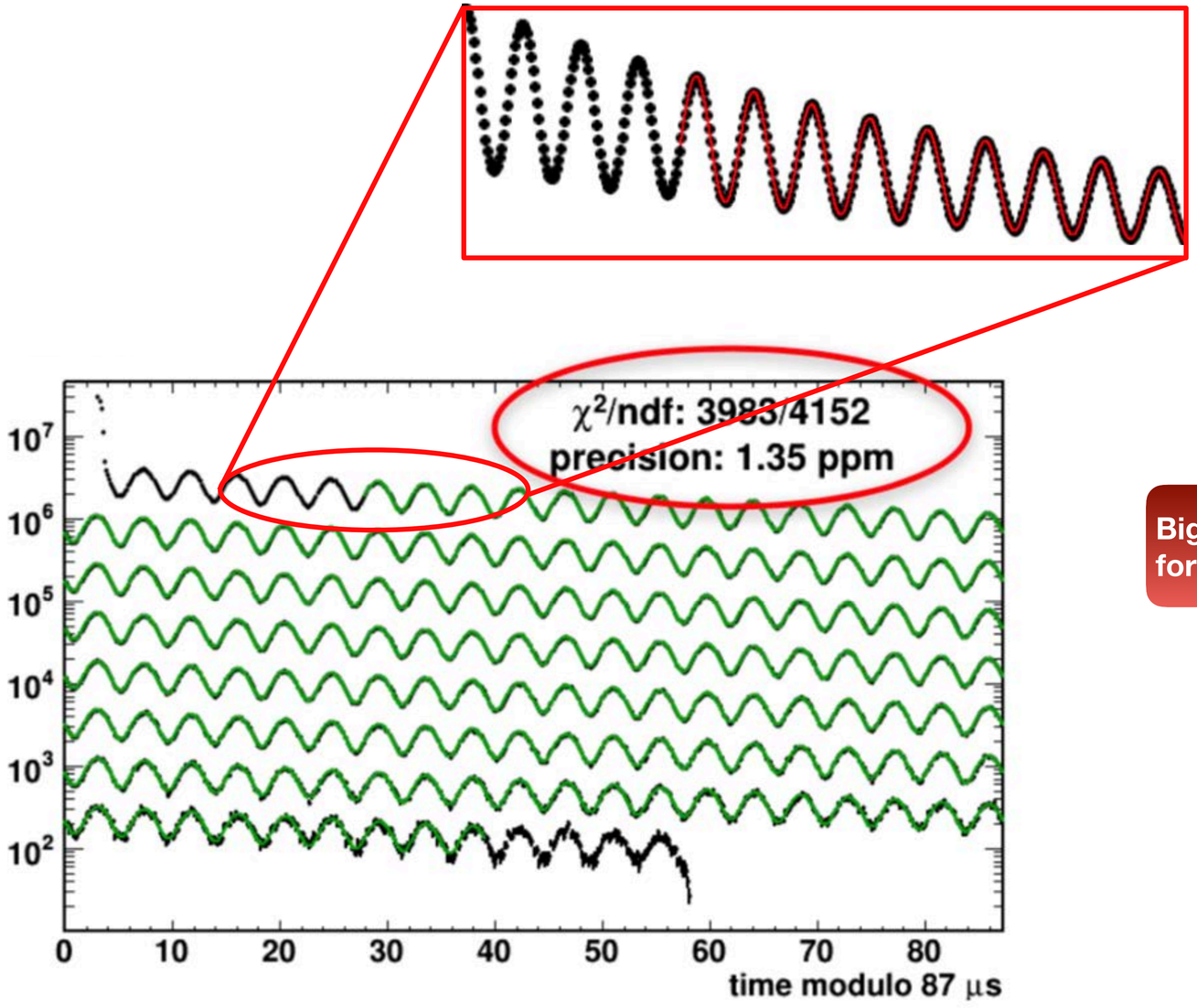

Simple five-parameter fit

FFT of fit residuals

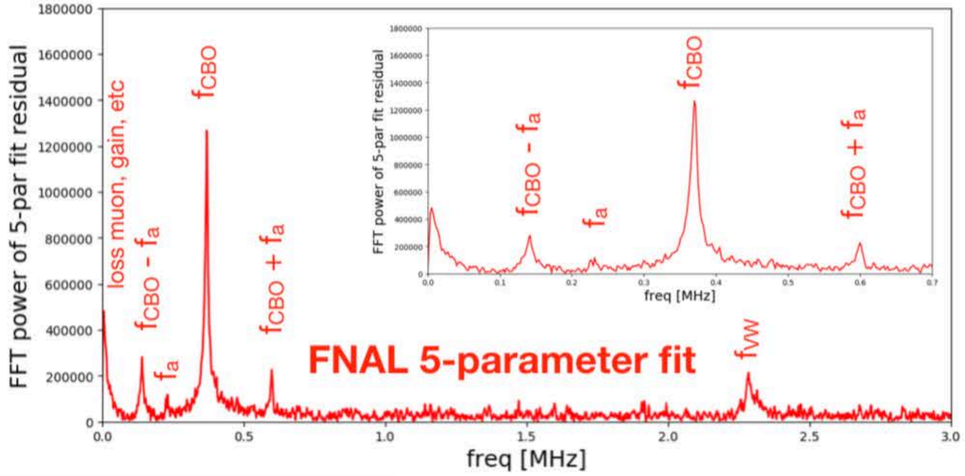

Big improvements when accounting for CBO, lost muons,…

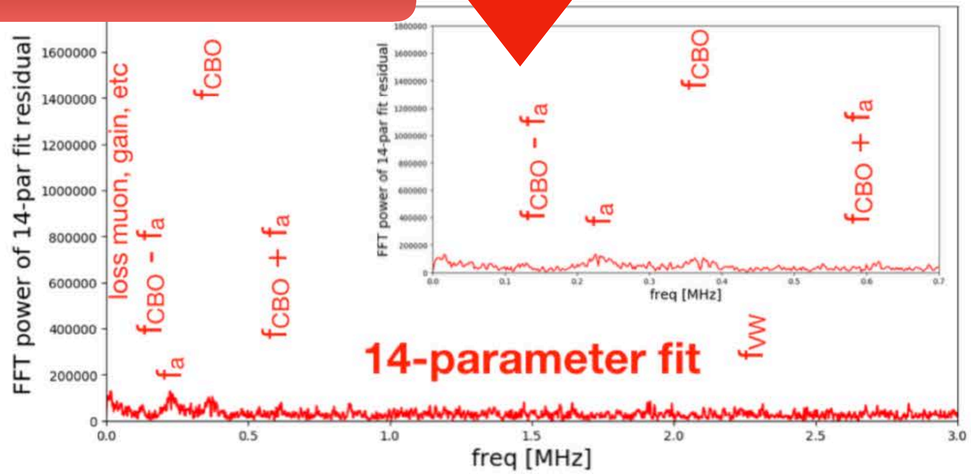

UMassAmherst

Run 1 Analysis Status: ω_a

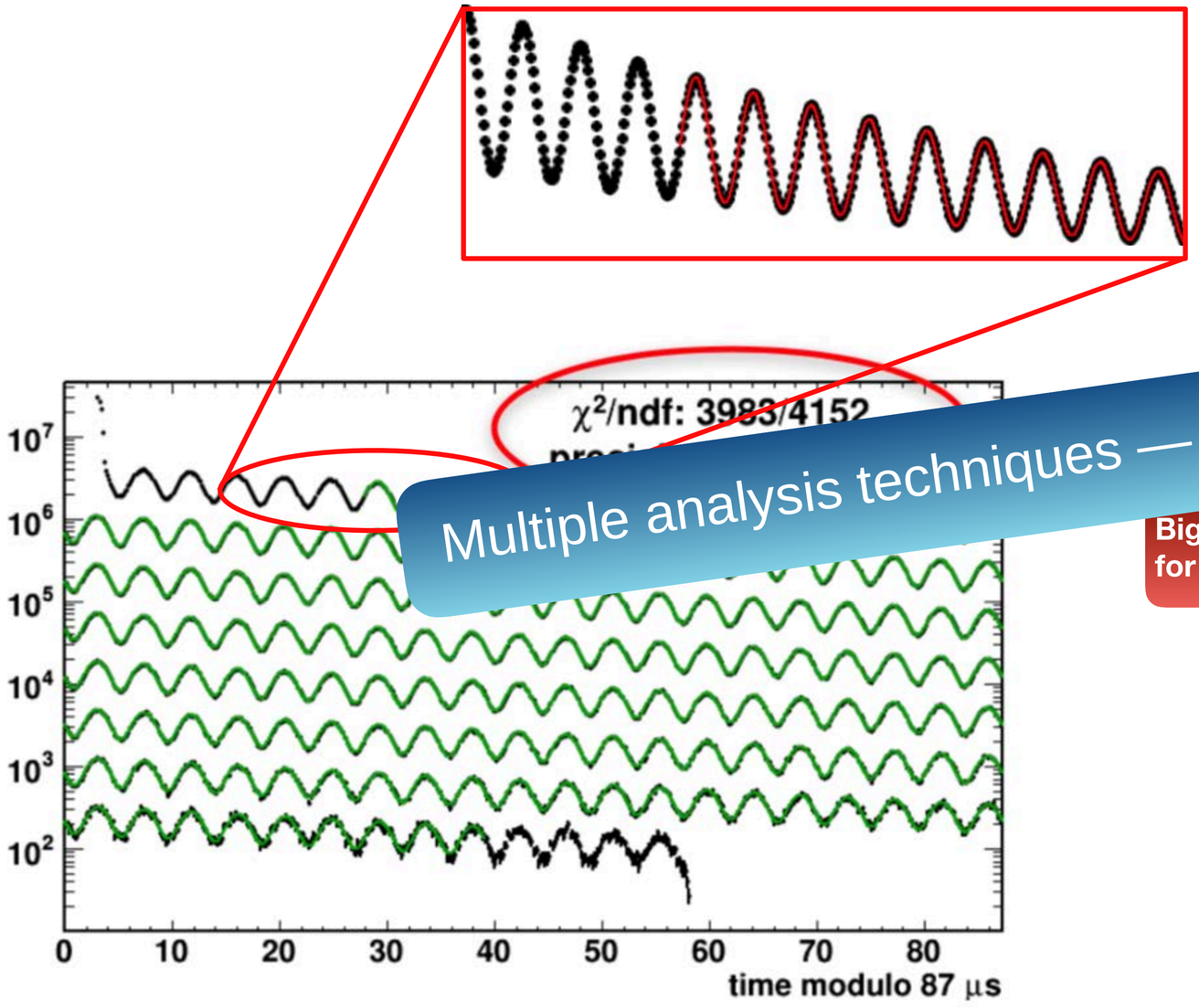

Simple five-parameter fit

FFT of fit residuals

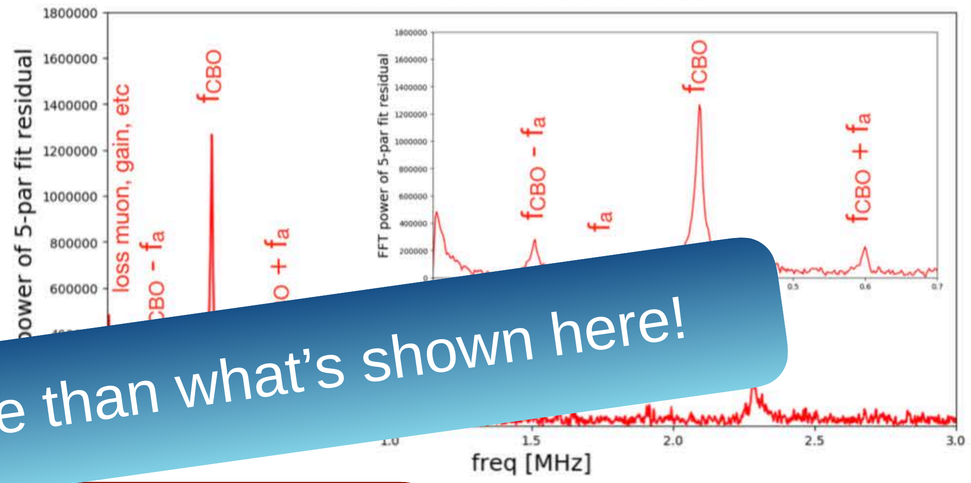

Multiple analysis techniques — more than what's shown here!

Big improvements when accounting for CBO, lost muons,…

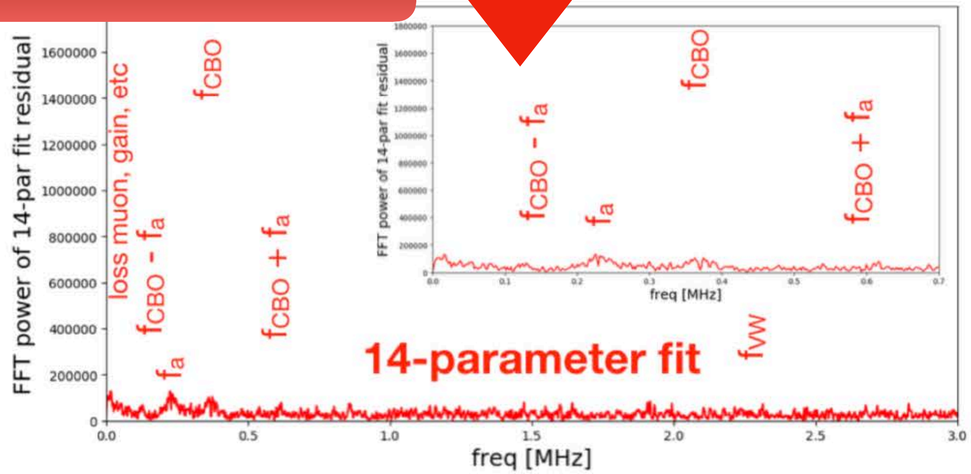

UMassAmherst

Run 1 Analysis Status: Relative Unblinding for ω_a

- Doubly-blinded in ω_a measurement: Clock tuned to 40 MHz ± 25 ppm
- Analyzers' results come with random frequency offset $\omega_a \rightarrow \omega_a \pm 25$ ppm
- Recently compared results on **subset of data** at a **common blinded value**

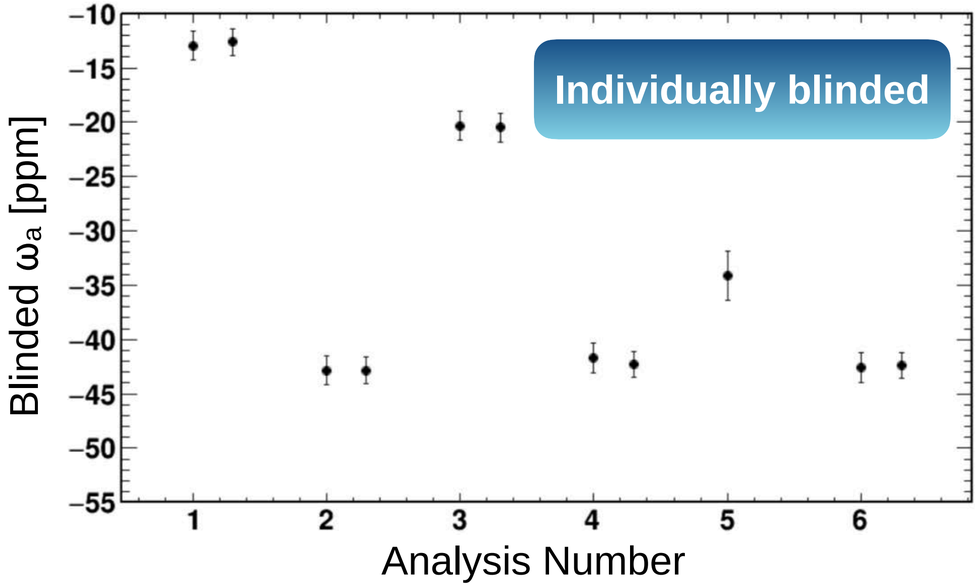

Run 1 Analysis Status: Relative Unblinding for ω_a

- Doubly-blinded in ω_a measurement: Clock tuned to 40 MHz ± 25 ppm
- Analyzers' results come with random frequency offset $\omega_a \rightarrow \omega_a \pm 25$ ppm
- Recently compared results on **subset of data** at a **common blinded value**

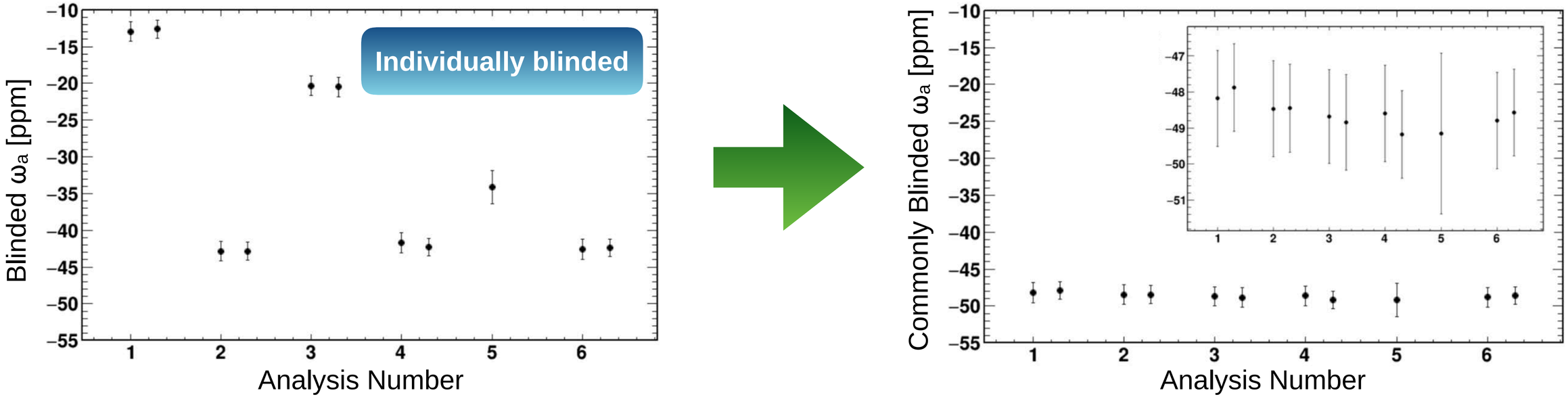

- Consistent results at **common blinded value** builds confidence in our analyses

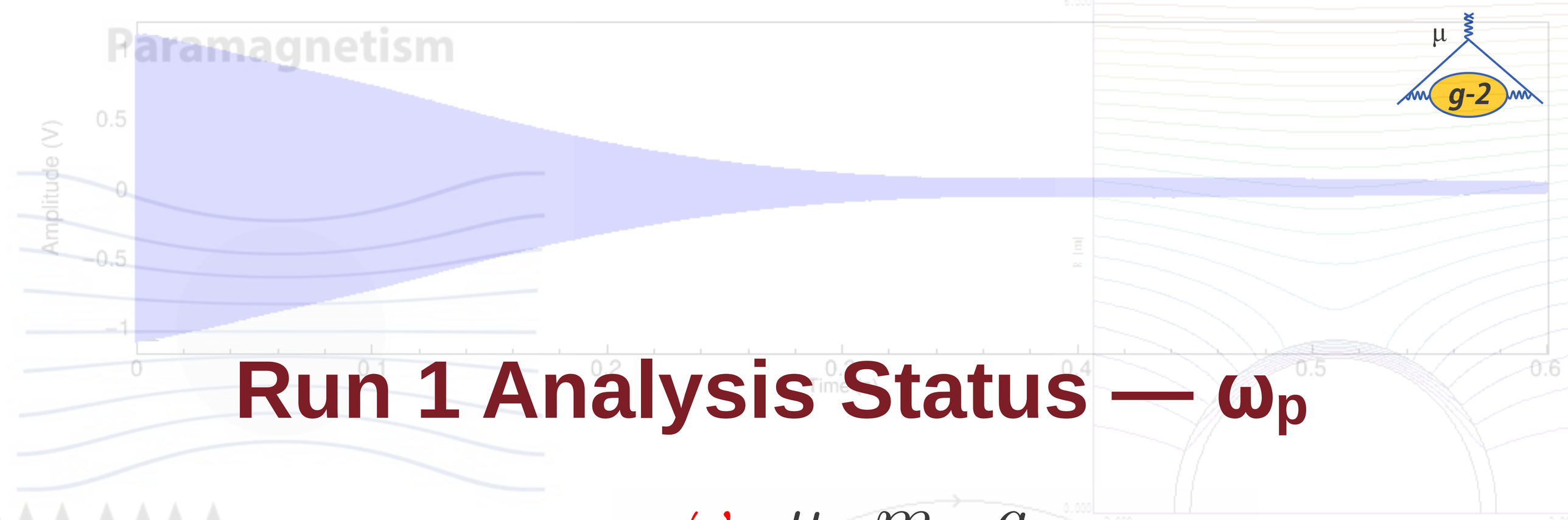

Run 1 Analysis Status — ω_p

$$a_\mu = \frac{\omega_a}{\tilde{\omega}_p} \frac{\mu_p}{\mu_e} \frac{m_\mu}{m_e} \frac{g_e}{2}$$

Run 1 Analysis Status: ω_p — Field Calibration

- In the experiment, need to extract ω_p; however, don't have free protons
  - Need a calibration
- Field at the proton differs from the applied field

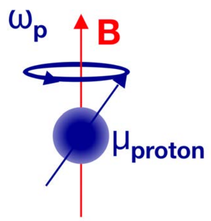

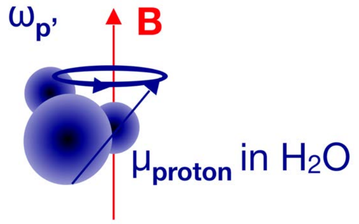

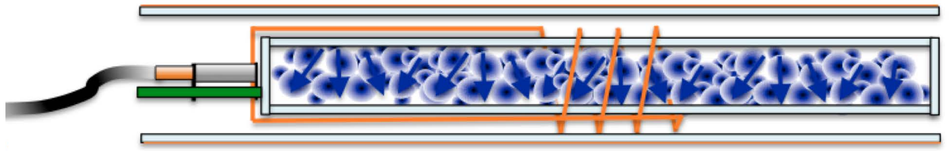

$$\omega_p^{\mathrm{meas}} \approx \omega_p^{\mathrm{free}}$$

Run 1 Analysis Status: ω_p — Field Calibration

- In the experiment, need to extract ω_p; however, don't have free protons
  - Need a calibration
- Field at the proton differs from the applied field

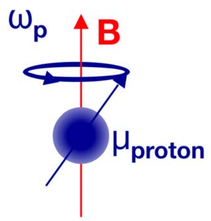

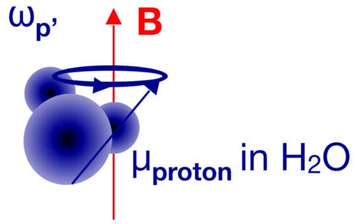

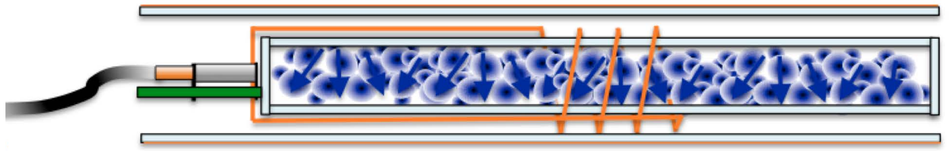

$$\omega_p^{\mathrm{meas}} = \omega_p^{\mathrm{free}} \left[1 - \sigma\left(\mathrm{H_2O}, T\right) \right.$$

Protons in H_2O molecules, diamagnetism of electrons screens protons => local B changes

- σ = 25 691(11) x 10^{-9} at 25 deg C [P.J. Mohr et al, Rev. Mod. Phys. **84**, 1527 (2012)]

Run 1 Analysis Status: ω_p — Field Calibration

- In the experiment, need to extract ω_p; however, don't have free protons
  - Need a calibration
- Field at the proton differs from the applied field

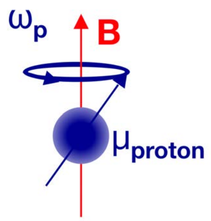

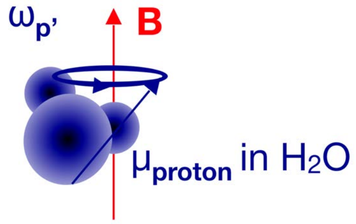

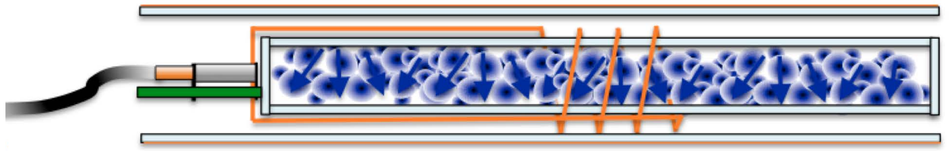

$$\omega_p^{\mathrm{meas}} = \omega_p^{\mathrm{free}} \left[1 - \sigma\left(\mathrm{H_2O}, T\right) - \left(\frac{\varepsilon}{4\pi} - \frac{1}{3} \right) \chi\left(\mathrm{H_2O}, T\right) \right.$$

Protons in H_2O molecules, diamagnetism of electrons screens protons => local B changes

- σ = 25 691(11) x 10^{-9} at 25 deg C [P.J. Mohr et al, Rev. Mod. Phys. **84**, 1527 (2012)]

Magnetic susceptibility of water gives shape-dependent perturbation

- $\varepsilon = 4\pi/3$ (perfect sphere)
- $\varepsilon = 2\pi$ (infinite cylinder) when probe is perpendicular to B
- χ_{H_2O}(T = 20°C) = -9049(9) x 10^{-9} [world average]

Run 1 Analysis Status: ω_p — Field Calibration

- In the experiment, need to extract ω_p; however, don't have free protons
  - Need a calibration
- Field at the proton differs from the applied field

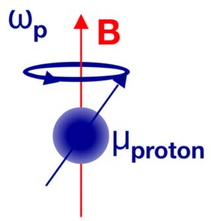

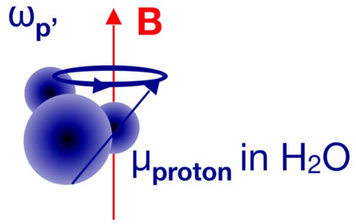

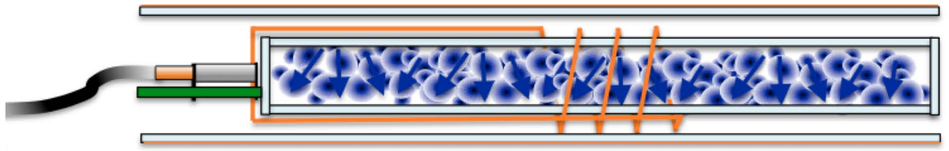

$$\omega_p^{\mathrm{meas}} = \omega_p^{\mathrm{free}} \left[1 - \sigma\left(\mathrm{H_2O}, T\right) - \left(\frac{\varepsilon}{4\pi} - \frac{1}{3} \right) \chi\left(\mathrm{H_2O}, T\right) - \delta_s \right.$$

Protons in H_2O molecules, diamagnetism of electrons screens protons => local B changes

- σ = 25 691(11) x 10^{-9} at 25 deg C [P.J. Mohr et al, Rev. Mod. Phys. **84**, 1527 (2012)]

Magnetic susceptibility of water gives shape-dependent perturbation

- $\varepsilon = 4\pi/3$ (perfect sphere)
- $\varepsilon = 2\pi$ (infinite cylinder) when probe is perpendicular to B
- χ_{H_2O}(T = 20°C) = -9049(9) x 10^{-9} [world average]

Magnetization of probe materials, geometry perturbs field experienced by protons

Run 1 Analysis Status: ω_p — Field Calibration

- In the experiment, need to extract ω_p; however, don't have free protons
  - Need a calibration
- Field at the proton differs from the applied field

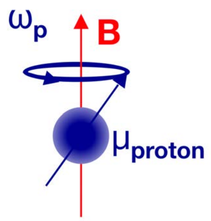

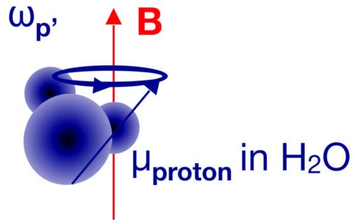

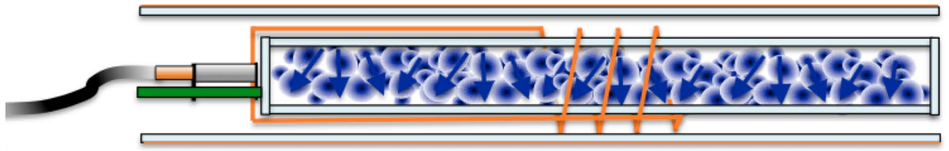

paramagnetic impurities in water sample

$$\omega_p^{\mathrm{meas}} = \omega_p^{\mathrm{free}} \left[1 - \sigma\left(\mathrm{H_2O}, T\right) - \left(\frac{\varepsilon}{4\pi} - \frac{1}{3} \right) \chi\left(\mathrm{H_2O}, T\right) - \delta_s - \delta_p \right.$$

Protons in H_2O molecules, diamagnetism of electrons screens protons => local B changes

- σ = 25 691(11) x 10^{-9} at 25 deg C [P.J. Mohr et al, Rev. Mod. Phys. **84**, 1527 (2012)]

Magnetic susceptibility of water gives shape-dependent perturbation

- $\varepsilon = 4\pi/3$ (perfect sphere)
- $\varepsilon = 2\pi$ (infinite cylinder) when probe is perpendicular to B
- $\chi_{H_2O}(T = 20°C)$ = -9049(9) x 10^{-9} [world average]

Magnetization of probe materials, geometry perturbs field experienced by protons

Run 1 Analysis Status: ω_p — Field Calibration

- In the experiment, need to extract ω_p; however, don't have free protons
  - Need a calibration
- Field at the proton differs from the applied field

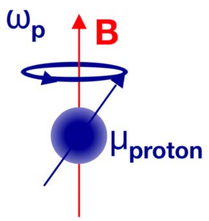

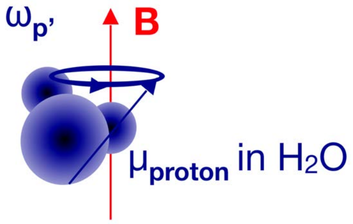

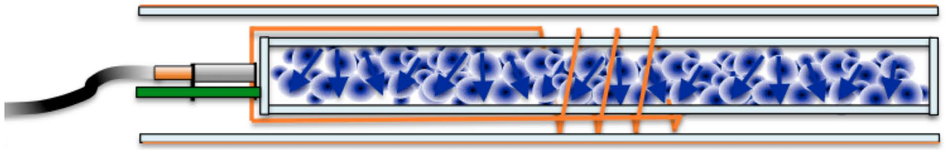

paramagnetic impurities in water sample

$$\omega_p^{\mathrm{meas}} = \omega_p^{\mathrm{free}} \left[1 - \sigma\left(\mathrm{H_2O}, T\right) - \left(\frac{\varepsilon}{4\pi} - \frac{1}{3} \right) \chi\left(\mathrm{H_2O}, T\right) - \delta_s - \delta_p - \delta_{\mathrm{RD}} - \delta_d \right]$$

Protons in H_2O molecules, diamagnetism of electrons screens protons => local B changes

- σ = 25 691(11) x 10^{-9} at 25 deg C [P.J. Mohr et al, Rev. Mod. Phys. **84**, 1527 (2012)]

Magnetic susceptibility of water gives shape-dependent perturbation

- $\varepsilon = 4\pi/3$ (perfect sphere)
- $\varepsilon = 2\pi$ (infinite cylinder) when probe is perpendicular to B
- $\chi_{H_2O}(T = 20°C)$ = -9049(9) x 10^{-9} [world average]

Magnetization of probe materials, geometry perturbs field experienced by protons

Dynamic effects: radiation damping, dipolar field from protons

Run 1 Analysis Status: ω_p — Field Calibration

- In the experiment, need to extract ω_p; however, don't have free protons
  - Need a calibration
- Field at the proton differs from the applied field

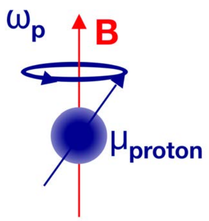

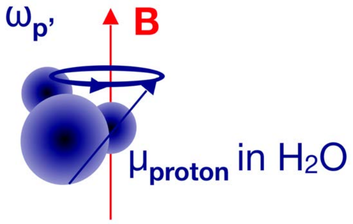

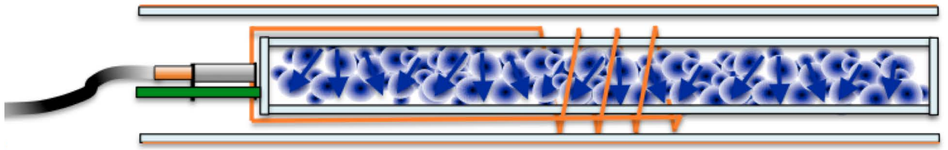

paramagnetic impurities in water sample

$$\omega_p^{\mathrm{meas}} = \omega_p^{\mathrm{free}} \left[1 - \sigma\left(\mathrm{H_2O}, T\right) - \left(\frac{\varepsilon}{4\pi} - \frac{1}{3} \right) \chi\left(\mathrm{H_2O}, T\right) - \delta_s - \delta_p - \delta_{\mathrm{RD}} - \delta_d \right]$$

Protons in H_2O molecules, diamagnetism of electrons screens protons => local B changes

- σ = 25 691(11) x 10^{-9} at 25 deg C [P.J. Mohr et al, Rev. Mod. Phys. **84**, 1527 (2012)]

Magnetic susceptibility of water gives shape-dependent perturbation

- $\varepsilon = 4\pi/3$ (perfect sphere)
- $\varepsilon = 2\pi$ (infinite cylinder) when probe is perpendicular to B
- $\chi_{H_2O}(T = 20°C)$ = -9049(9) x 10^{-9} [world average]

Magnetization of probe materials, geometry perturbs field experienced by protons

Dynamic effects: radiation damping, dipolar field from protons

Goal: Determine total correction to ≤ 35 ppb accuracy

Run 1 Analysis Status: ω_p — Field Calibration

Plunging Probe

- Achieved **small perturbation of plunging probe ($\delta_s + \delta_p + \delta_{RD} + \delta_d$): (-0.2 ± 11.4) ppb**
- Quantified uncertainties on plunging probe material, dynamic effects — **under budget of 35 ppb by a factor of > 2**

Plunging Probe Perturbations		
Quantity	**Symbol**	**Uncertainty (ppb)**
Material Perturbation	δ_s	10.9
Paramagnetic Impurities	δ_p	1.1
Radiation Damping	δ_{RD}	2
Proton Dipolar Fields	δ_d	2.3
Bulk Magnetic Susceptibility	δ_b	2
Water Diamagnetic Shielding	σ	11
TOTAL		**15.9**

Run 1 Analysis Status: ω_p — Field Calibration

Plunging Probe

Plunging Probe Perturbations		
Quantity	**Symbol**	**Uncertainty (ppb)**
Material Perturbation	δ_s	10.9
Paramagnetic Impurities	δ_p	1.1
Radiation Damping	δ_{RD}	2
Proton Dipolar Fields	δ_d	2.3
Bulk Magnetic Susceptibility	δ_b	2
Water Diamagnetic Shielding	σ	11
TOTAL		**15.9**

Run 1 Analysis Status: ω_p — Field Interpolation

- Need to determine ω_p at all times while storing muons => interpolate between trolley maps using fixed probe data

Run 1 Analysis Status: ω_p — Field Interpolation

- Need to determine ω_p at all times while storing muons => interpolate between trolley maps using fixed probe data

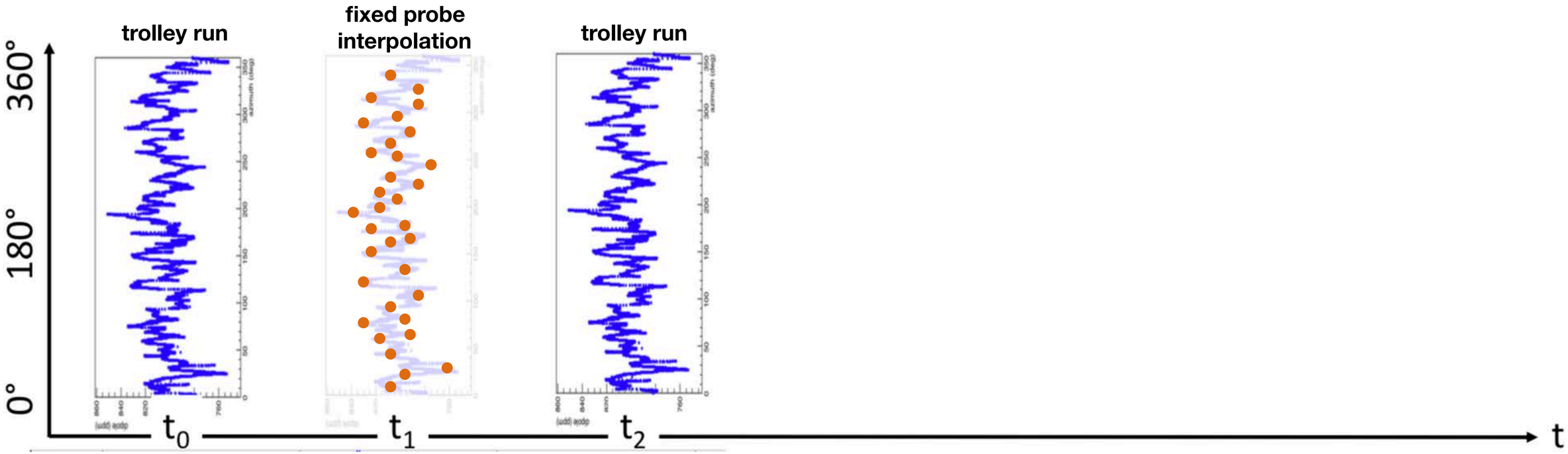

Run 1 Analysis Status: ω_p — Field Interpolation

- Need to determine ω_p at all times while storing muons => interpolate between trolley maps using fixed probe data

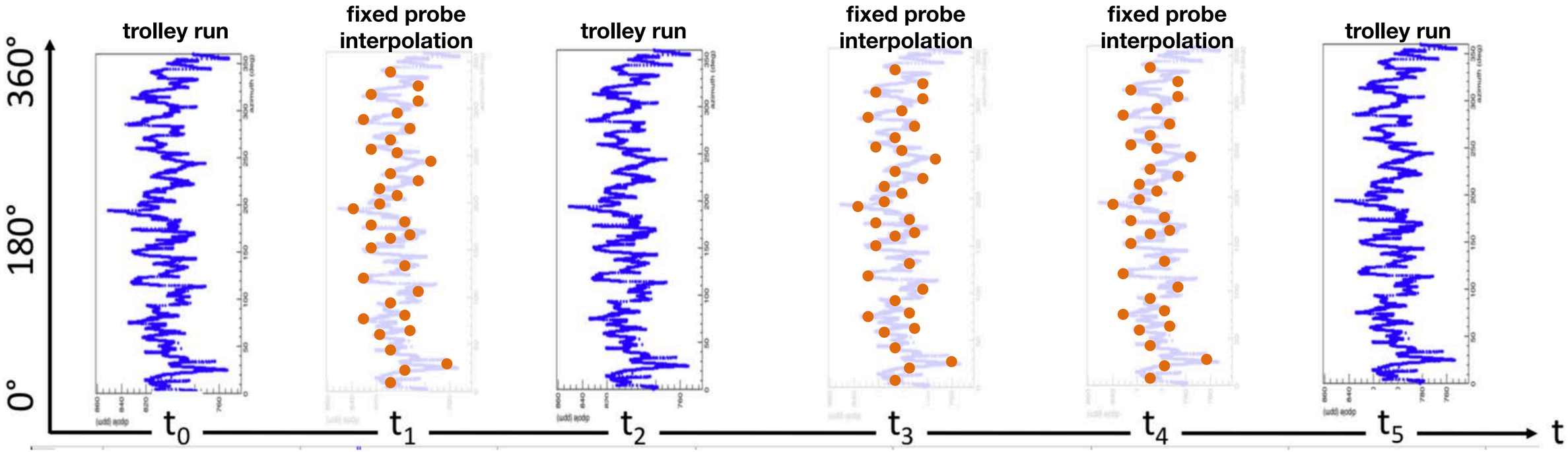

UMassAmherst

Run 1 Analysis Status: ω_p — Field Interpolation

- Example from subset of data
- Tracking algorithms showing good agreement with trolley runs
- Also tracking higher-order multipole moments — important for extracting muon-weighted field $\tilde{\omega}_p$

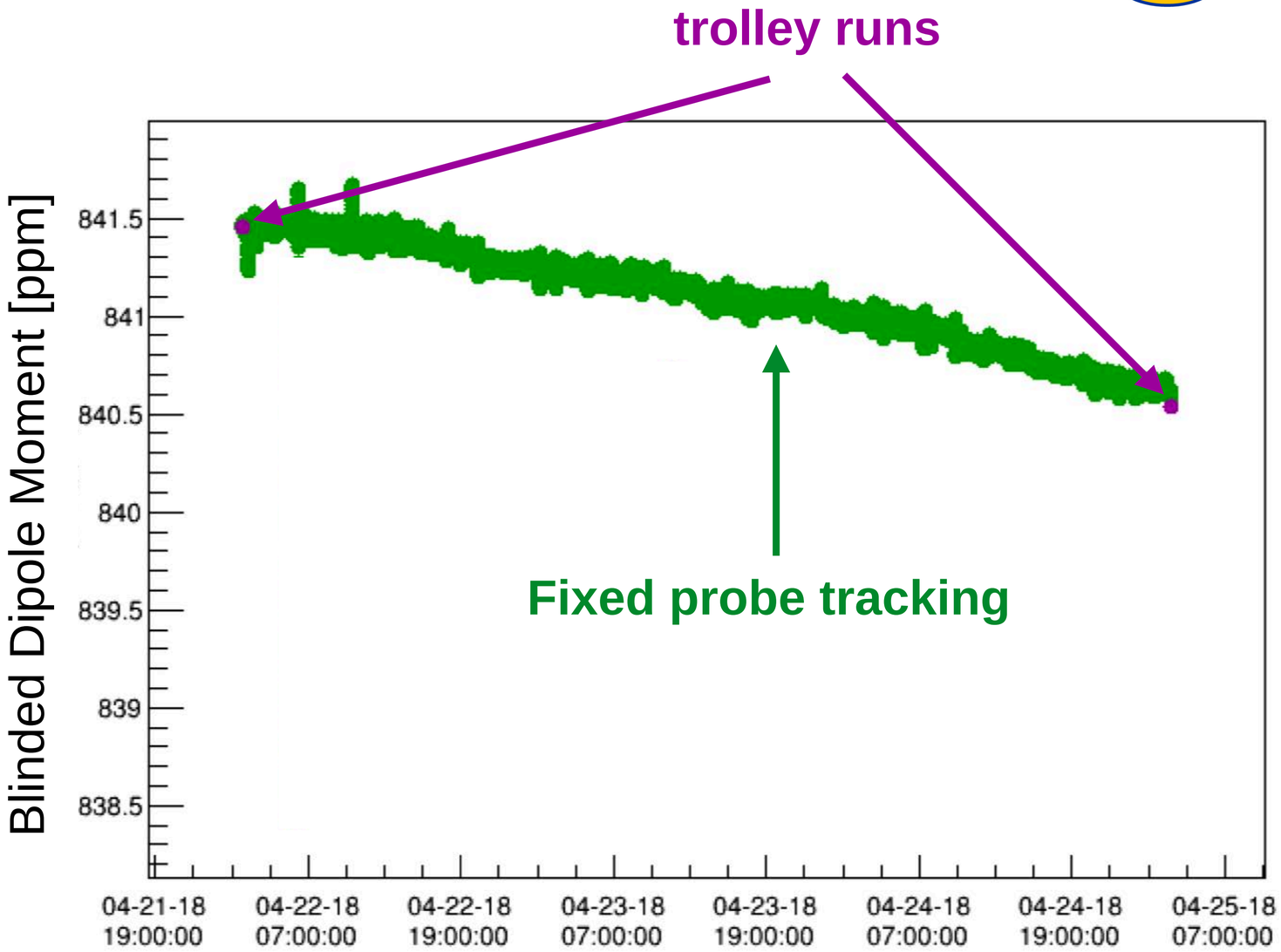

Summary

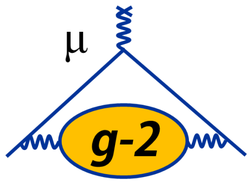

- **The Muon g-2 Experiment** is a highly sensitive test of the SM
  - Discrepancy between theory and experiment for a_μ > ~3σ

✓ Completed Run 1 in July 2018 (1.1x BNL statistics)

→ Analyses are mature and progressing towards a result in ***early 2020***

✓ Completed Run 2 in July 2019 (1.9x BNL statistics)

  - Starting to organize analysis efforts

- Run 3 starting this November: aiming to **triple** statistics to date


Thank You!


Backup

The Big Move: Transporting the Ring from BNL to FNAL

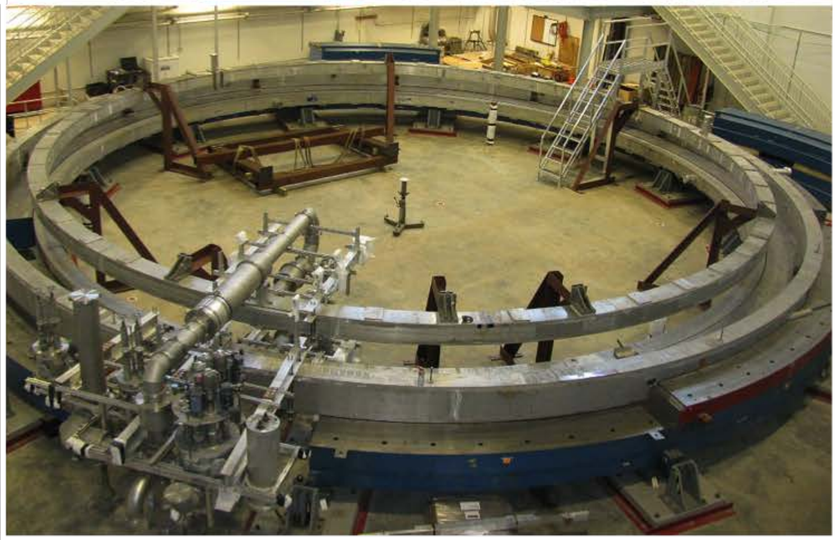

- June 2013—June 2015
- Ring deconstructed at BNL, transported by barge/ flatbed trailer
- Reassembled at FNAL
- Ring successfully cooled and powered to 1.45 T in September 2015 — remarkable achievement!

Getting Muons Into the Ring: Inflector Magnet

- Outside ring: B = 0 T, inside: B = 1.45 T
- Need to cancel field in order to get muons in (strong deflection otherwise)
- No perturbation to field outside shield
- New inflector design with higher transmission under development
- **Improve injection by 40%**

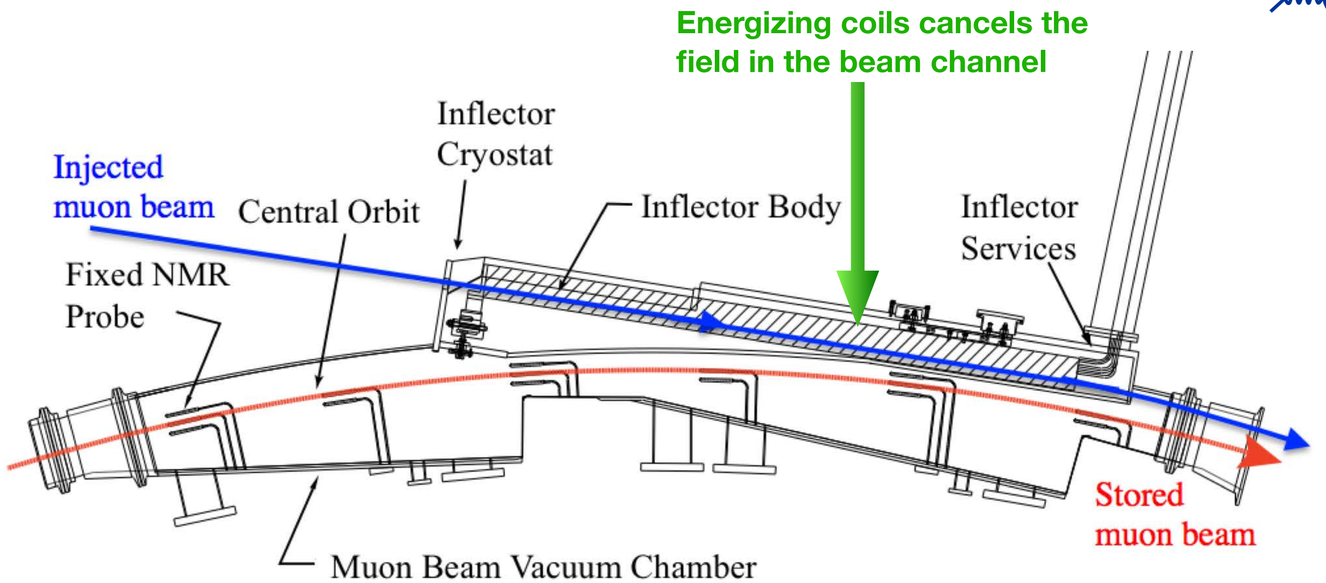

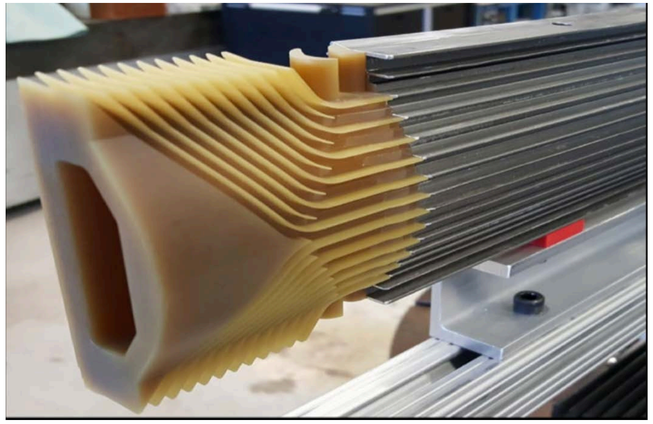

New inflector coil winding mount

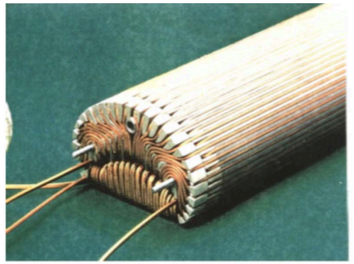

Present inflector

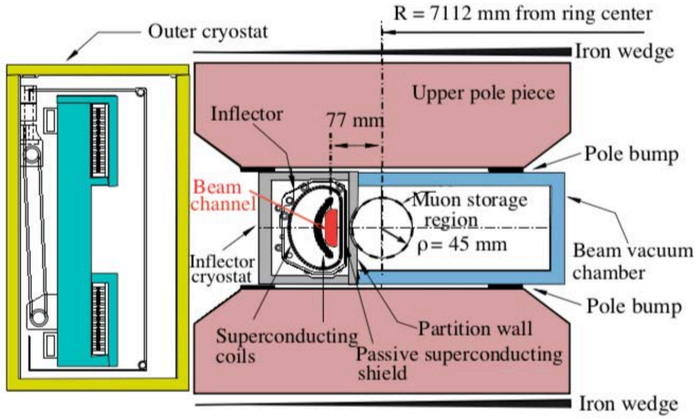

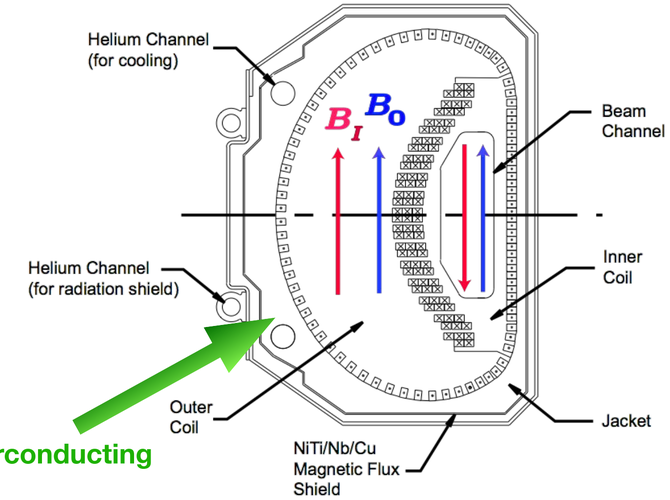

Super currents in passive superconducting shield prevents flux leakage

UMassAmherst

Theory Status of Hadronic Contribution to a_μ

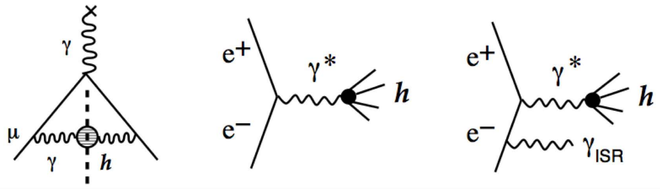

$$a_\mu^{\mathrm{had;LO}} = \left(\frac{\alpha m_\mu}{3\pi}\right)^2 \int_{m_\pi^2}^{\infty} \frac{ds}{s^2} K(s) R(s)$$

$$R \equiv \frac{\sigma_{\mathrm{tot}}(e^+e^- \to \mathrm{hadrons})}{\sigma(e^+e^- \to \mu^+\mu^-)}$$

- **Critical input to HVP** from e^+e^- colliders (SND, CMD3, BaBar, KLOE, Belle, BESIII)
- **BESIII:** 3x more data available, luminosity measurement improvements
- **VEPP-2000:** Aiming for 0.3% (fractional) uncertainty; radiative return + energy scan
- **CMD3:** Will measure up to 2 GeV (energy scan, ISR — good cross check)

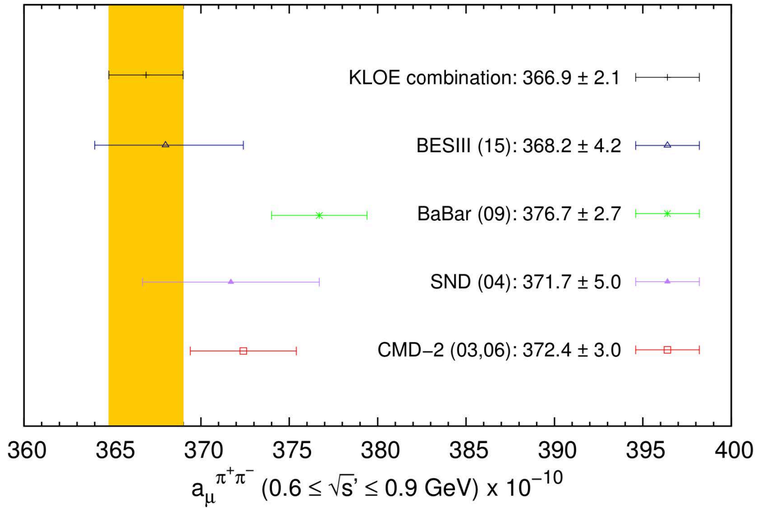

A. Anastasi et al., arXiv:1711.03085 [hep-ex]

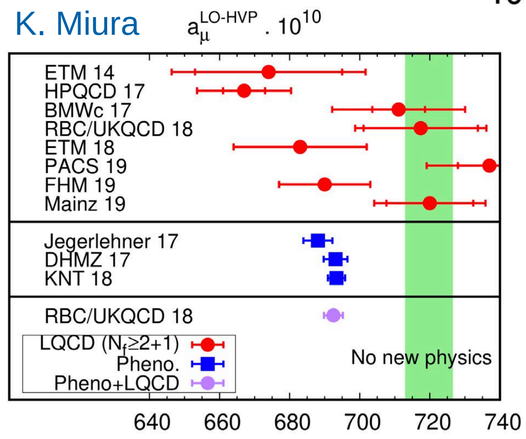

M. Davier et al., arXiv:1706.09436 [hep-ph]

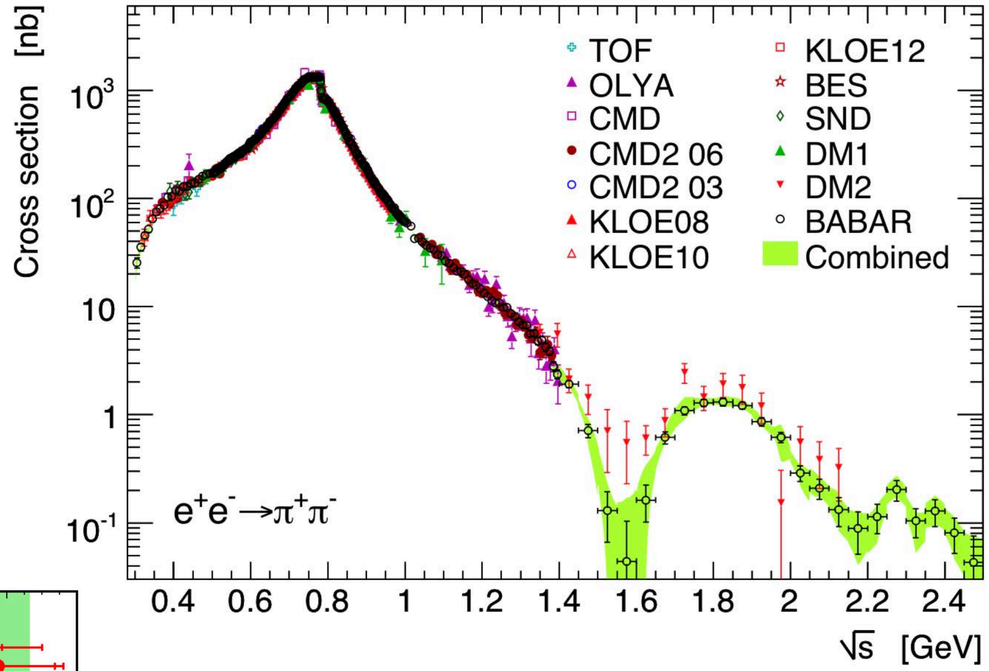

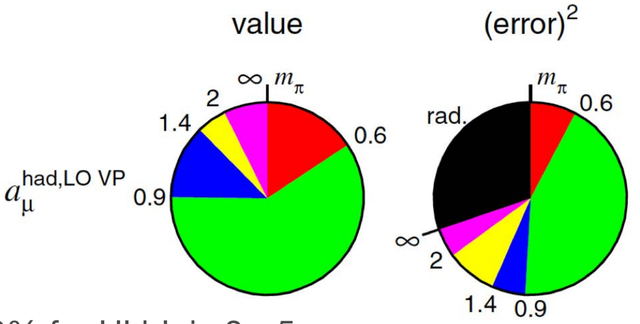

- **Lattice calculations** of a_μ^{HVP} to 1% soon, 30% for HLbL in 3—5 years

Physics Beyond the Standard Model?

SUSY, TeV-Scale Models

- Higgs measured at the LHC to be 125 GeV
- Theory: Higgs should acquire much heavier mass from loops with heavy SM particles (e.g., top quark)
  - **Supersymmetry: new class of particles** that enters such loops and **cancels this contribution**

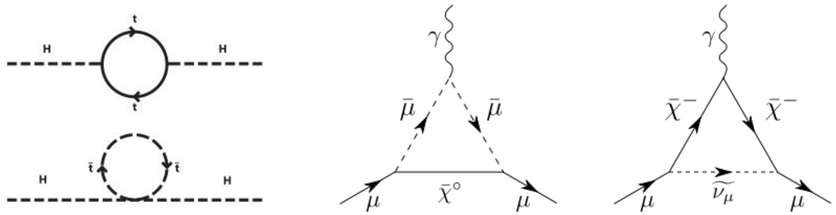

- **Complementary to direct searches at the LHC**
  - Sensitivity to sgn(μ), tan(β)
  - Contributions to a_μ arise from charginos, sleptons
  - LHC searches sensitive to squarks, gluinos

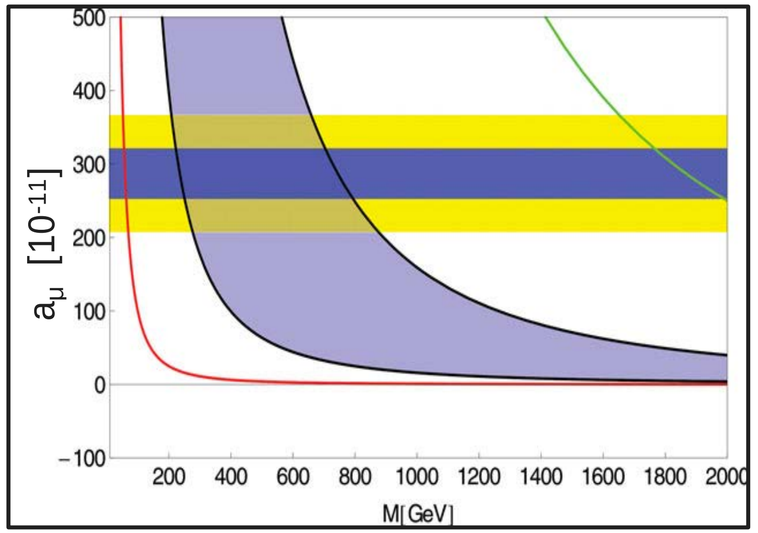

D. Hertzog, Ann. Phys. (Berlin), 2015, courtesy D. Stockinger

Z', W', UED, Littlest Higgs
- Assumes typical weak coupling

Radiative muon mass generation

Unparticles, Extra Dimension Models, SUSY (tan β = 5 to 50)

Z' Possibilities

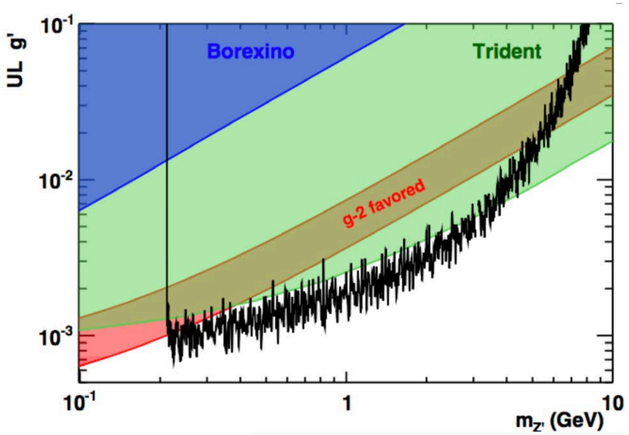

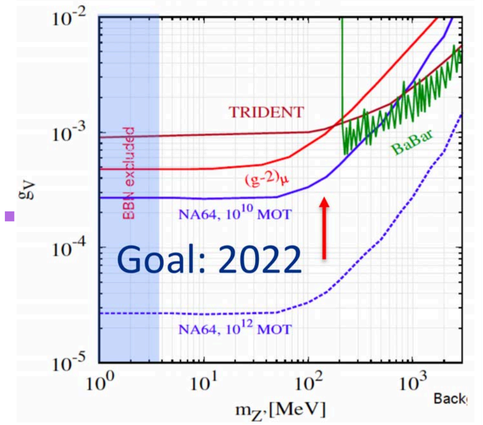

Others…

- Axion-like particles
- Dark photons (invisible)
- Extended Higgs/ leptoquarks

Analysis Details: ω_a

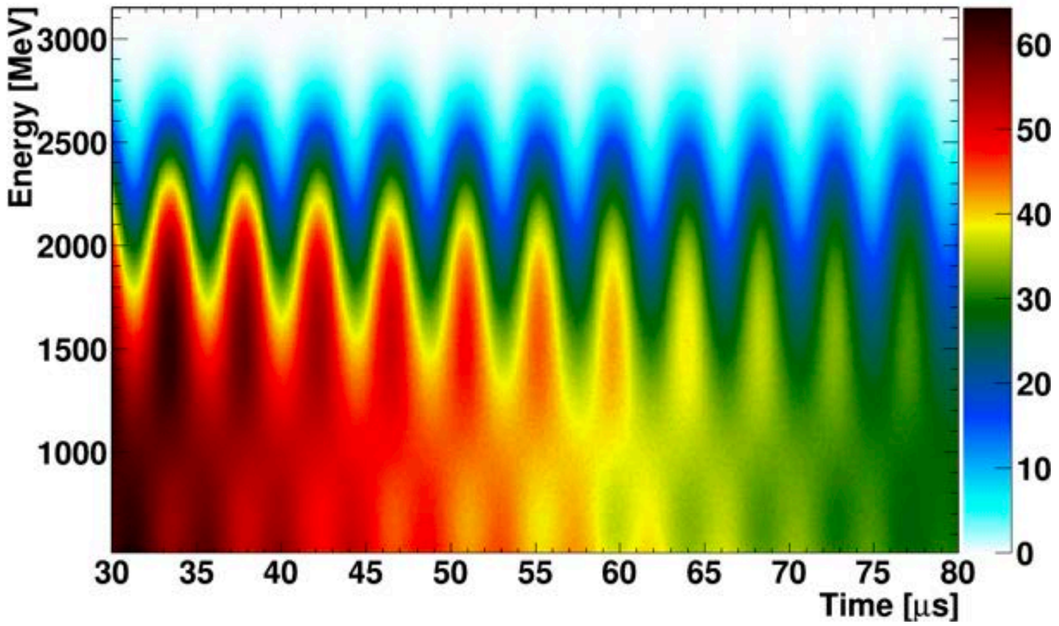

$$\frac{\delta\omega_a}{\omega_a} = \frac{\sqrt{2}}{2\pi f_a \tau_\mu N^{\frac{1}{2}} A}$$

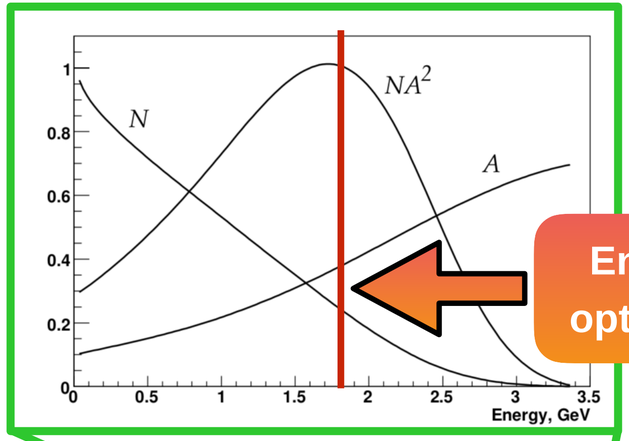

Energy cut chosen to optimize figure-of-merit

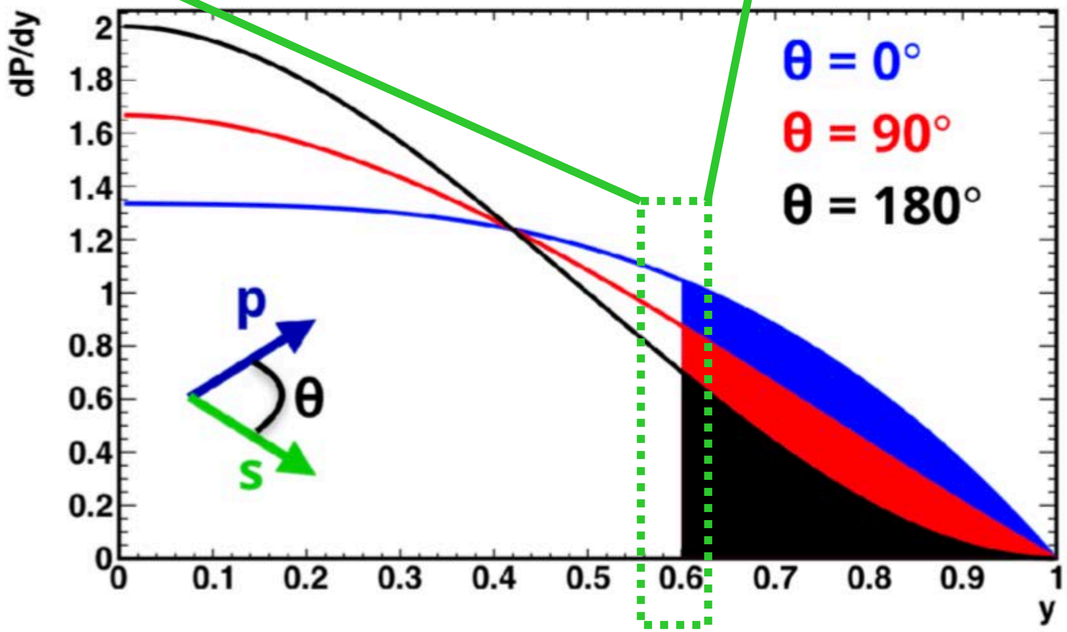

UMassAmherst

Analysis Details: ω_a

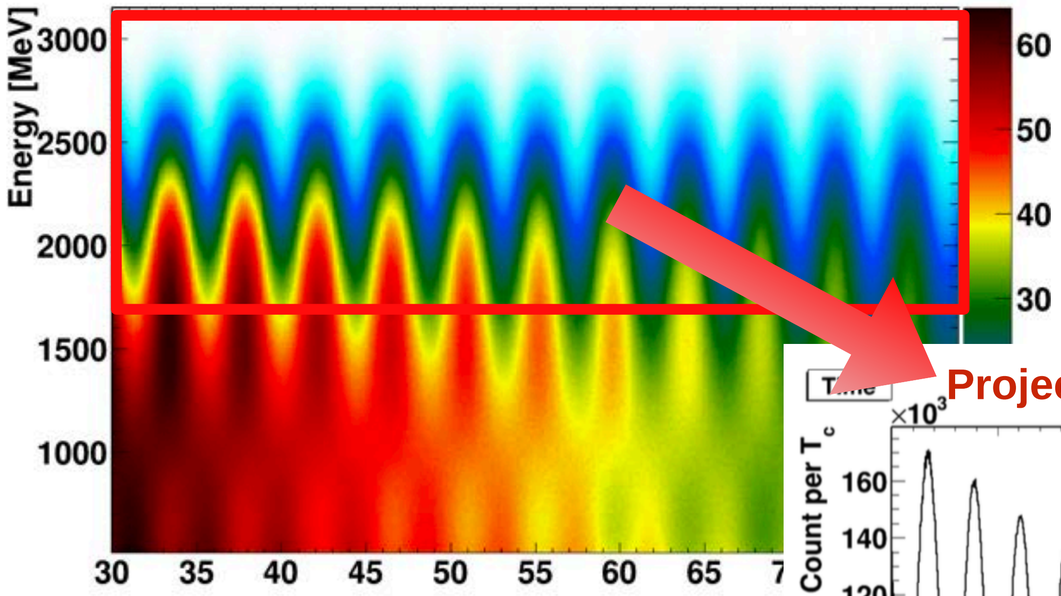

$$\frac{\delta\omega_a}{\omega_a} = \frac{\sqrt{2}}{2\pi f_a \tau_\mu N^{\frac{1}{2}} A}$$

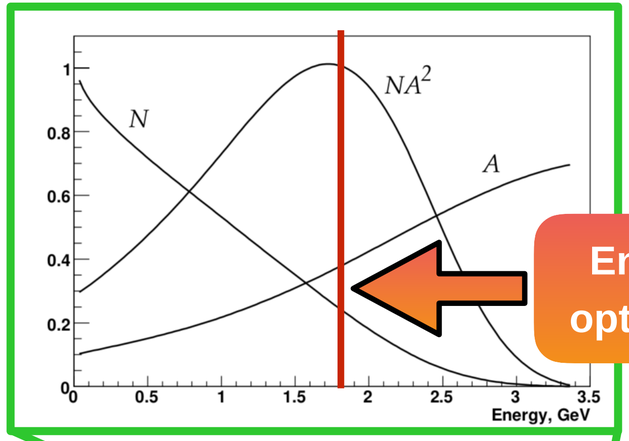

Energy cut chosen to optimize figure-of-merit

Project along time axis, energy cut

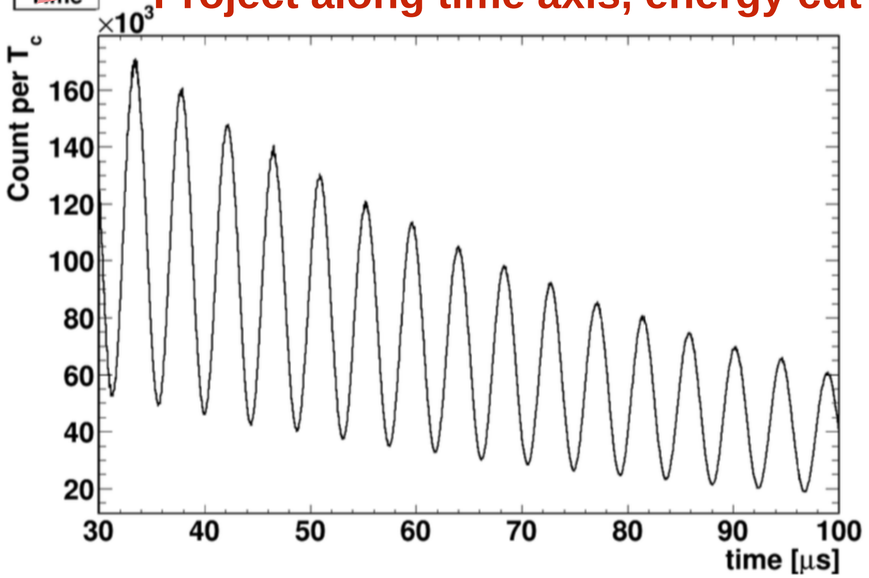

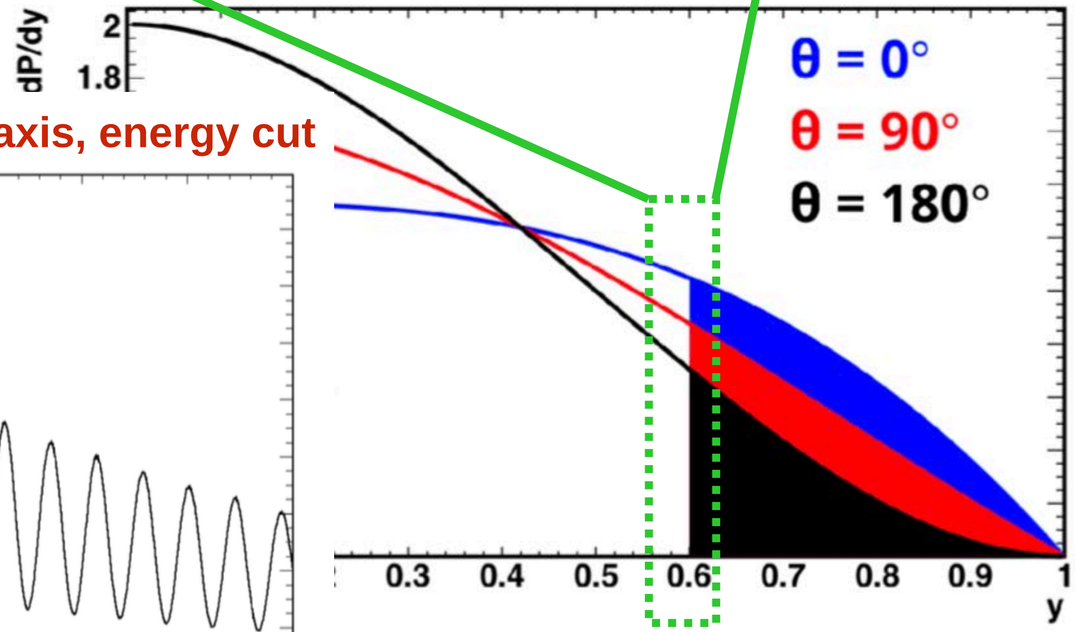

Analysis Details: ω_a

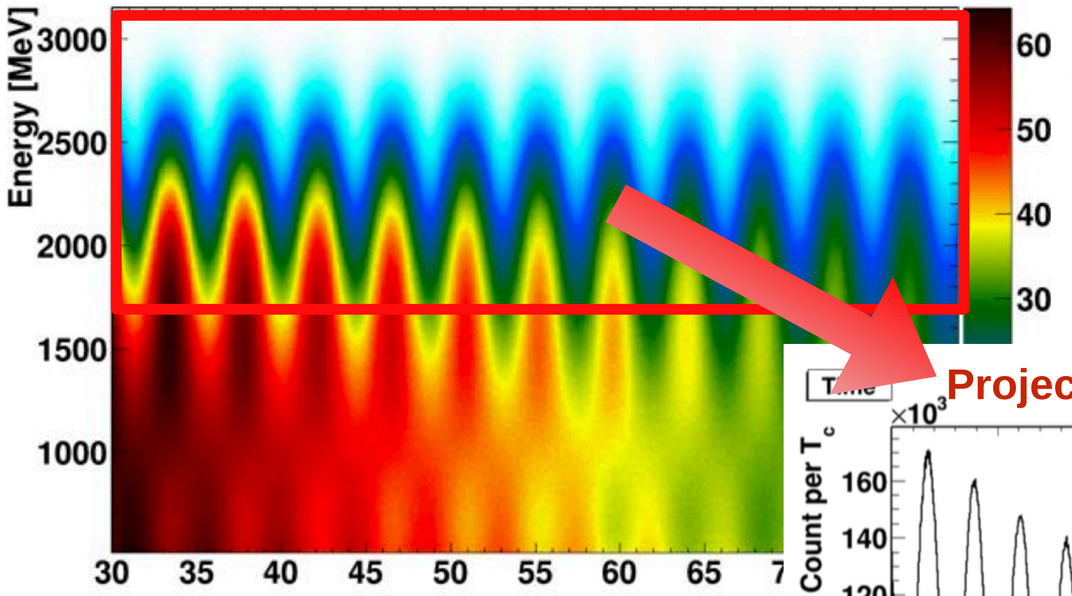

$$\frac{\delta\omega_a}{\omega_a} = \frac{\sqrt{2}}{2\pi f_a \tau_\mu N^{\frac{1}{2}} A}$$

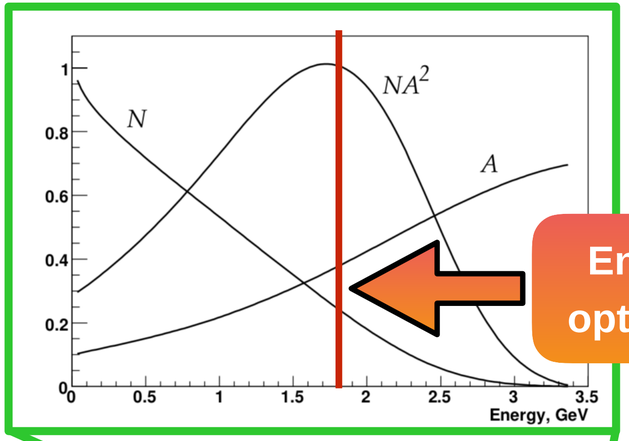

Energy cut chosen to optimize figure-of-merit

Project along time axis, energy cut

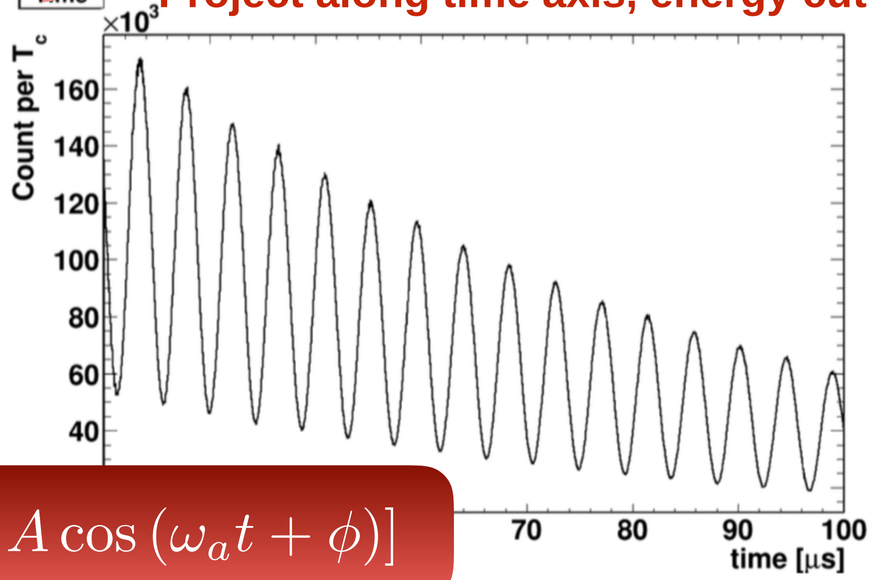

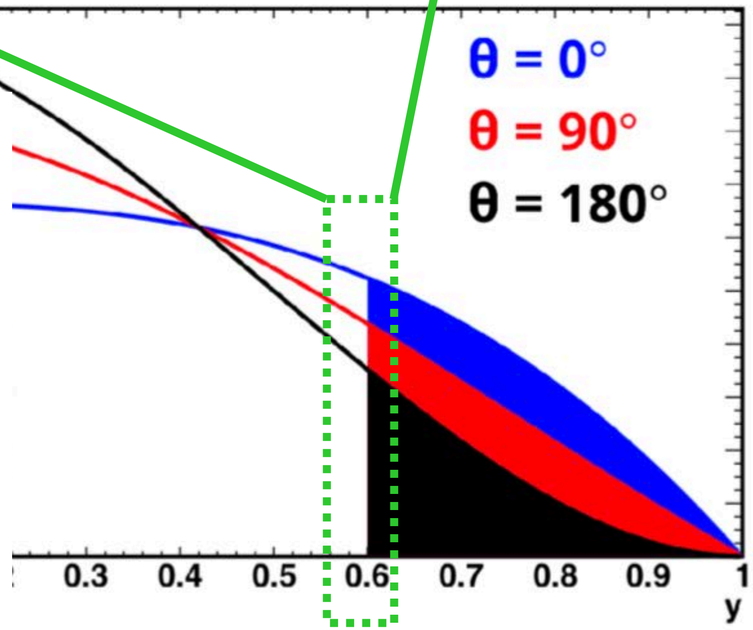

Fit to: $N(t) = N_0 e^{-t/\tau}\left[1 - A\cos\left(\omega_a t + \phi\right)\right]$

Beam Dynamics Corrections

- Full expression for ω_a:

$$\vec{\omega}_a = \vec{\omega}_S - \vec{\omega}_C = -\frac{e}{mc}\left[a_\mu \vec{B} - \left(a_\mu - \frac{1}{\gamma^2-1}\right)\vec{\beta}\times\vec{E} - a_\mu\left(\frac{\gamma}{\gamma+1}\right)\left(\vec{\beta}\cdot\vec{B}\right)\vec{\beta}\right]$$

- Choose $\gamma = 29.3$ ($p_\mu = 3.094$ GeV/c)

Not all μ^+ at this γ → **E-field correction**

$$C_E = -2n(1-n)\beta^2\frac{\langle x_e^2\rangle}{R_0^2}$$

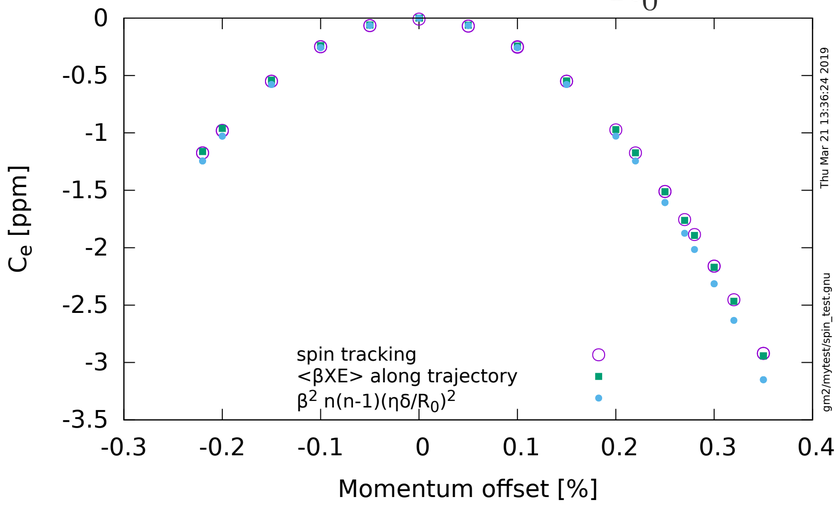

Vertical beam oscillations → **pitch correction**

$$C_p = -\frac{n}{4}\frac{\langle y^2\rangle}{R_0^2}$$

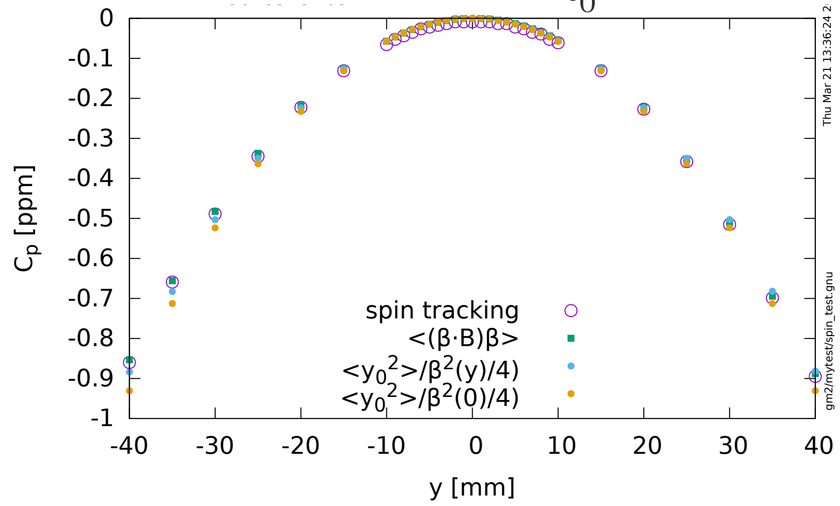

Quad Challenges (Run 1)

- 2 of 32 HV resistors on quad plates were flawed => did not stabilize in time for “fit start time”
- Mean of vertical muon distribution moves down by 0.6 mm
  - Investigating impact on ω_a (calculations, systematic measurements)
- Problem was fixed for Run 2

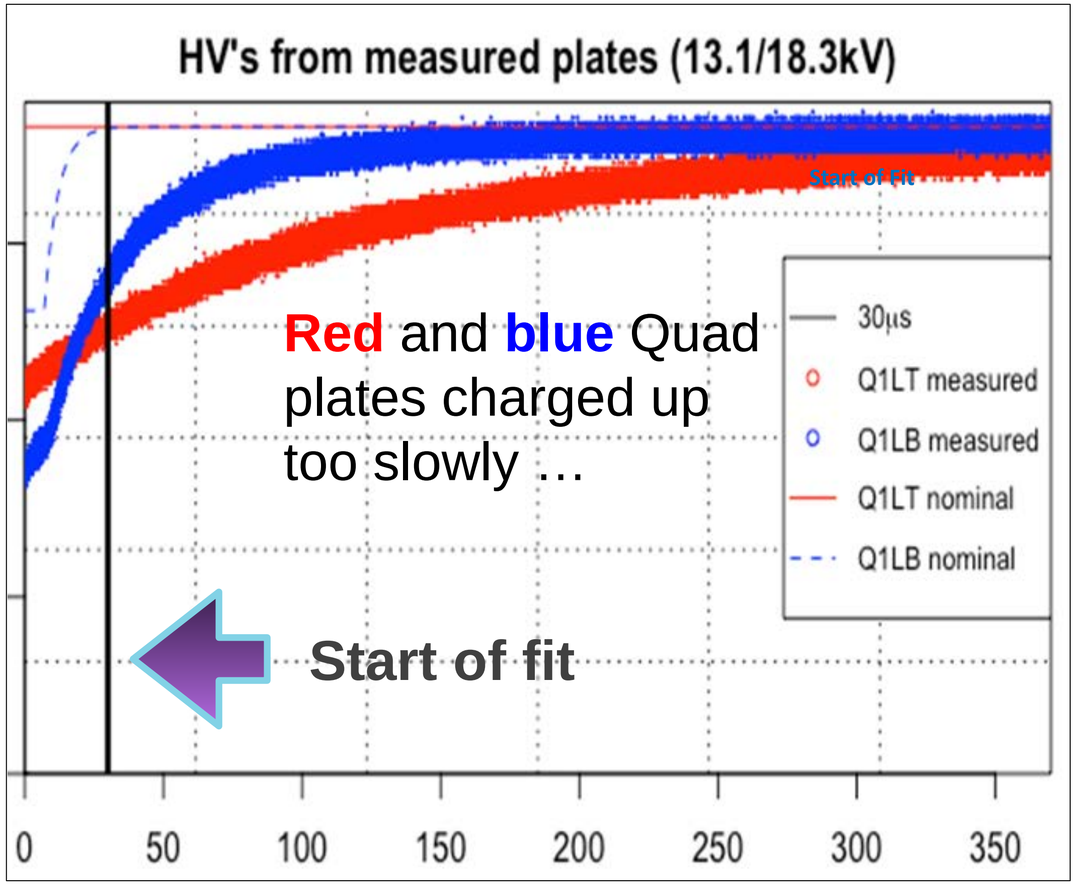

How is a Kick Made?

- A **charging power supply** charges up a **capacitor bank** to 700 V
- Capacitors are **discharged** through a transformer into a **Blumlein** (a HV capacitor up to 55 kV)
- Current in **Blumlein** is discharged into a **resistive load (Z = 12.5 Ω)**
- Current delivered to plates, producing a **~200 G magnetic field**, rotating muon's momentum vector

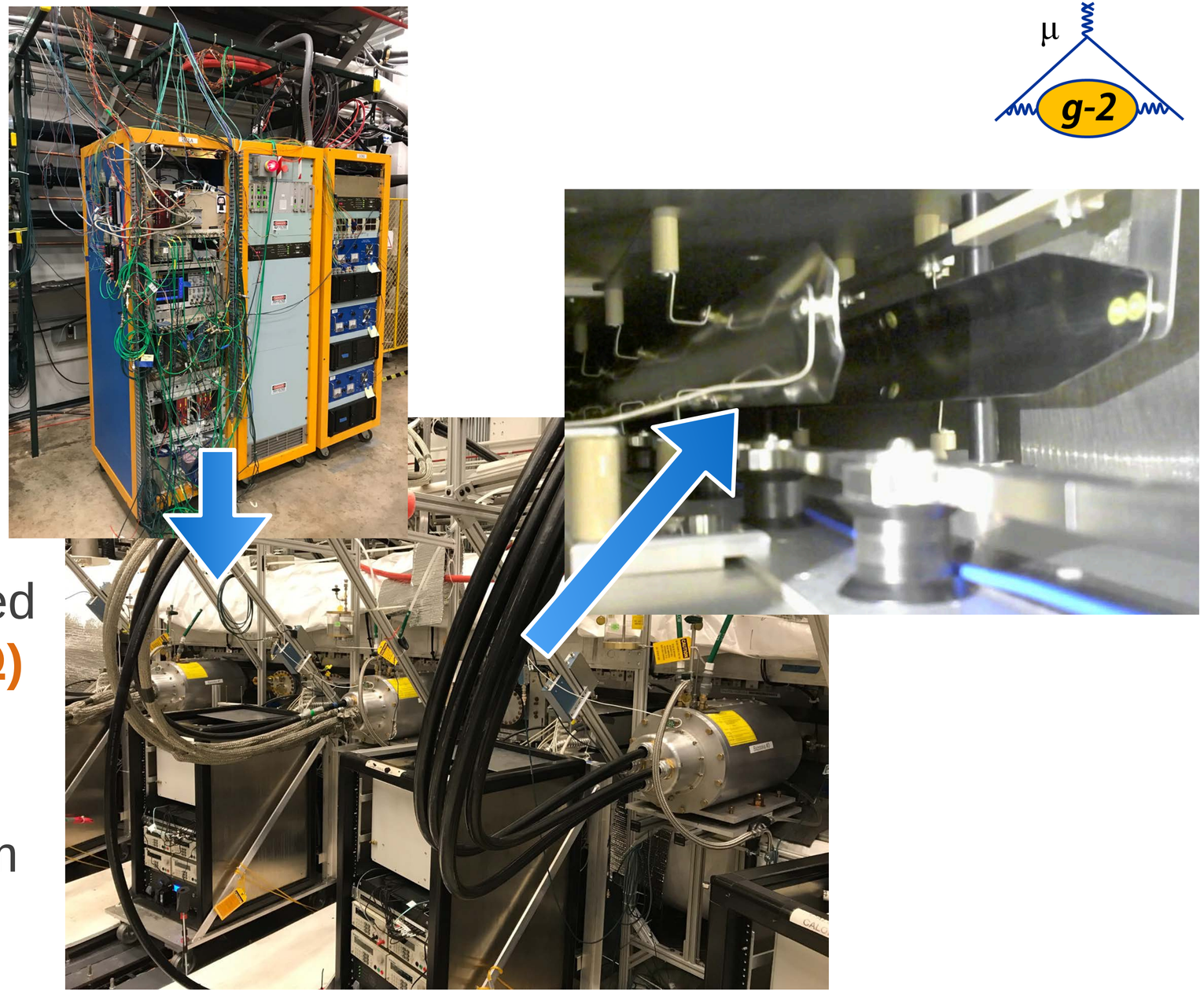

What Affects the Beam Shape?

- **Kicker pulse** strength, shape affects structure of beam
- **Beam width** affected by dynamics

Kicker Pulse

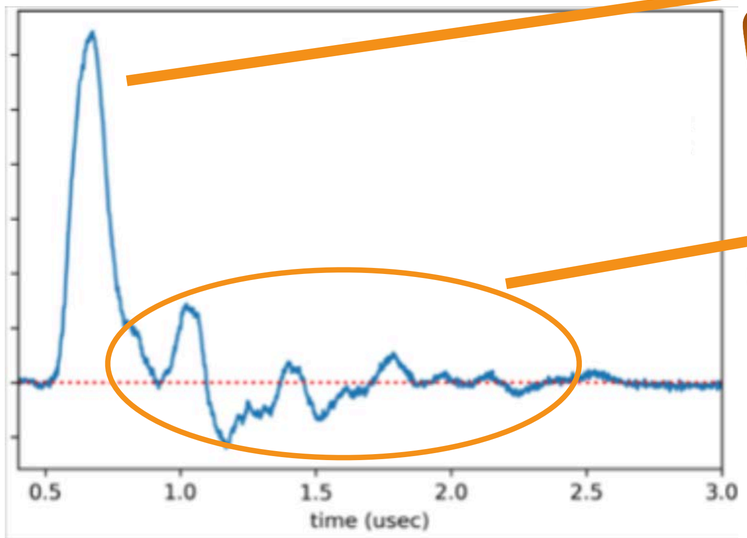

Higher kick → lower radius

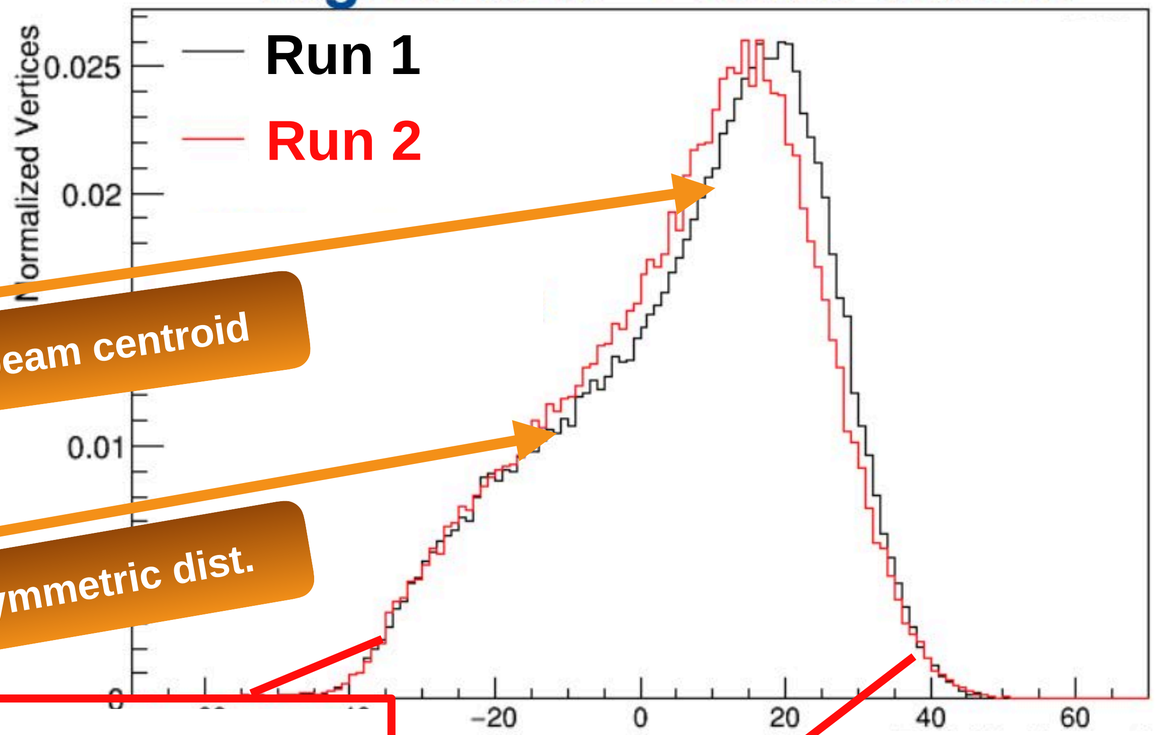

kick strength → beam centroid

ringing kick → asymmetric dist.

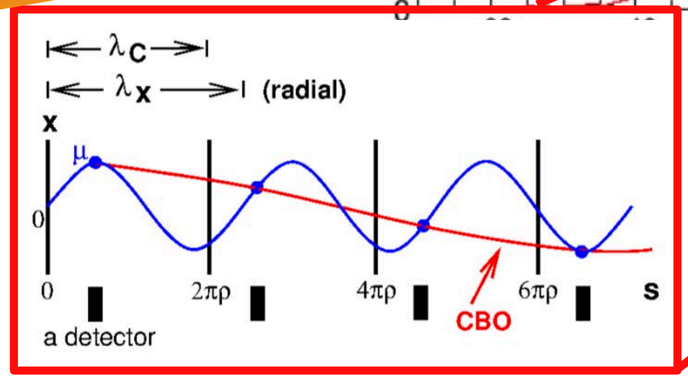

CBO → radial width

Kicker Challenges

- Need to deflect beam by ~11 mrad on the first turn, then turn off (< 149 ns)
- Engineering challenge never fully realized at BNL— and not yet for us

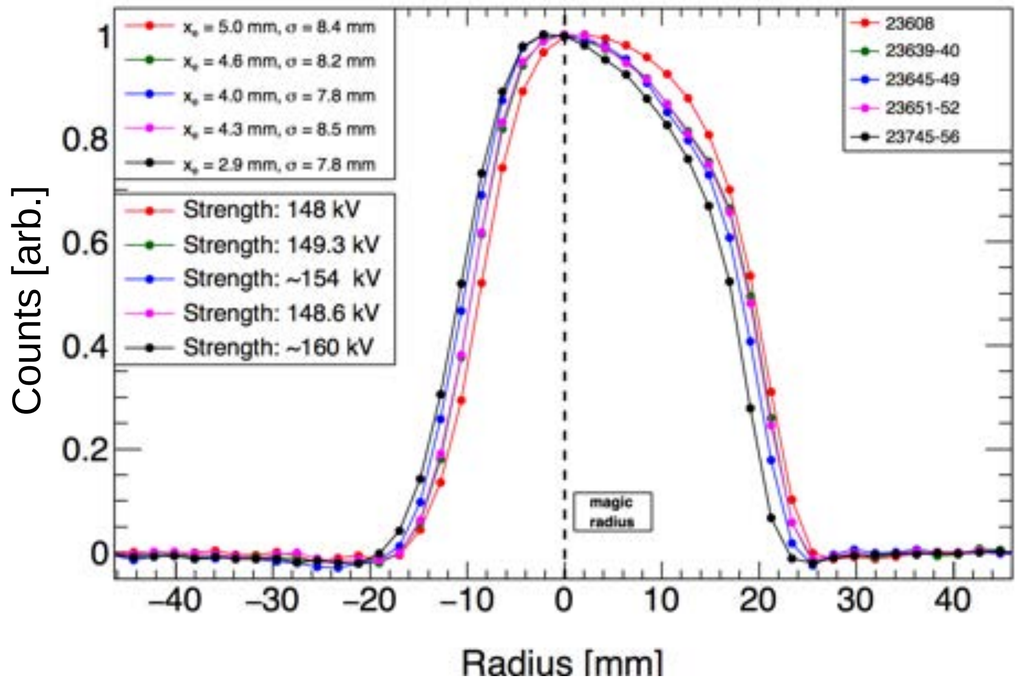

Radial beam distribution at various kick strengths; well contained, but not centered

Take away: we can live with this — we just don't like it

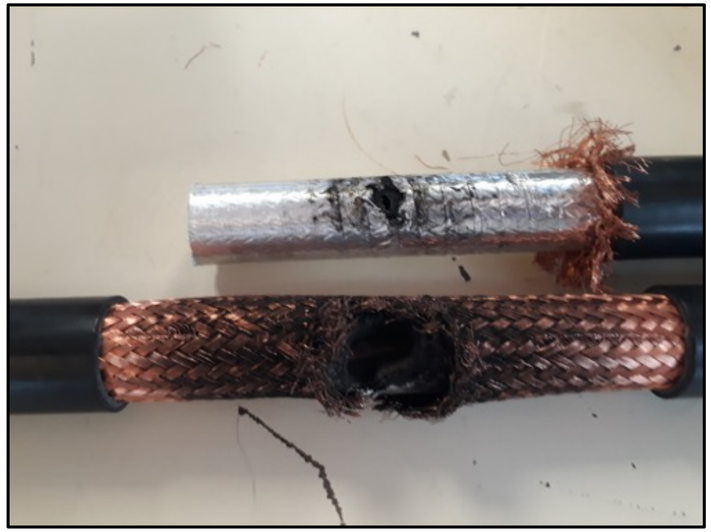

Running at high voltages (~ 50 kV) burns out cables — had to back off

What Drives the ω_a Fit Start Time?

- Start fit window to extract ω_a at ~ 30 μs to avoid:

Kicker eddy currents affect the magnetic field

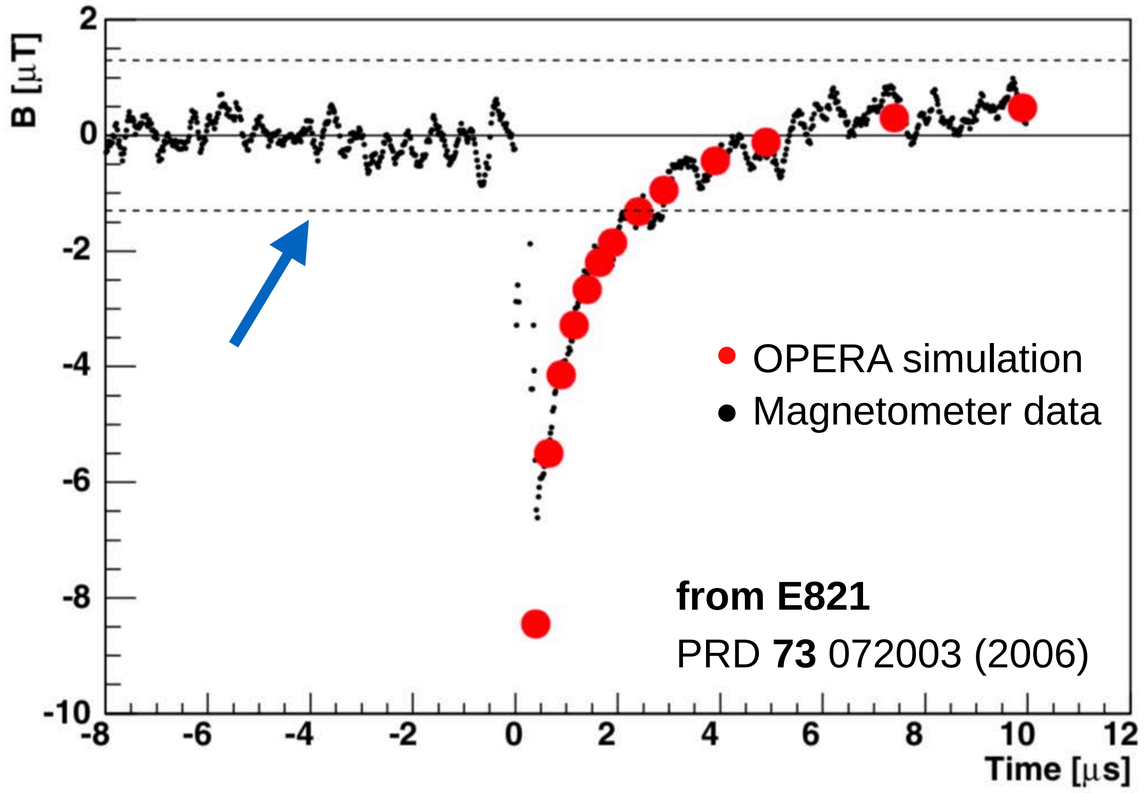

Quad scraping at early times to reduce losses

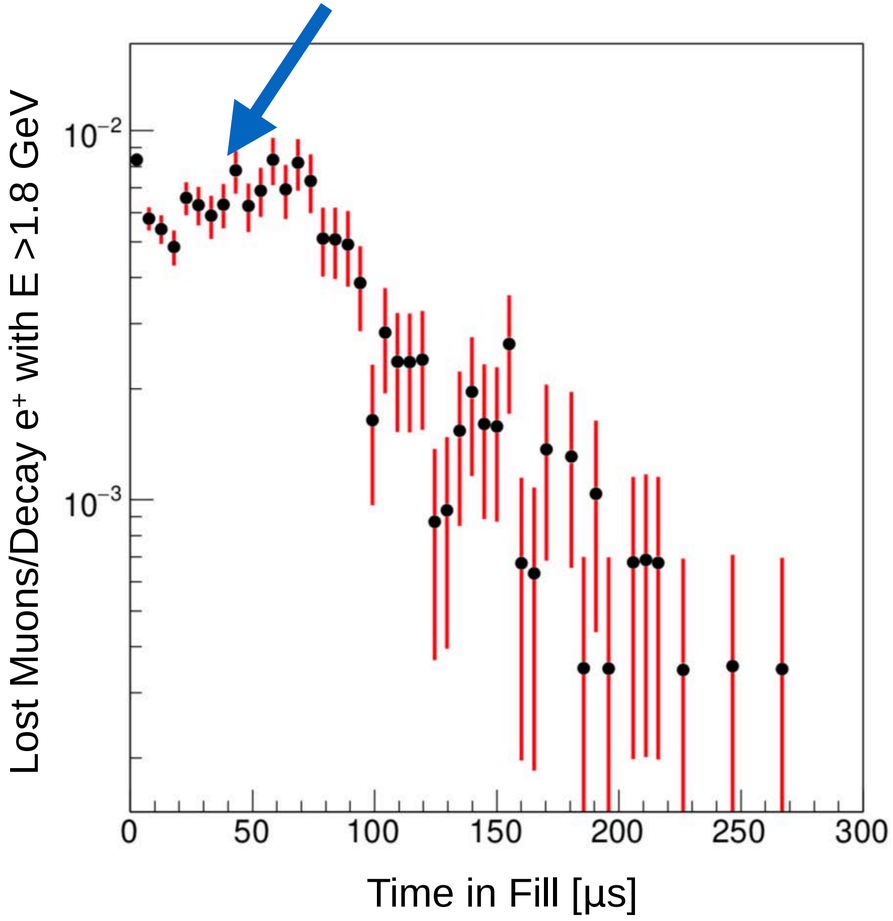

Pulsed Nuclear Magnetic Resonance

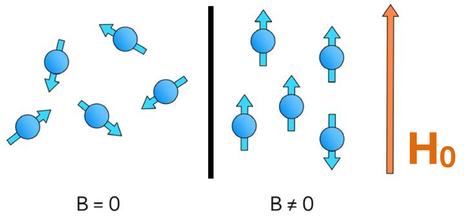

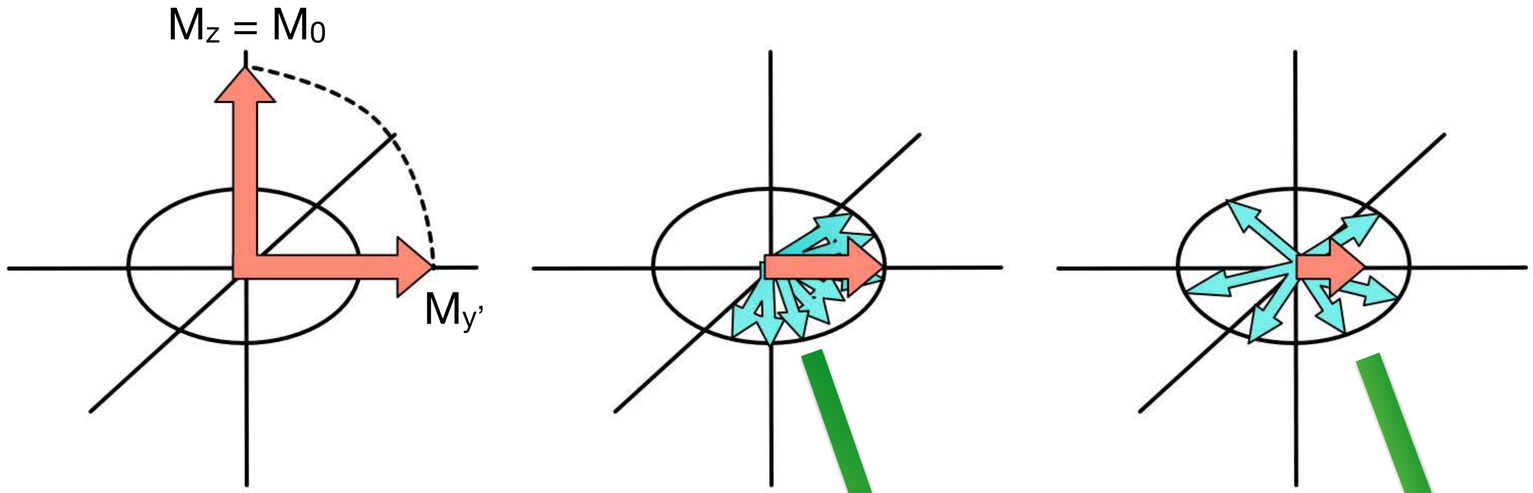

- Apply an RF pulse for a short time to the sample at Larmor frequency — tips spins perpendicular to external B field (**π/2 pulse**)
- Spin precession induces an EMF in the pickup coil
  - So-called **Free-Induction Decay** (**FID**)
- Decay of signal driven by:
  - Spin-spin interactions (dephasing) (pure T_2)
  - Field inhomogeneities (T_2^*)
  - Simultaneously, spins relax back to alignment with holding field (spin-lattice relaxation, T_1)

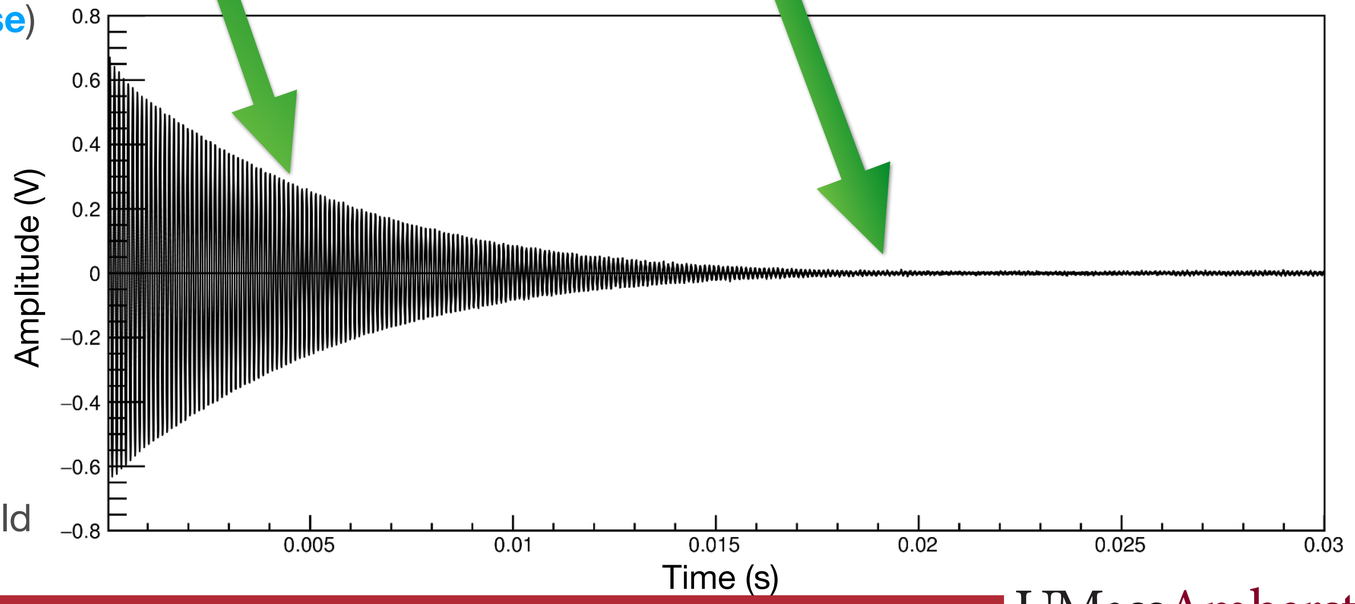

UMassAmherst

Magnetic Circuits

$$\mathcal{E} = \oint \vec{f}_s \cdot d\vec{\ell} = V = IR$$

Can write a similar equation for magnets

$$\mathcal{F} = \oint \vec{H} \cdot d\vec{\ell} = NI$$

Magnetomotive Force (mmf)

$$\vec{B} = \mu_0 (1 + \chi_m) \vec{H} = \mu \vec{H}$$

Rewrite H in terms of B

$$\Phi = \vec{B} \cdot \vec{A} = \mu \vec{H} \cdot \vec{A}$$

Consider magnetic flux

$$\Phi \oint \frac{d\ell}{\mu A} = \mathcal{F} \Rightarrow \boxed{\mathcal{R} = \oint \frac{d\ell}{\mu A} = \frac{\mathcal{F}}{\Phi}}$$

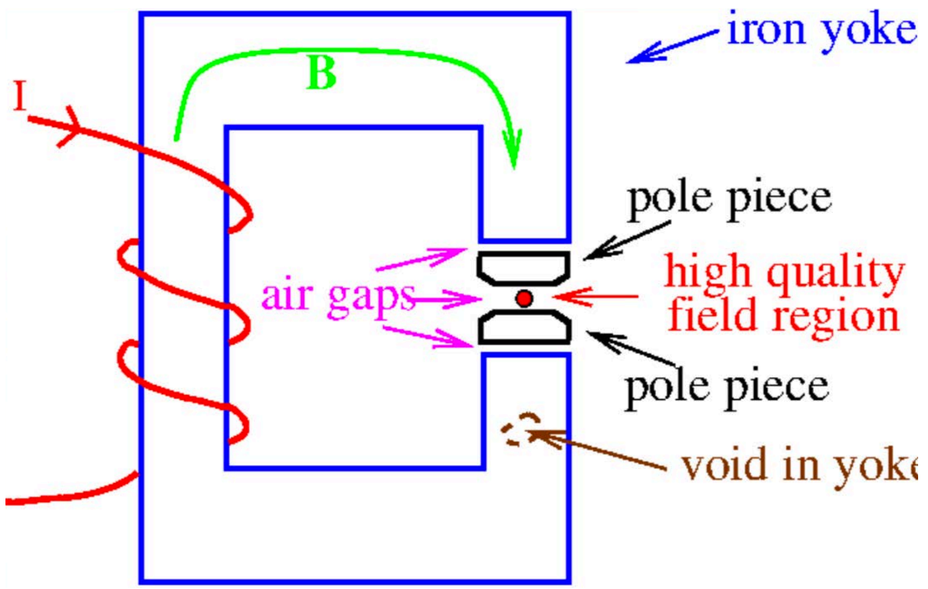

Magnetic Reluctance

- Analogous to resistance in an electrical circuit $\boxed{V = IR \Leftrightarrow \mathcal{F} = \Phi\mathcal{R}}$
- Current flows along a path of least resistance while field lines will take a path of least reluctance
- While the emf drives electric charges (Ohm's Law), the mmf "drives" magnetic field lines (Hopkinson's Law)

Magnet Anatomy

- For E821, Gordon Danby had a brilliant magnet design

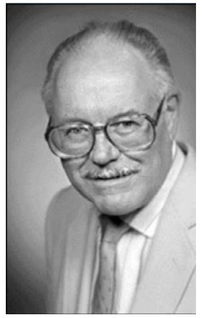

B = 1.45 T (~5200 A)

- Non-persistent current: fine-tuning of field in real time

12 C-shaped yokes

- 3 upper and 3 lower poles per yoke
- 72 total poles

Shimming knobs

- Pole separation determines field: pole tilts, non-flatness affect uniformity
- Top hats (30 deg effect, dipole)
- Wedges (10 deg effect, dipole, quadrupole)
- Edge shims (10 deg effect, dipole, quadrupole, sextupole)
- Laminations (1 deg effect, dipole, quadrupole, sextupole)
- Surface coils (360 deg effect, quadrupole, sextupole,…)

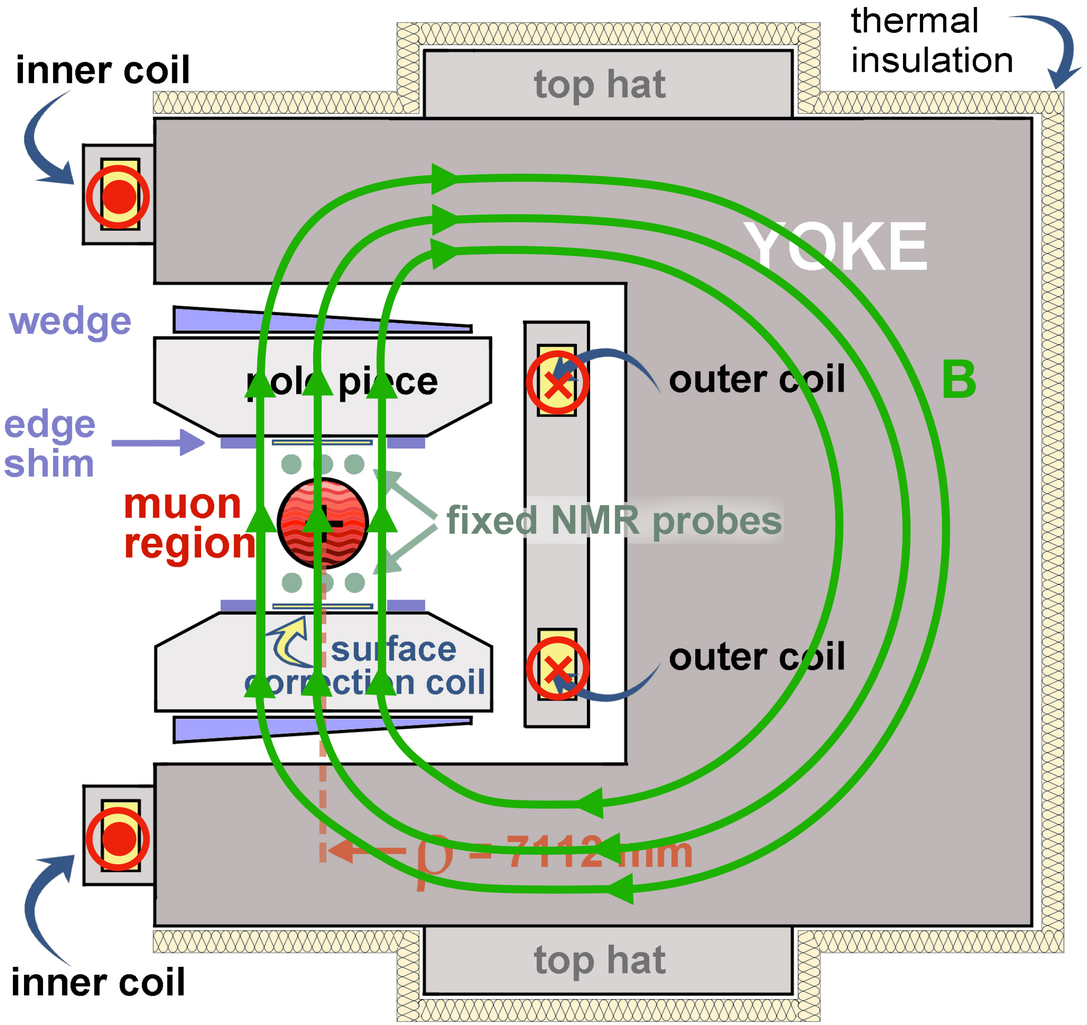

Current direction indicated by red markers

UMassAmherst

Optimizing the Dipole Moment

- Want to optimize the vertical component of the field
- Step and tilt discontinuities in pole surfaces yield large variations in the field
- To reduce/remove such effects, make adjustments to pole feet, which changes the magnet gaps and tilts
  - Use 0.001—0.010” thick shims
  - Requires removal of poles from the ring
- Informed by a computer model that optimizes the pole configurations
  - Requires global continuity between pole surfaces
  - Allows only three adjacent poles to be moved at a time (preserves alignment)

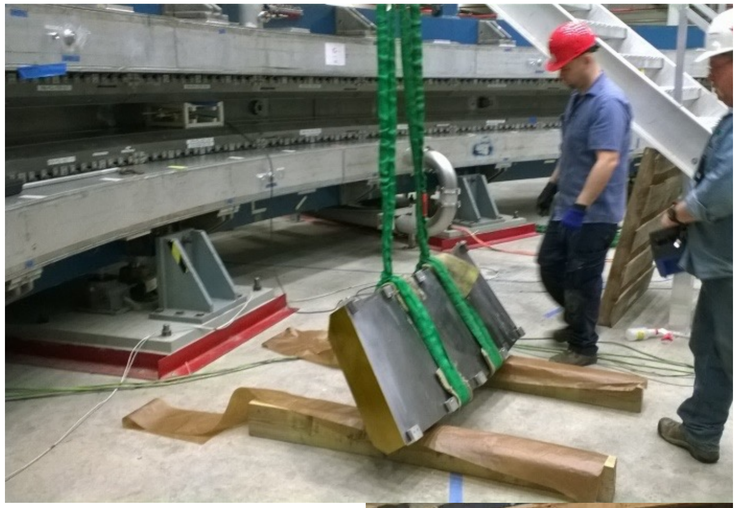

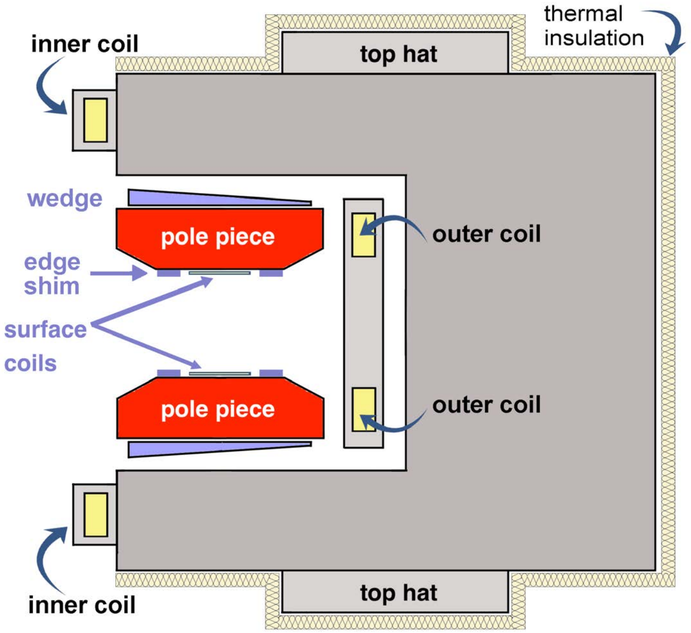

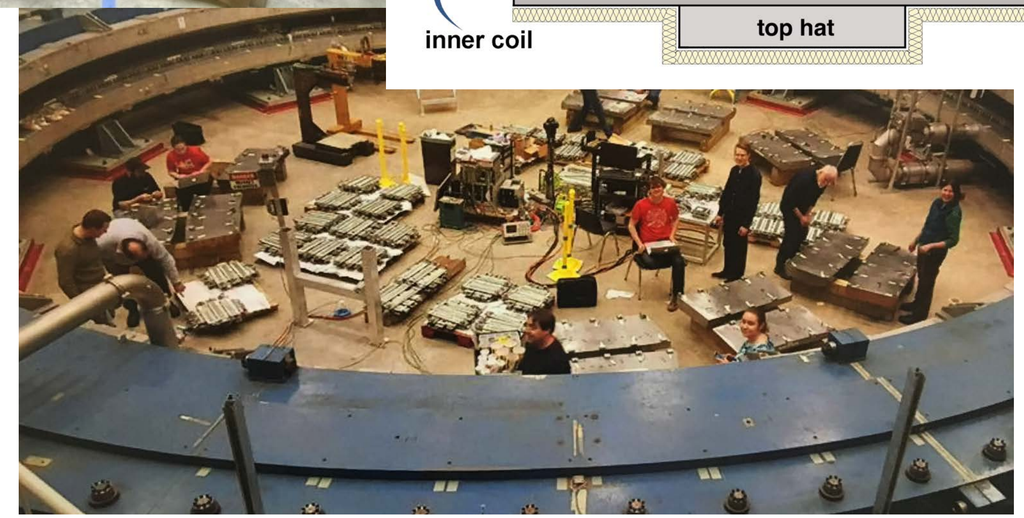

Minimizing the Quad, Sext, Octu Moments

Calibrated shimming knobs

- 48 top hats
- 864 wedges
- ~8400 iron foils (on pole surfaces)

Coarse tuning: top hat & wedge adjustments (**dipole, quadrupole**)

- Least-squares fit to field maps predicts top hat and wedge positions

Fine tuning: iron foils (**quadrupole, sextupole,…**)

- Modeled as saturated dipoles in 1.45 T field
- Computer code predicts foil width (mass) distribution to fill in the valleys of the field map

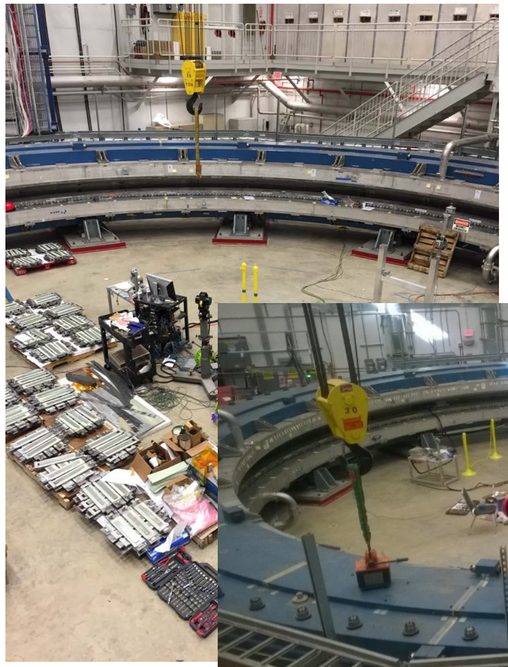

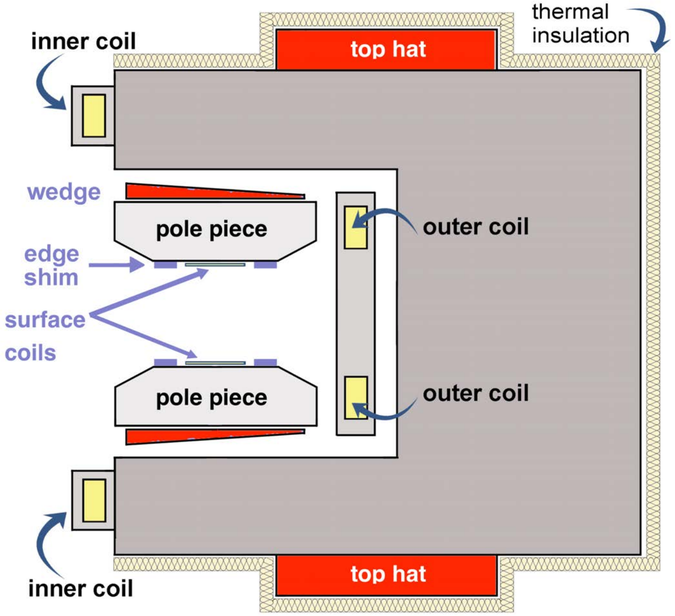

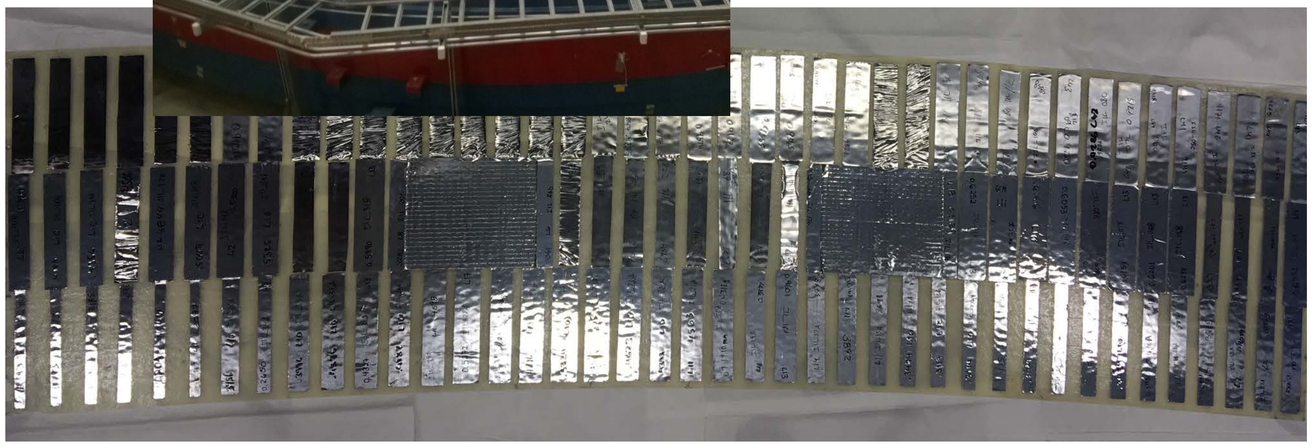

UMassAmherst

Rough Shimming Results

Oct 2015 → Aug 2016

Goal

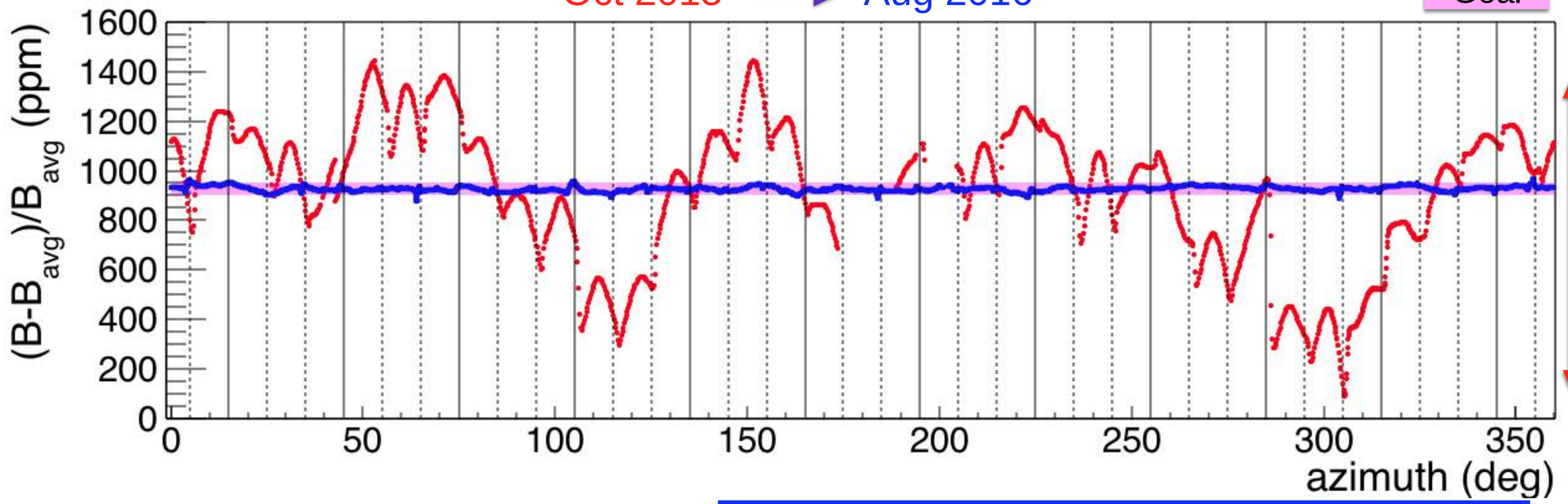

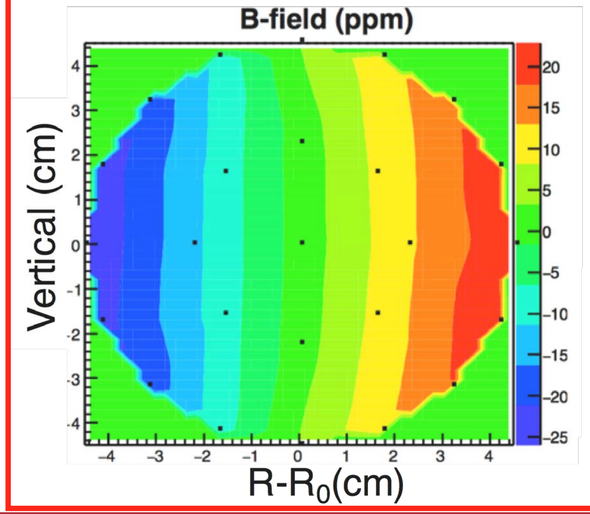

	Norm	Skew
Quad	25.13	-0.53
Sext	-1.99	-0.11
Octu	-1.16	-0.31
Decu	0.95	-0.07

Oct 2015

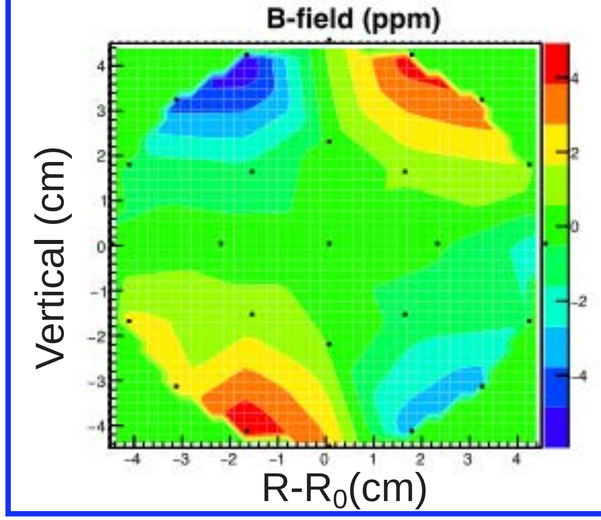

	Norm	Skew
Quad	-0.02	-0.57
Sext	-0.70	3.84
Octu	-0.76	0.56
Decu	0.44	-1.61

Aug 2016

UMassAmherst

Magnetic Field Comparison: BNL 821 and FNAL E989

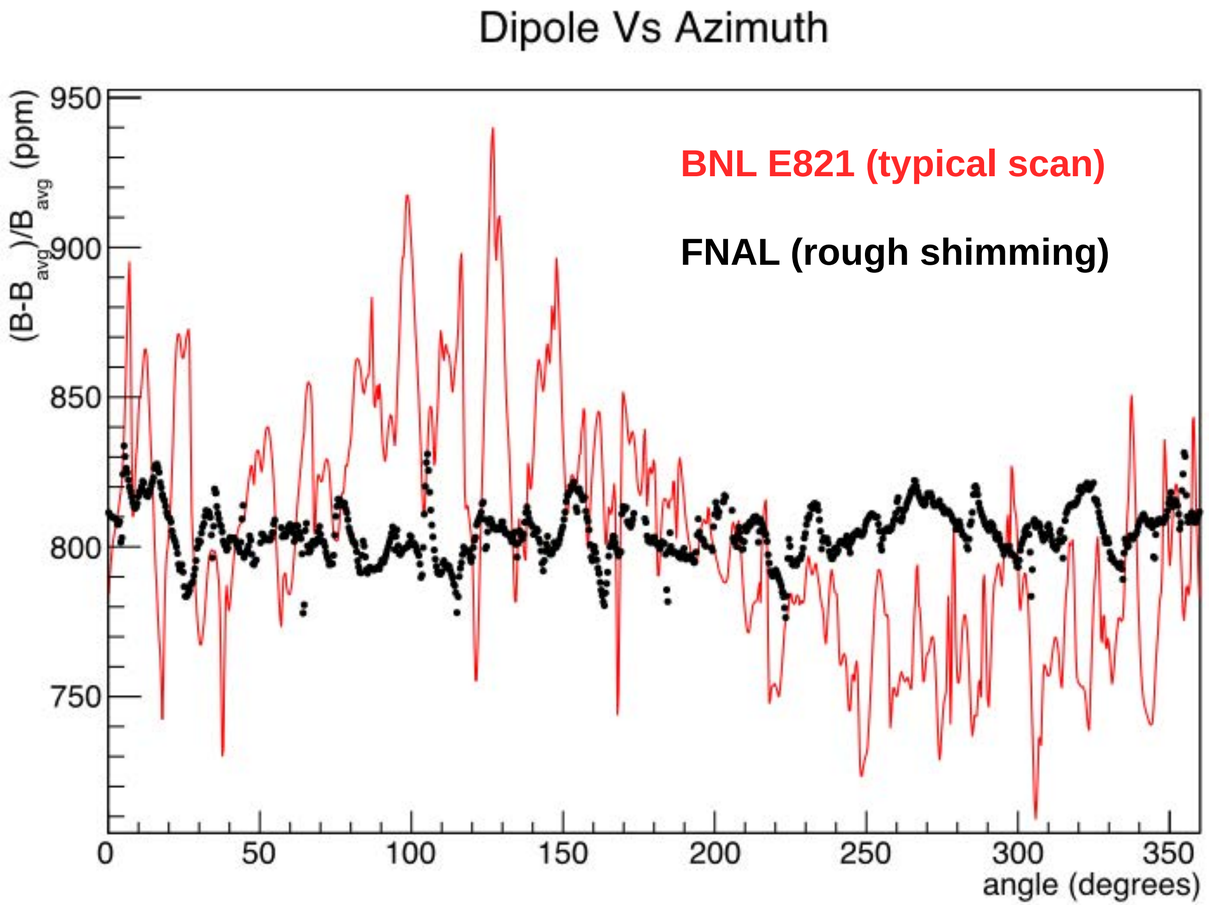

- Laminations very successful in reducing field variations

- BNL E821: 39 ppm RMS (dipole), 230 ppm peak-to-peak
- FNAL rough shimming: 10 ppm RMS (dipole), 75 ppm peak-to-peak

Magnetic Field Variations

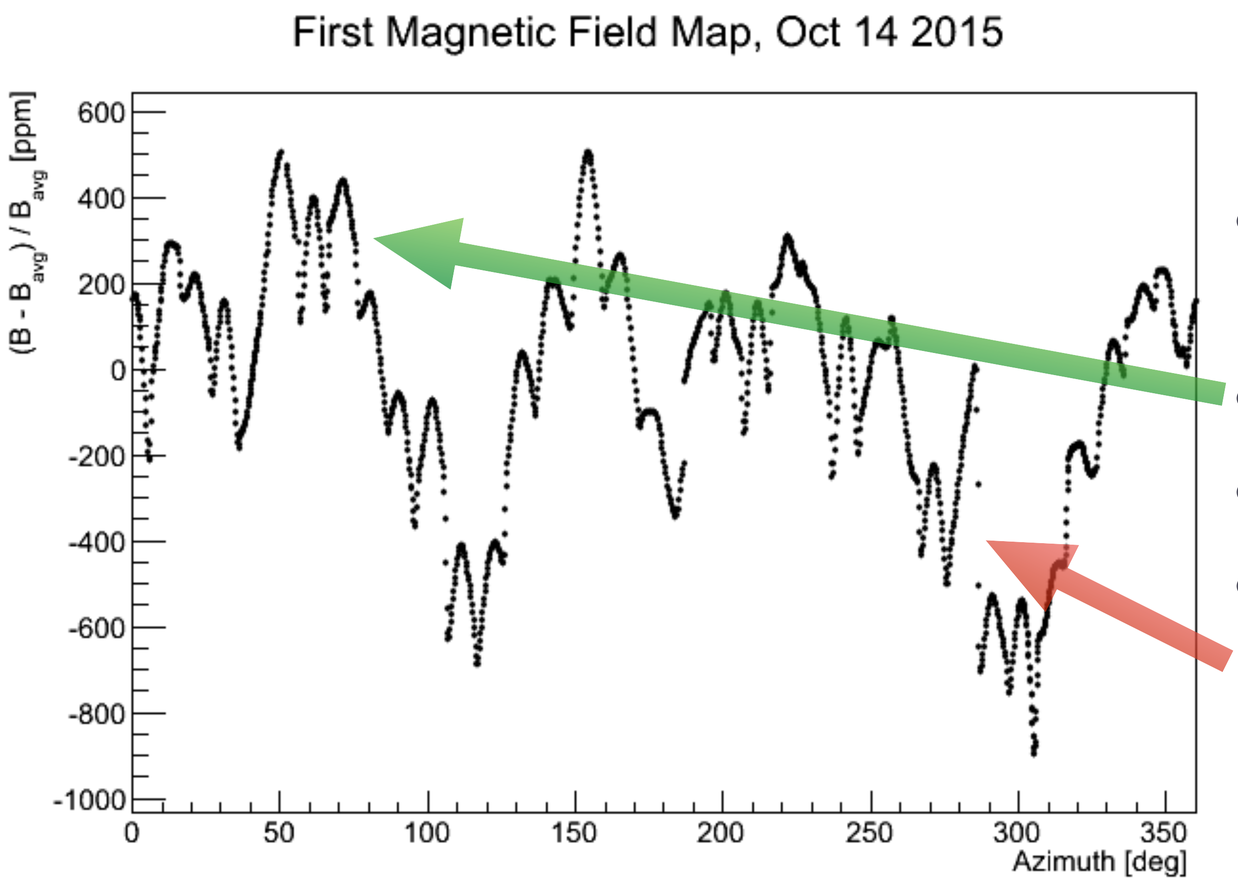

- Gradual drift from materials, pole gap changes
- 36 pairs of poles → 10-degree structure
- Pole shape: 
- Pole-to-pole discontinuities

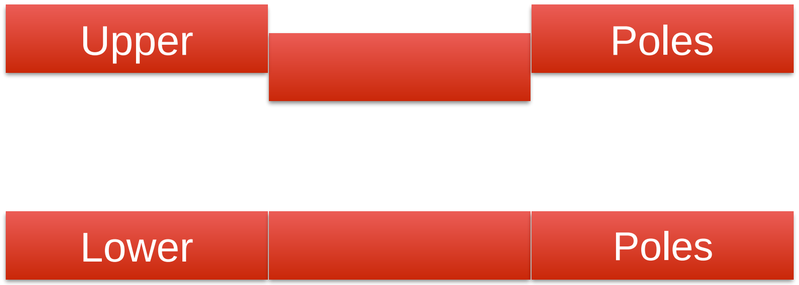

Auxiliary Field Systems

Surface Correction Coils

- Continuous PCB traces going around the ring on pole surfaces
- 100 concentric traces on upper poles, 100 on lower poles
- Programmable range: ± 20 ppm on the field
- Used to cancel higher-order multipole moments in the magnetic field (on average)

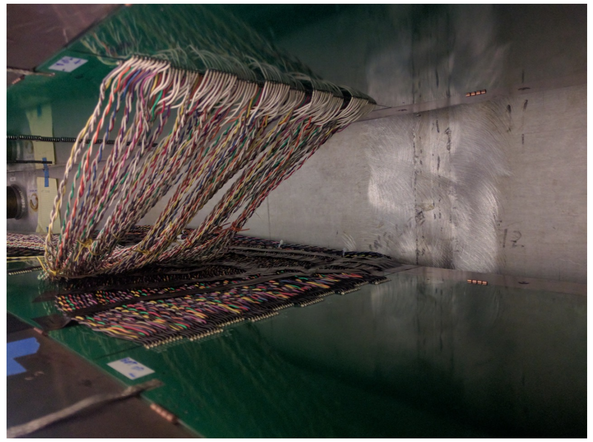

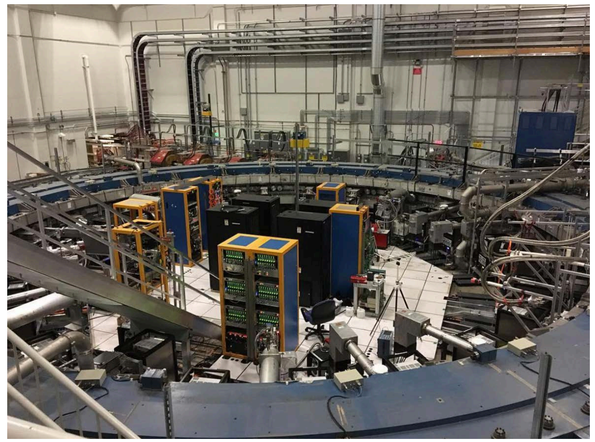

Power Supply Feedback

- Programmable current source with a range of ± 5 ppm on the field
- Uses data from **fixed probe** system to stabilize the field at a specified set point

Fluxgates

- Measure (x,y,z) components of transient fields in the hall
- Sensitive down to 10^{-9} T (DC or AC) fields
- Bandwidth up to 1 kHz

Magnet Insulation

- Temperature variations in the hall affect the quality of the magnetic field
  - Observed ~ 20 ppm/deg C effects on the dipole moment during the run
  - Also affects ability to track higher-order multipoles
- Two main issues
  - Large changes in average temperature over time (2–3°C)
  - Differential changes across the magnet (~3°C)
- Two-pronged solution:
  - Improved cooling system in the hall
  - Install fiberglass insulation blanket on magnet steel

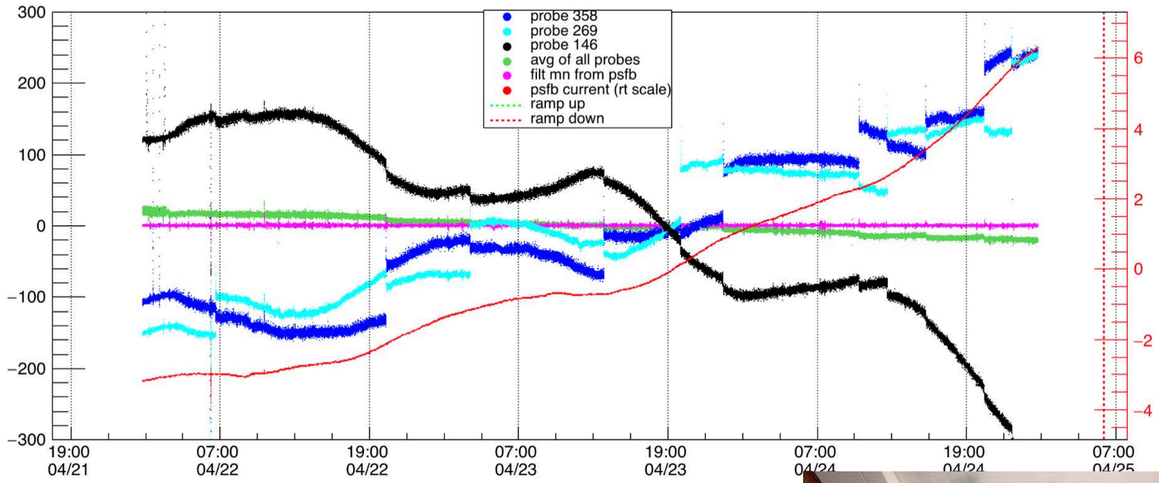

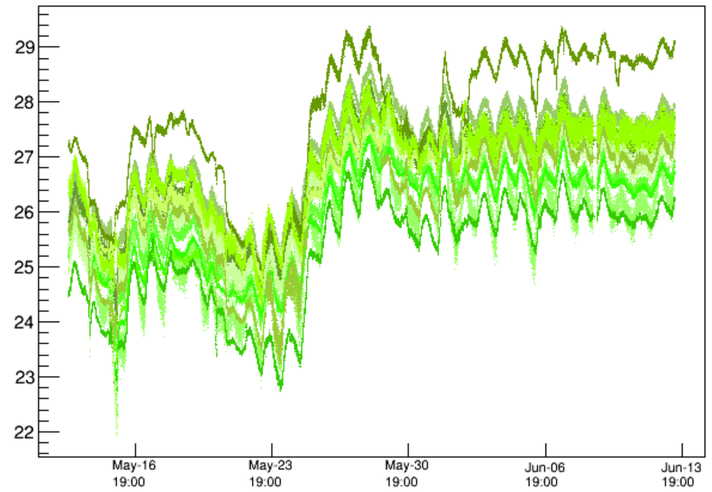

Fixed probe on yoke D vacuum chamber (top)

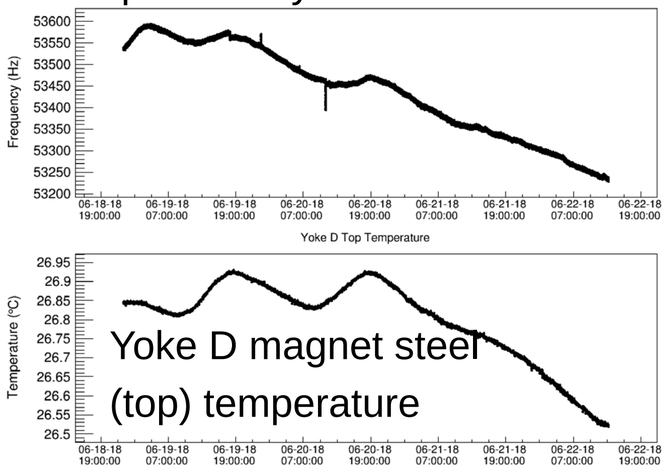

Installed blankets summer 2018

UMassAmherst

Plunging Probe Design

- Used to calibrate the **trolley** NMR probes
- **Symmetry** is very important => minimizes field perturbations => reduced systematic uncertainties
- **RF coil support**: 15-mm OD high-precision glass cylinder
  - Macor supports ensure alignment of **RF coil** (zero-χ 0.97-mm OD wire)
- **Ground shield**: 1” OD, 1-mm wall 2024-T3 Al
  - Stabilizes probe tune, reduces noise pickup
- **Vacuum compatible**

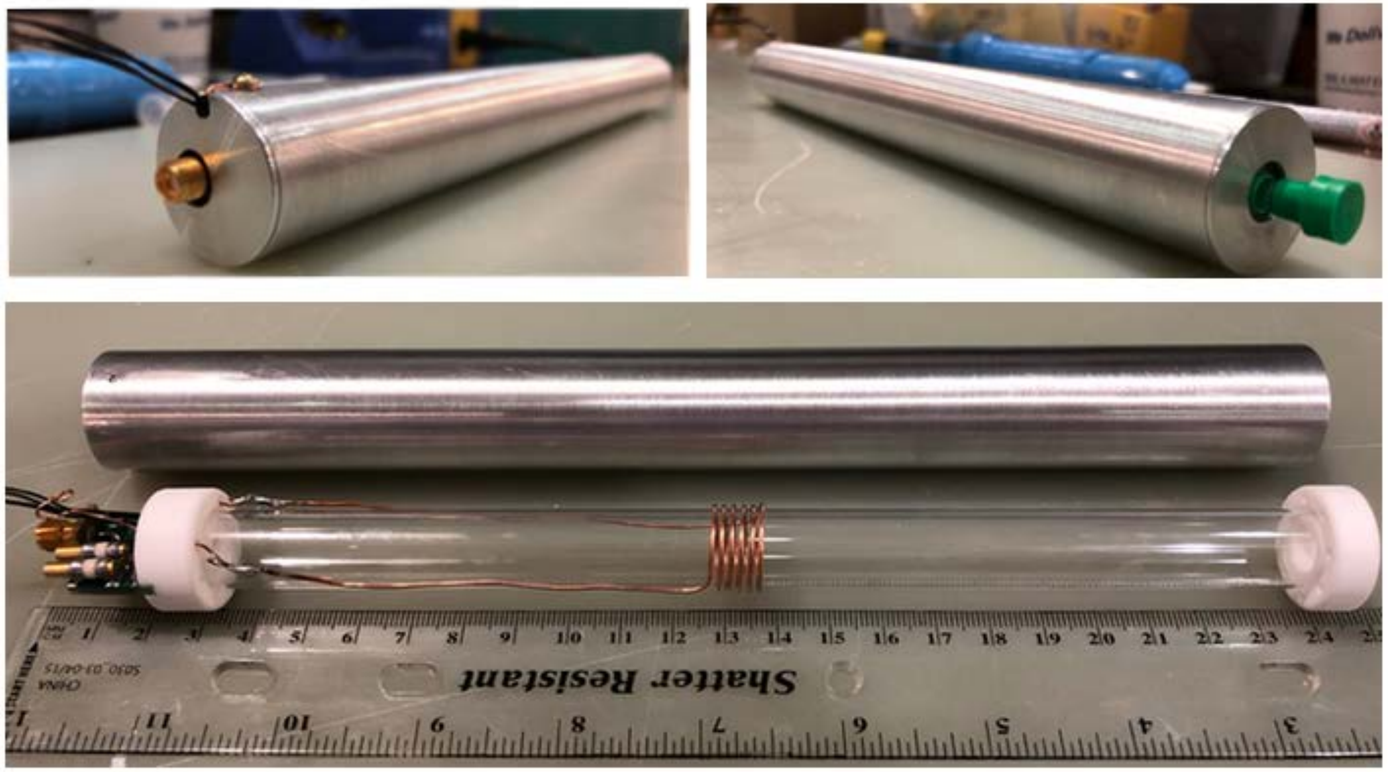

Plunging Probe: Measuring Perturbations

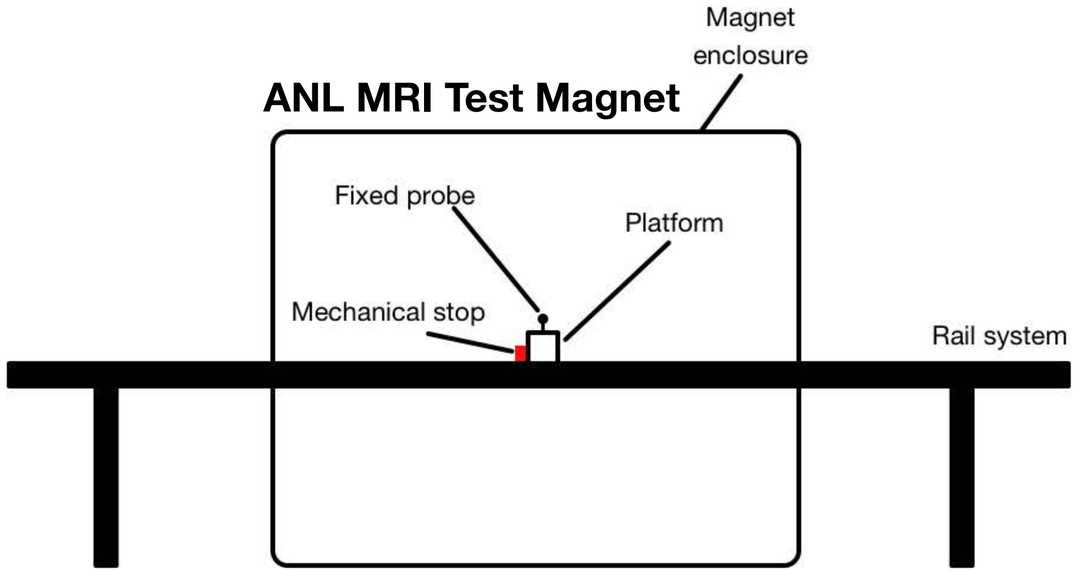

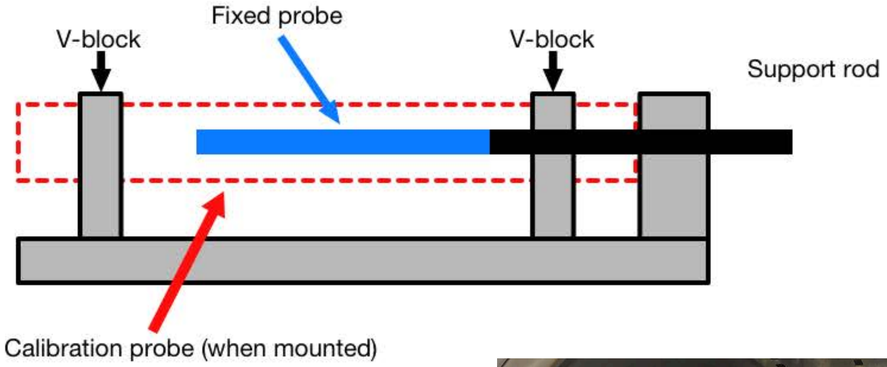

- Take measurements of the field using the **fixed probe**
- **Compare** measurements without and with the PP mounted on stand
- **Difference** with and without gives the effect

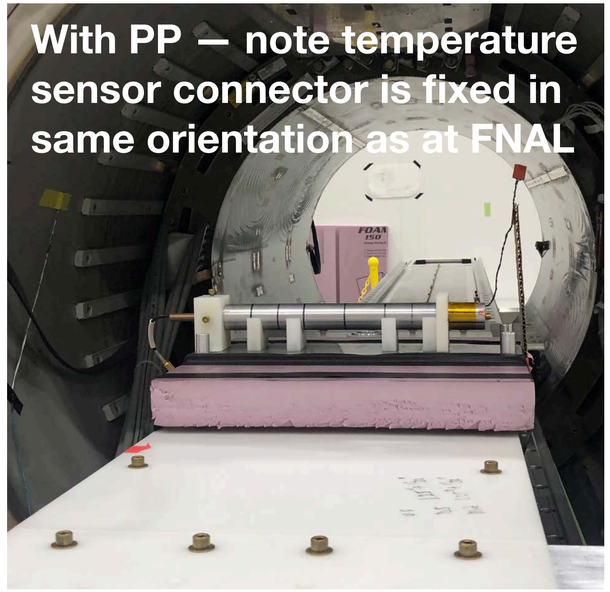

Plunging Probe: Material Perturbations (δ_s)

How much the field changes due to probe presence

Dependence on orientation about its **own** axis

Dependence on orientation relative to **field** axis

Quantity	Symbol	Value (ppb)
General Material Perturbation	$\delta_{mat} + \delta_{mag}$	4.2 ± 8.0
SMA Cable Perturbation	δ_{cable}	-1.4 + 3.0
Probe Temperature	δ_T	0 ± 5
Roll Effect	δ_{roll}	0 ± 1
Pitch Effect	δ_{pitch}	-4.4 ± 4.4
Water Sample Camber	δ_c	0 ± 1
TOTAL	δ_s	**-1.6 ± 10.9**

Plunging Probe: Water Purity (δ_p)

- Impurities in the water sample will perturb the field — paramagnetic contamination (e.g., dissolved oxygen) will increase the field
- Conduct two tests:
  1. Measure field when we **degas** the water — that is, heat up water just enough so that oxygen escapes. Compare to nominal water sample (at same T)
  2. Compare field measurements using water from two different vendors
- **Define** $\delta_p = \delta_{O2} + \delta_w$

dissolved oxygen

different vendors

Quantity	Symbol	Value (ppb)
Oxygen Contamination	δ_{O2}	1.4 ± 0.5
Different Vendors	δ_w	0 ± 1
TOTAL	**δ_p**	**1.4 ± 1.1**

Plunging Probe: Magnetic Images

- Need to account for the effect due to magnetic images of the PP in the pole pieces

- For an infinite plane with magnetic permeability μ_r, the field due to the image of a material with perturbation ΔB is:

$$\Delta B' \approx \left(\frac{\mu_r - 1}{\mu_r + 1}\right) \Delta B\,(x, y, z') \approx \Delta B\,(x, y, z')$$

For $\mu_r >> 1$ (~ 1450 for the magnet*). Evaluate the perturbation at image distance z' in the pole piece (upper **and** lower)

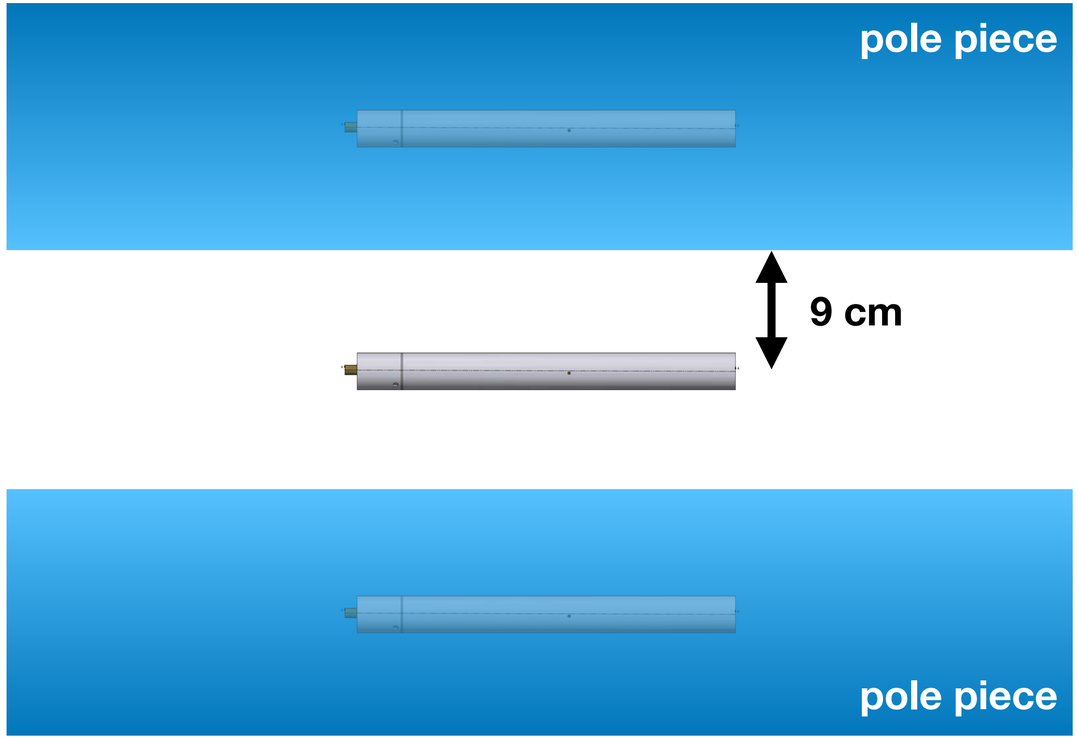

* G. T. Danby *et al*, Nucl. Insrum. Meth. A **457**, 151 (2001)

Plunging Probe: Measuring the Images at FNAL

- Use a stage to mount a fixed probe along the axis of the PP, which can slide over fixed probe
- Compare field measurements with and without PP installed on the stage
- Repeat measurements at height of center trolley probe, and highest trolley probe location
- Also conduct measurements with PP mounting rod attached/detached

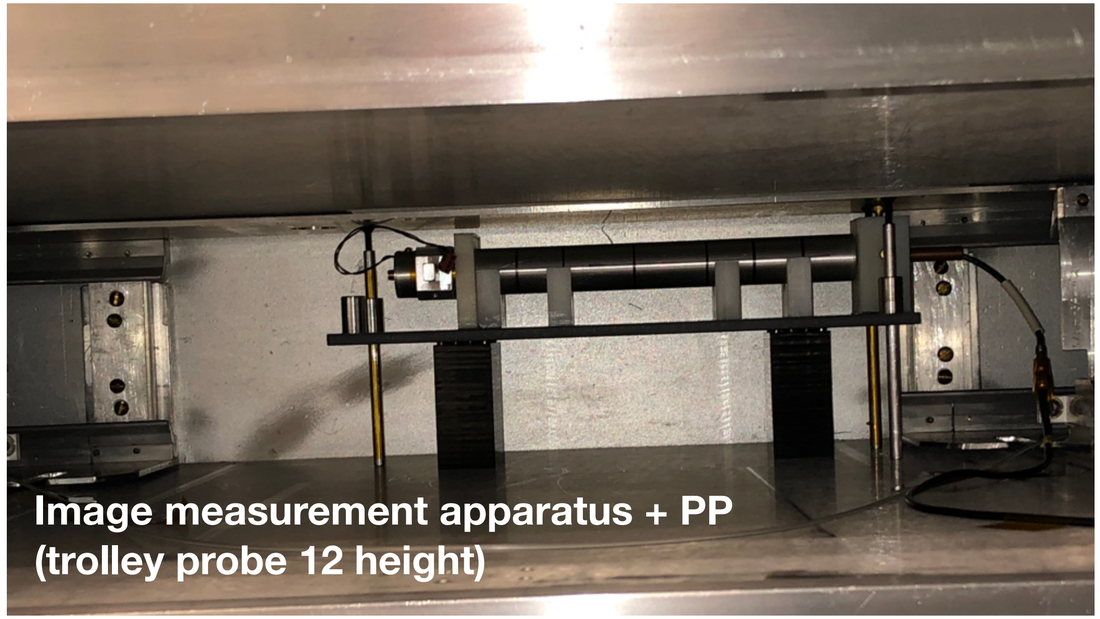

Type	Height Above Midplane (mm)	Image + Perturbation (ppb)	Calculated Prediction (ppb)
PP + Holder	35.5	6.1 ± 4.4	11.5
PP + Holder	-0.2	7.3 ± 5.4	4.3
Rod	-0.2	-3.1 ± 5.6	-12.9
TOTAL	**-0.2**	**4.2 ± 8.0**	**-8.6**

Rod composition may not be pure aluminum (typically up to ~20% variation in χ => imperfect predictions)

Radiation Damping

What is it?

- Precessing spins induce emf in pickup coil; this in turn generates an alternating magnetic field that **acts to rotate spins back towards the main field**
- **Size of effect: $\delta_{RD} \sim [(f_0-f_L)/f_0]\eta Q M_z(t)/\tau_{RD}$**
  - f_0 = resonant frequency of circuit; f_L = Larmor frequency
  - η = filling factor; Q = quality factor of circuit
  - $M_z(t)$ = magnetization of sample, τ_{RD} = time scale of effect

How to quantify?

- Use coils to produce a longitudinal field
  - Precise control over main field to mimic damping effect
- Vary π/2 pulse => vary $M_z(t)$ => changes δ_{RD}

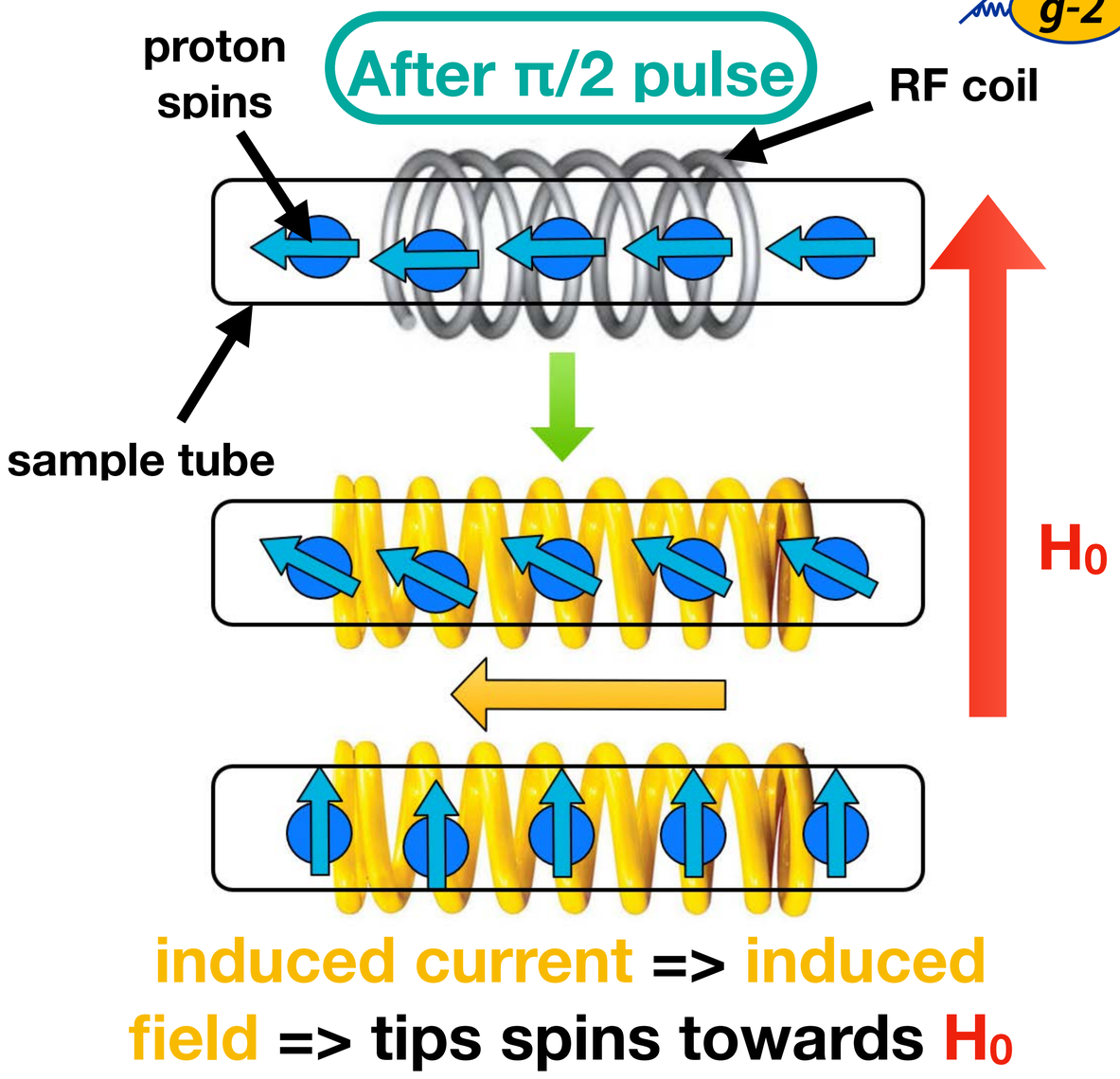

Calibrating the Trolley

Procedure

- Select **trolley** probe to calibrate

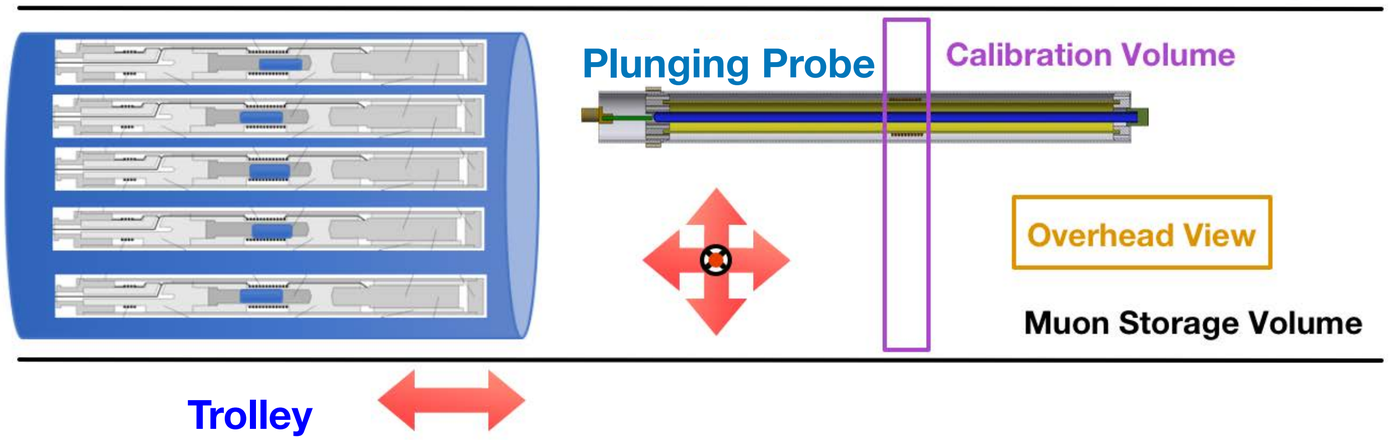

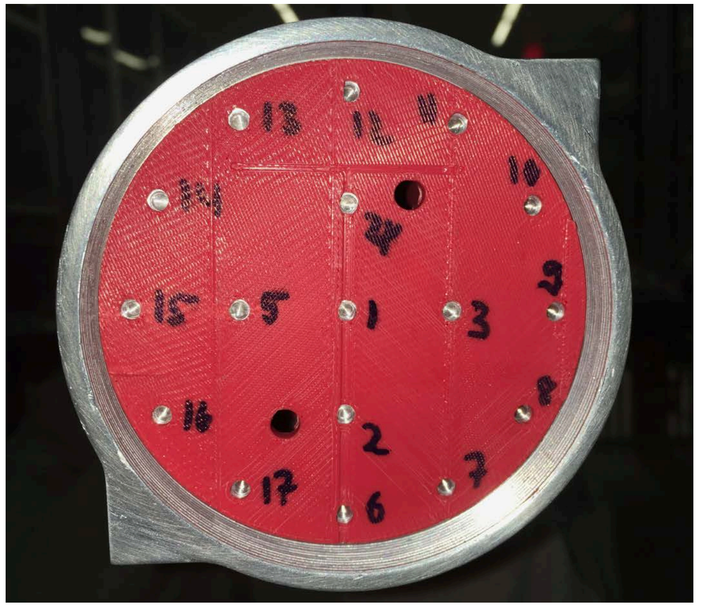

Calibrating the Trolley

Procedure

- Select **trolley** probe to calibrate
- Impose a **known gradient** across the trolley; compare to **bare field B_0**. **Define $\Delta B = B(I \neq 0) - B(I=0)$**
- Unique ΔB for each **trolley** probe gives position

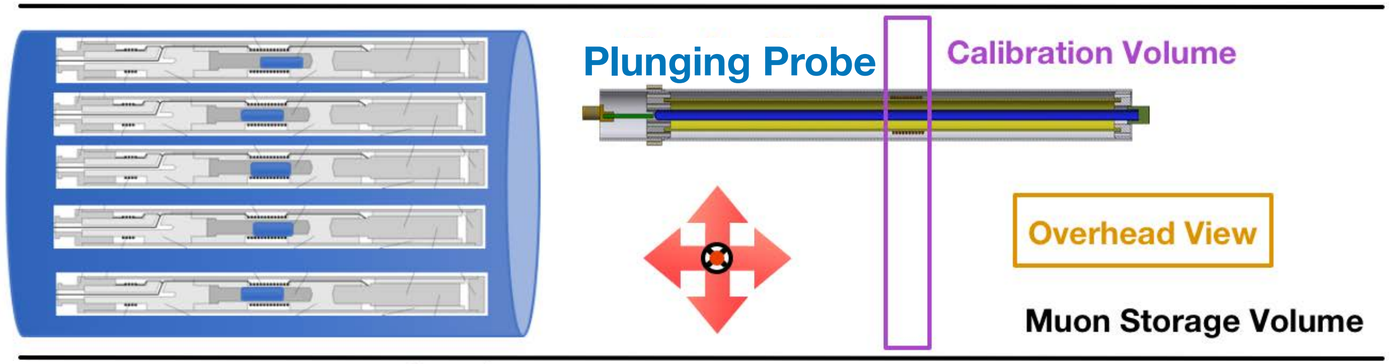

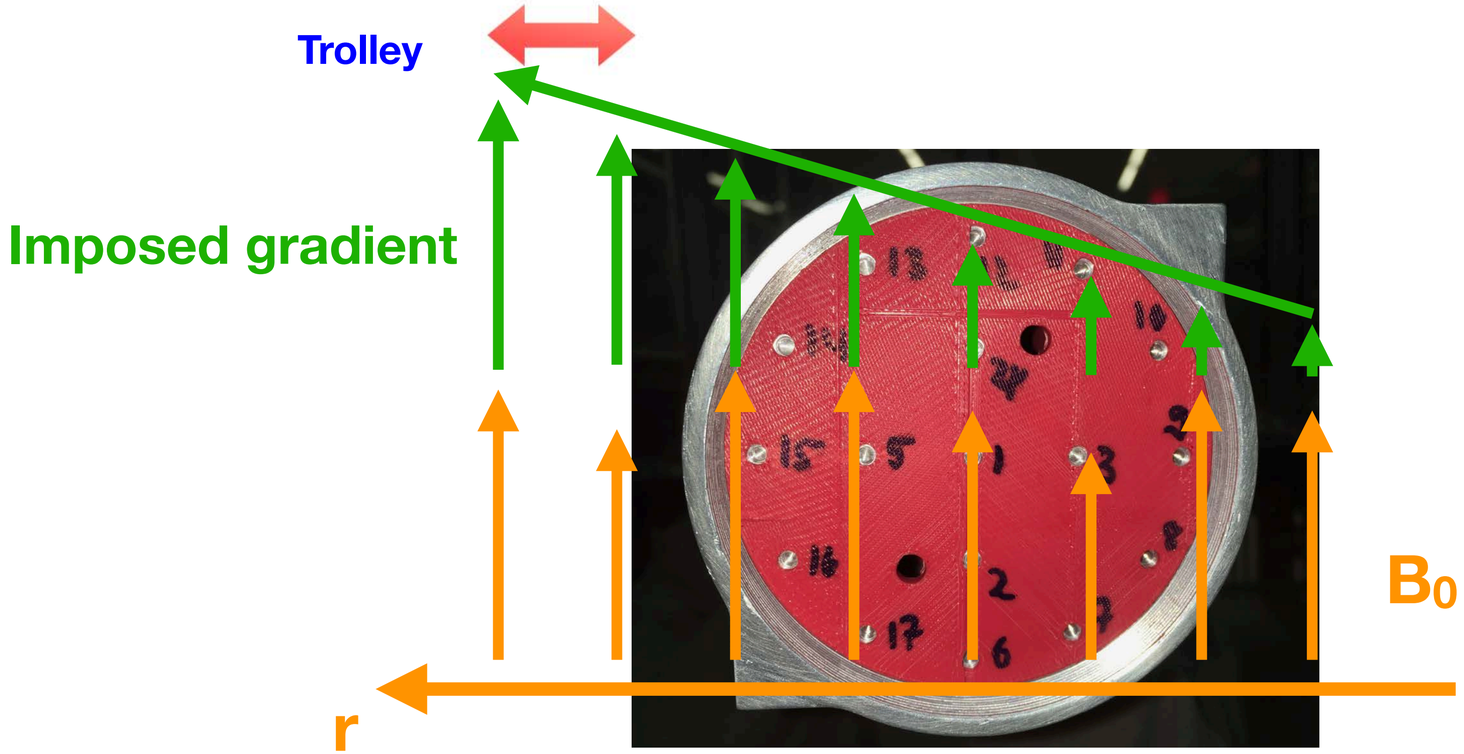

Calibrating the Trolley

Procedure

- Select **trolley** probe to calibrate
- Impose a **known gradient** across the trolley; compare to **bare field B_0**. **Define $\Delta B = B(I \neq 0) - B(I=0)$**
- Unique ΔB for each **trolley** probe gives position
- Move **plunging probe** into volume; measure ΔB and determine distance to move **plunging probe**
- Iterate until **plunging probe** ΔB matches **trolley** probe ΔB
- Perform for radial, vertical, azimuthal coordinates

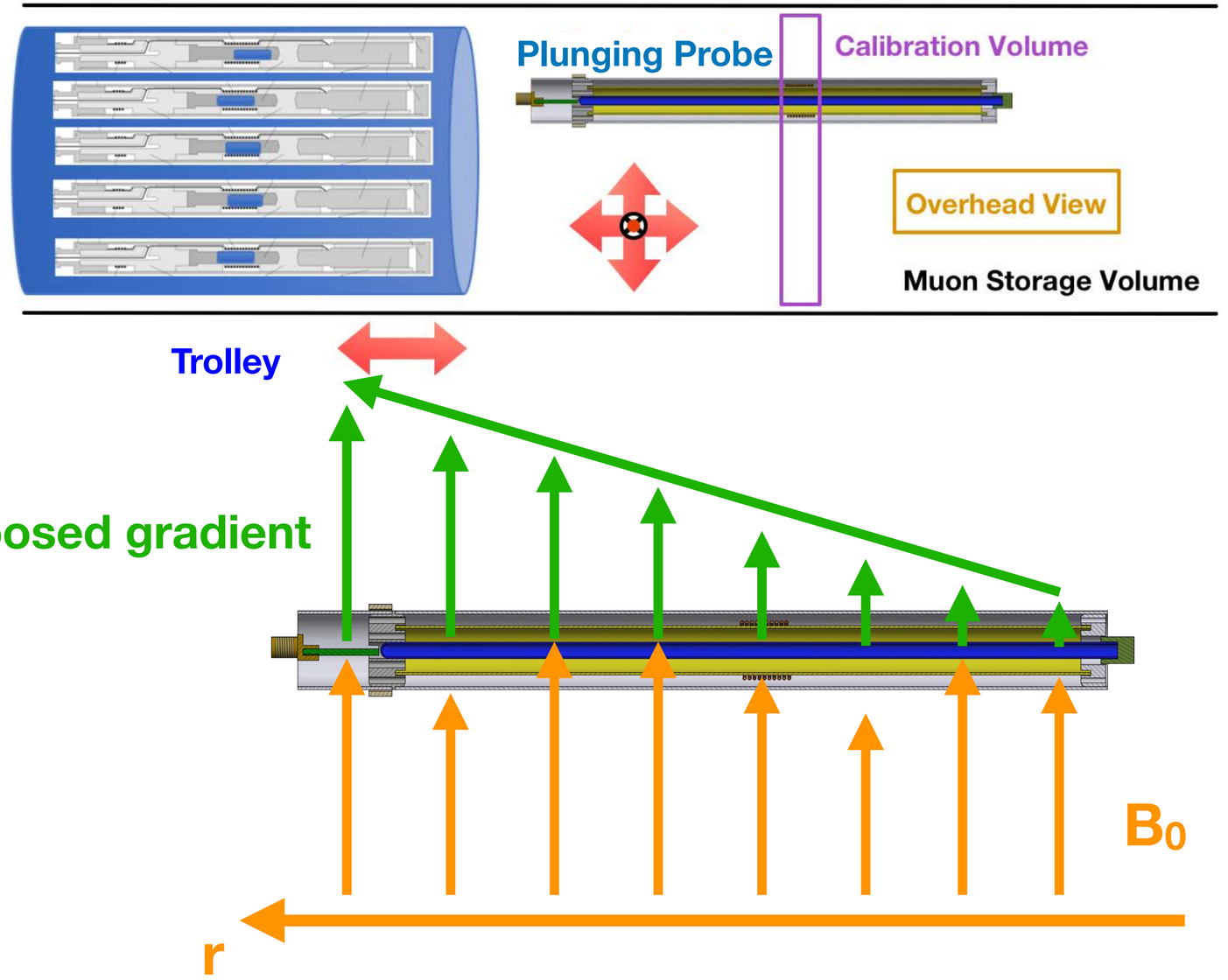

Calibrating the Trolley

Procedure

- Select **trolley** probe to calibrate
- Impose a **known gradient** across the trolley; compare to **bare field B_0**. **Define $\Delta B = B(I \neq 0) - B(I=0)$**
- Unique ΔB for each **trolley** probe gives position
- Move **plunging probe** into volume; measure ΔB and determine distance to move **plunging probe**
- Iterate until **plunging probe** ΔB matches **trolley** probe ΔB
- Perform for radial, vertical, azimuthal coordinates
- Shim the field to be highly uniform, and measure using the **PP** and the **trolley** (rapid swapping)